Impact of atmospheric reactive nitrogen compounds on marine biogeochemical cycles over the Pacific Ocean

(太平洋における海洋大気中反応性窒素化合物の生物地球化学的過程への影響)

鄭進永

The University of Tokyo

Abstract

Aerosol, rain and sea fog (only in the subarctic western North Pacific) samples were collected between 48°N and 55°S during the KH-08-2 (R/V *Hakuho Maru*, 29 July–17 September 2008, the subarctic and subtropical western North Pacific), the MR08-06 (R/V *Mirai*, 15 January–8 April 2009, the North and South Pacific) and the KT-09-5 (R/V *Tansei Maru*, 1 May–6 May 2009, the semi-pelagic western North Pacific) cruises conducted over the North and South Pacific Oceans, in order to estimate deposition fluxes for atmospheric reactive inorganic N species, including ammonium (NH_4^+) and nitrate (NO_3^-), and evaluate their impact on marine biogeochemical cycle.

Concentrations of NH_4^+ and NO_3^- in marine aerosols collected over the semi-pelagic western North Pacific Ocean varied from 59–182 nmol m^{-3} and 13–86 nmol m^{-3}, with averages of 117 ± 42 nmol m^{-3} and 36 ± 22 nmol m^{-3}, respectively. Aerosol inorganic N was composed of ~77% NH_4^+ and 23% NO_3^- (median values for all data). Most NH_4^+ (mean 90%) was found in fine mode aerosols (D < 2.5 μm), suggesting that it was formed by gas-to-particle conversion. In contrast, NO_3^- (mean 55%) was predominantly found in coarse mode aerosols (D > 2.5 μm), indicating a chemical reaction between nitric acid gas (HNO_3) and sea-salt/crustal aerosol in the marine atmosphere. Both NH_4^+ and NO_3^- showed strong correlations with nss-SO_4^{2-} and nss-K^+ (r = 0.73–0.96), suggesting that fossil fuel combustion and biomass burning are significant sources of NH_4^+ and NO_3^-, and/or that they experienced similar transport and removal mechanisms. The fractions of atmospheric inorganic N species derived from specific sources were estimated that 97–99% (mean 98%) of NH_4^+ and 78–88% (mean 84%) of NO_3^- were derived from agricultural activity and fossil fuel combustion, respectively. Mean dry deposition fluxes for NH_4^+ and NO_3^- were estimated to be 31 ± 17 μmol m^{-2} d^{-1} and 33 ± 17 μmol m^{-2} d^{-1}, respectively. Although the mean concentration of NH_4^+ was 3 times higher than that of NO_3^-, dry deposition fluxes of both were approximately the same since fluxes to the ocean are dominated by the coarse mode, resulting in NO_3^- being deposited much more rapidly. Atmospheric bioavailable N deposition flux (64 ± 31 μmol m^{-2} d^{-1}) over the semi-pelagic western North Pacific Ocean was found to be maximally responsible for the carbon uptake of 420 ± 210 μmol C m^{-2} d^{-1} (139–669 μmol C m^{-2} d^{-1}) by using the Redfield C/N ratio of 6.6, indicating that it can support 1.9–8.9% of the new primary production.

Over the subarctic western North Pacific Ocean (> 40°N), sea fog occurred predominantly when the difference between the air and sea surface temperatures is observed to be positive. This result indicates that the warm and humid air masses form the low and middle latitudes of the North Pacific were cooled down to a saturation temperature by the relatively cold sea surface, making a favorable condition for sea fog formation. Mean particle number densities during non sea fog events were 25 ± 31 cm^{-3} for aerosols in the range of 0.3 < D < 0.5 μm, 2.6 ± 3.0 cm^{-3} for 0.5 < D < 1.0 μm, 0.53 ± 0.70 cm^{-3} for 1.0 < D < 2.0 μm, and 0.17 ± 0.27 cm^{-3} for D > 2.0 μm. In comparison, the mean particle number densities during sea

fog events decreased by 4% (mean particle number density 24 ± 20 cm^{-3}) for aerosols in the range of 0.3 < D < 0.5 μm, 12% (2.3 ± 3.1 cm^{-3}) for 0.5 < D < 1.0 μm, 55% (0.24 ± 0.52 cm^{-3}) for 1.0 < D < 2.0 μm, and 78% (0.038 ± 0.091 cm^{-3}) for D > 2.0 μm. This result suggests that the growth of aerosol particles to liquid droplets leads to the acceleration of particle removal from the atmosphere, and that particles with diameters larger than 0.5 μm could act preferentially as condensation nuclei for sea fog droplets. Although the mean pH values of rainwater (4.1 ± 0.37) and sea fog water (4.2 ± 0.64) collected over the subarctic western North Pacific Ocean were similar, non sea-salt chloride (nss-Cl^-) and non sea-salt sulfate (nss-SO_4^{2-}) exerted larger influences on acidity of rainwater and sea fog water, respectively. In addition, mean concentrations of methanesulfonic acid (MSA), which is formed exclusively from dimethylsulfide (DMS) produced by phytoplankton in the ocean, and nss-SO_4^{2-} in sea fog water were 15 times and 13 times higher than those in rainwater, respectively. These results suggest that sea fog scavenged biogenic sulfur species more efficiently than rain, and that scavenging processes of aerosols and gases by sea fog are different to those by rain. While the mole equivalent ratio of NO_3^-/Na^+ in sea fog water was higher than that in aerosols, the NO_3^-/Na^+ ratio in rainwater was lower than in aerosols. Moreover, mean concentration of NO_3^- in sea fog water was approximately 6 times higher than that in rainwater, whereas those of NH_4^+ were almost similar in both sea fog water and rainwater. This result reveals that sea fog scavenged more effectively coarse mode particles (e.g., sea salt particles and $NaNO_3$) that acted as condensation nuclei of sea fog droplets as well as gaseous HNO_3. Mean dry, wet and sea fog deposition for atmospheric total inorganic N (TIN; i.e., $NH_4^+ + NO_3^-$) over the subarctic western North Pacific Ocean were estimated to be 4.9 ± 2.6 μmol m^{-2} d^{-1}, 33 ± 47 μmol m^{-2} d^{-1} and 7.8 ± 8.7 μmol m^{-2} d^{-1}, respectively. The contribution of dry, wet and sea fog deposition to total deposition flux for TIN (46 ± 48 μmol m^{-2} d^{-1}) were 11%, 72% and 17%, respectively, suggesting that ignoring sea fog deposition would lead to underestimate of the total influx of atmospheric inorganic N into the subarctic western North Pacific Ocean, especially in summer periods.

Total concentrations of NH_4^+ and NO_3^- in bulk (fine + coarse) aerosols collected over the Pacific Ocean varied from 0.93–12 nmol m^{-3} and 0.44–5.6 nmol m^{-3}, respectively. Aerosol inorganic N in entire data set was composed of ~68% NH_4^+ and ~32% NO_3^- (median values for all data), with ~81% and ~45% of each species being present on fine mode aerosol, respectively. The total NH_4^+ and NO_3^- concentrations showed similar trends, with higher concentrations in samples collected over the western North Pacific and lower values over the South Pacific. These distributions likely resulted from large terrestrial emission sources of N in the northern hemisphere, deposition during transport across the ocean, and the intertropical convergence zone (ITCZ) by which cross-equatorial transport is suppressed. Concentration of NH_4^+ (0.93–4.1 nmol m^{-3}) in aerosols collected over the South Pacific were a factor of 1.2–6.3 higher than the results of model study (0.65–0.78 nmol m^{-3} STP) calculated aerosol NH_4^+ concentrations without natural emissions in the South Pacific, suggesting that emissions of ammonia gas (NH_3) from the ocean could become a significant source of aerosol NH_4^+ in the South Pacific because

NH_3 is emitted into the atmosphere from the ocean as a result of biological activity, and that much of observed aerosol NH_4^+ in the open ocean aerosols could be recycled oceanic NH_3. Overall, NO_3^- mainly was found in coarse mode aerosols, while NH_4^+ was largely associated with the fine mode. Interestingly, 73 ± 4.2% of NO_3^- collected in the coast of Chile was found in fine mode aerosols, although it is known that NO_3^- in the marine atmosphere is predominantly associated with coarse mode aerosol, suggesting that NO_3^- accumulated in the coarse mode could have been removed more rapidly by dry or wet deposition during transport because of the larger particle size, and that NO_3^- could be produced by lightning in the free troposphere and by injection from the stratosphere because there are few chances to react with coarse mode sea-salt that is continuously supplied from the sea surface.

Concentrations of NH_4^+ and NO_3^- in rainwater collected over the Pacific Ocean ranged from 1.7–55 μmol L^{-1} and 0.16–18 μmol L^{-1}, respectively. Inorganic N in rainwater was composed of ~87% NH_4^+ and ~13% NO_3^- (median values for all data), suggesting that NH_4^+ is more abundant in rainwater collected over the North and South Pacific Ocean, and that it is a more important inorganic N species supplied by wet deposition. A significant correlation ($r = 0.74$, $p < 0.05$, $n = 10$) between NH_4^+ and MSA was found in rainwater samples collected over the South Pacific Ocean and the coast of Chile. In addition, NH_4^+ showed no clear relationship with Na^+ in rainwater collected over these regions, suggesting that emissions of NH_3 by marine biological activity from the ocean could become a significant source of NH_4^+ in rainwater over the South Pacific Ocean.

The estimated mean dry deposition fluxes for atmospheric TIN in the Pacific Ocean varied from 1.5–5.7 μmol m^{-2} d^{-1}, contributing ~47% by NH_4^+ and ~53% by NO_3^- to the dry deposition flux for atmospheric TIN. Mean wet deposition fluxes of atmospheric TIN in the Pacific Ocean varied from 31 to 62 μmol m^{-2} d^{-1}, accounting for ~81% by NH_4^+ and ~19% by NO_3^- of TIN from wet deposition flux. While NO_3^- was the dominant inorganic N species in dry deposition, inorganic N supplied to surface waters by atmospheric wet deposition was predominantly by NH_4^+. Total (dry + wet) mean deposition fluxes of atmospheric TIN in the Pacific Ocean were estimated to be 32–64 μmol m^{-2} d^{-1}, with 66–99% of this in the form of wet deposition, indicating that wet deposition plays an important role in the supply of atmospheric inorganic N to the Pacific Ocean compared to dry deposition, although the relative contributions are highly variable among regions. The total mean deposition fluxes of atmospheric TIN over the Pacific Ocean were found to be maximally responsible for the carbon uptake of 210–420 μmol C m^{-2} d^{-1} in the Pacific Ocean, suggesting that inorganic N deposited to the Pacific Ocean from the atmosphere can support 0.86–1.7% of the total primary production.

Contents

1. Introduction

Nitrogen (N) is an essential nutrient in terrestrial and marine ecosystems. Most N in the atmosphere and ocean is present as nitrogen gas (N_2) and is available only to diazotrophs, a restricted group of microorganisms that can fix N_2. Most organisms can only assimilate forms of reactive N (N_r) species, including oxidized (e.g., NO_x, HNO_3, N_2O, NO_2^- and NO_3^-) and reduced (e.g., NH_3 and NH_4^+) inorganic and organic forms (e.g., urea, amines, and proteins) (Galloway, 2004; Duce et al., 2008). Compared to N_2, N_r species are minor constituents; however, they play important roles in contemporary environmental problems, including the formation of acidic precipitation, photochemical smog and eutrophication of coastal waters (Brasseur et al., 1999).

1.1. Sources and transport of atmospheric reactive nitrogen

Sources of atmospheric reactive inorganic N species such as ammonium (NH_4^+) and nitrate (NO_3^-) are comparatively well understood (Spokes et al., 2000; Cornell et al., 2003; Baker et al., 2007). Fossil fuel combustion is a major source for nitrogen oxides (NO_x = NO + NO_2) (Levy and Moxim, 1987; Duce et al., 1991) and a smaller source of ammonia gas (NH_3). Atmospheric NO_3^- is an end product of a series of gas-phase photochemical and heterogeneous reactions involving NO_x, which are primarily derived from fossil fuel combustion and certain natural N fixing processes (Seinfeld and Pandis, 1998). Atmospheric NO_3^- is formed from nitrogen monoxide (NO) and nitrogen dioxide (NO_2) gases which are generated via the high temperature oxidation of N in internal combustion engines and during industrial activity. Reaction of ozone (O_3) or peroxy radicals with NO rapidly produces NO_2. This either reacts directly with hydroxyl radical (OH) to form nitric acid gas (HNO_3) or with O_3 to produce the highly reactive NO_3 radical which is rapidly photolyzed. At night, significant concentrations of NO_3 radical build up, reacting with NO_2 to set up an equilibrium with dinitrogen pentoxide (N_2O_5). Heterogeneous reactions of HNO_3 and NO_3 radical with water on aerosols result in the formation of aerosol NO_3^- since they are highly soluble (Seinfeld and Pandis, 1998; Brasseur et al., 1999; Spokes et al., 2000). Atmospheric NH_4^+ is produced by heterogeneous reactions involving NH_3 whose major sources are animal wastes, ammonification of humus followed by emission from soils, losses of NH_3-based fertilizers from soils, oceans, biomass burning and industrial emissions (Dentener and Crutzen, 1994). Ammonia is the only natural alkaline gas in the atmosphere and can be converted to an aerosol NH_4^+ in an acid–base reaction with a gas (e.g., HNO_3) or aerosol (e.g., sulfate; SO_4^{2-}) (Brasseur et al., 1999).

Atmospheric particulate N released or delivered to the atmosphere can be transported by the prevailing wind hundreds to thousands of kilometers horizontally and vertically several kilometers (Graham and Duce, 1979; Duce et al., 1991; Seinfeld and Pandis, 1998; Brasseur et al., 1999; Galloway, 2004). During transport, atmospheric N is removed from by dry and wet deposition. Dry and wet

deposition is the ultimate paths by which gas and particle are removed from the atmosphere. Dry deposition is a removal process of gaseous and particulate species from the atmosphere onto the earth's surfaces in the absence of precipitation (including removal by fog deposition). Factors governing the dry deposition of atmospheric aerosols include the level of atmospheric turbulence, the properties of the particle (e.g., size, density, shape and composition), and the nature of the surface itself (Duce et al., 1991; Pryor and Barthelmie, 2000). Wet deposition, on the other hand, involves all processes by which airborne species are transferred to the earth's surface in aqueous form (i.e., rain, snow or fog): (1) dissolution of atmospheric gases in airborne droplets (e.g., cloud, rain and fog drops); (2) removal of atmospheric particles when they serve as nuclei for the condensation of atmospheric water to form a cloud or fog droplet and are subsequently incorporated in the droplet; and (3) removal of atmospheric particles when the particle collides with a droplet both within and below clouds (Duce et al., 1991; Seinfeld and Pandis, 1998; Pryor and Barthelmie, 2000). While dry deposition is a continuous process occurring at all times over all surfaces, wet deposition is highly episodic occurring only when there is precipitation. The relative importance of dry and wet deposition fluxes varies between locations since wet deposition is intermittent and primarily functions of the rainfall frequency and amount in the region (Spokes et al., 2000).

1.2. Inputs of atmospheric reactive nitrogen to the ocean

Nutrient supply to the ocean surface layer is an important factor controlling the ocean ecosystem. The major paths of supplies of nutrients to the ocean surface layer have been considered as those from deep layers and river discharge, which is mostly taken up near the estuary region, but the nutrients transported through the atmosphere become important for the open ocean where the nutrients are limiting primary productivity (Uno et al., 2007). Biological N fixation, which is the natural process that converts N_2 to N_r, is the dominant source of new N to the ocean (Gruber and Galloway, 2008). The other new N sources to the ocean are riverine injection and atmospheric deposition; however, contributions of these two inputs are small (Galloway, 2004). Although contribution of atmospheric N deposition to total N input to the ocean is small, the relative contribution of atmospherically derived N to the total N demand can be much larger in regions where the vertical supply of N from deep nutrient rich water is very restricted, such as the subtropical ocean gyres (Benitez-Nelson, 2000).

Atmospheric N can reach by dry and wet deposition to waterbodies either directly, by falling onto the waterbody itself, or indirectly, after falling on the watershed and being delivered to the waterbody with groundwater and surface runoff (Clark and Kremer, 2005). Atmospheric transport of particulate matter from the continents to the oceans is well recognized as a major pathway for supply of natural and anthropogenic materials to open ocean surface waters, including nutrients (Duce et al., 1991; Jickells, 1995). Apart from supply of deep nutrient rich water by vertical mixing, the atmosphere is the only

significant pathway of nutrients to the photic zone of the open ocean where there is little riverine input (Bergametti et al., 1992; Benitez-Nelson, 2000). Atmospheric depositions of biologically available N into the ocean could fertilize the ocean's biosphere. Previous studies have highlighted the significance of the atmosphere as a pathway for transport of essential nutrients for biological growth, from continents to marine surface waters and their critical role in oceanic biogeochemical cycling (Graham and Duce, 1979, 1982; Duce et al., 1991; Prospero et al., 1996; Paerl, 1997; Mahowald et al., 2005, 2008).

1.3. Impact of anthropogenic nitrogen on marine biogeochemical cycles

Before anthropogenic sources became significant, the biogeochemical cycle of N was in a state of near equilibrium, balanced by transport among the atmosphere, hydrosphere, soils, and biota. However, anthropogenic inputs of N from industrial activities, transportation, agriculture, etc. have disrupted these balances (Gruber and Galloway, 2008). Human activities have altered the biogeochemical cycles of carbon (C) as well as that of N, since the cycles of C and N are tightly related (Fig. 1.1).

Anthropogenic activities have enhanced N supply to coastal and open oceans (Naqvi et al., 2000; Nevison et al., 2004). The increased N release from land due to agricultural use and fossil fuel consumption has resulted in a change in nutrient supply to the oceans (De Leeuw et al., 2001). Anthropogenic N inputs alter surface seawater alkalinity, pH, and inorganic carbon storage, increasing ocean acidification and affecting ecosystems, especially in coastal regions, which could have a significant effect on human populations (e.g., changes in species and productivity of marine organisms and climate change) (Doney et al., 2007).

Extensive use of fossil fuels and N in fertilizer has already impacted coastal as well as open ocean marine ecosystems due to increased nutrient deposition (Krishnamurthy et al., 2010). With increasing fluxes from anthropogenic sources of nutrients, atmospheric input of N may strongly impact terrestrial and oceanic biogeochemistry (Cornell et al., 2003; De Leeuw et al., 2003; Duce et al., 2008; Mahowald et al., 2008). Duce et al. (2008) reported that the total N_r deposition to the ocean in 2000 was estimated to be ~67 Tg N yr^{-1}, with ~80% being anthropogenic (Fig. 1.2). This anthropogenic increase in nutrient input is thought to increase the total amount of carbon fixed in the upper ocean and thus balance in part the global atmospheric increase in carbon dioxide (CO_2) (Herut et al., 1999). It has been suggested that atmospheric deposition of anthropogenic N to the ocean located downwind of populated and urbanized regions can lead to or shift toward greater phosphorus limitation (Fanning, 1989). Atmospheric inputs of anthropogenic N can result in a significant contribution to the new production in oceanic surface waters, especially in oligotrophic areas.

1.4. Objectives of study

Considerable effort has been devoted to quantifying the deposition flux of atmospheric N and its impact on biogeochemical cycles (Paerl, 1985; Benitez-Nelson, 2000; Spokes et al., 2000; Carrillo et al., 2002; Duce et al., 2008; Mahowald et al., 2008; Rolff et al., 2008; Krishnamurthy et al., 2010). A large fraction of the atmospheric N input is in the form of inorganic N, mainly NO_3^- and NH_4^+, and the biogeochemical cycles of these N species are of particular interest because they can be readily utilized by a variety of aquatic microorganisms and plants (Gilbert et al., 1991). Although recent studies have estimated impacts of atmospheric N inputs, there are still large uncertainties regarding the global atmospheric N cycle since most studies are based on the results of several models (e.g., Dentener et al., 2006; Duce et al., 2008). The atmospheric N cycle over the oceans contains the most uncertain part (Baker et al., 2010) because the validation of model output was primarily based on comparisons to terrestrial sampling sites (Dentener et al., 2006; Baker et al., 2010). So far, the field observation/data on the deposition flux of atmospheric N are mostly concentrated on the Atlantic Ocean and the Mediterranean Sea (e.g., Spoke et al. 2000; Baker et al. 2007; Sandroni et al. 2007; Baker et al. 2010), with a little data being reported for the Pacific Ocean (e.g., Duce et al. 1991; Nakamura et al. 2005; Matsumoto et al. 2009).

Because of rapid Asian economic growth, emissions of anthropogenic substances (e.g., NO_x) from the Asian continent have significantly increased (Uno et al., 2007). Since the western North Pacific receives a large influx of mineral dust and pollution aerosol from the Asian continent through atmospheric transport (Uematsu et al., 1983; Gao et al., 1992; Nakamura et al., 2005; Uematsu et al., 2010), estimating deposition flux of atmospheric N and its impacts on biogeochemical cycles over the western North Pacific have become increasingly important. Nevertheless, few studies have been carried out over this region to estimate the dry and wet deposition fluxes of atmospheric N, simultaneously. Moreover, atmospheric N in marine aerosols and rain over the South Pacific Ocean, which is expected to receive little influences from terrestrial and anthropogenic substances, has not been extensively investigated. It is therefore necessary to characterize atmospheric N in marine aerosols and rain (and/or sea fog) over the North and South Pacific and estimate its total (dry + wet) deposition fluxes in order to fill the data gaps and evaluate its impact on marine biogeochemical cycle over these regions. The objectives of this study therefore are to (1) investigate general characteristics of atmospheric reactive inorganic N species in marine aerosols, rainwater (and/or fog water) samples collected over the North and South Pacific Oceans, (2) estimate total deposition flux of atmospheric bioavailable N, and (3) evaluate their impact on marine biogeochemical cycles. This study focuses on atmospheric NH_4^+ and NO_3^- which are dominant reactive inorganic N components for N supply to the ocean (Krishnamurthy et al., 2010). The results for atmospheric N deposition from this study should be valuable for filling the data gap, especially for the South Pacific, and be useful for validation of N deposition flux model on a global ocean scale.

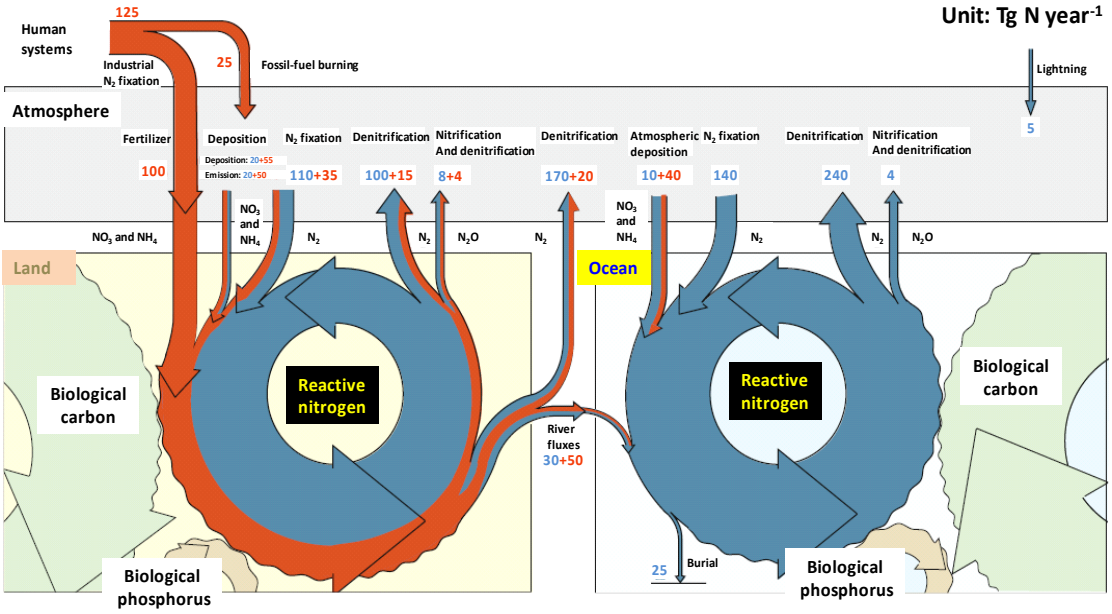

Fig. 1.1. Depiction of the global nitrogen cycle on land and in the ocean. Major processes that transform molecular nitrogen into reactive nitrogen (N_r), and back, are shown. Also shown is the tight coupling between the nitrogen cycles on land and in the ocean with those of carbon and phosphorus. Blue fluxes denote 'natural' (unperturbed) fluxes in Tg N yr^{-1}; orange fluxes denote anthropogenic perturbation in Tg N yr^{-1}. The plot is taken from Gruber and Galloway (2008).

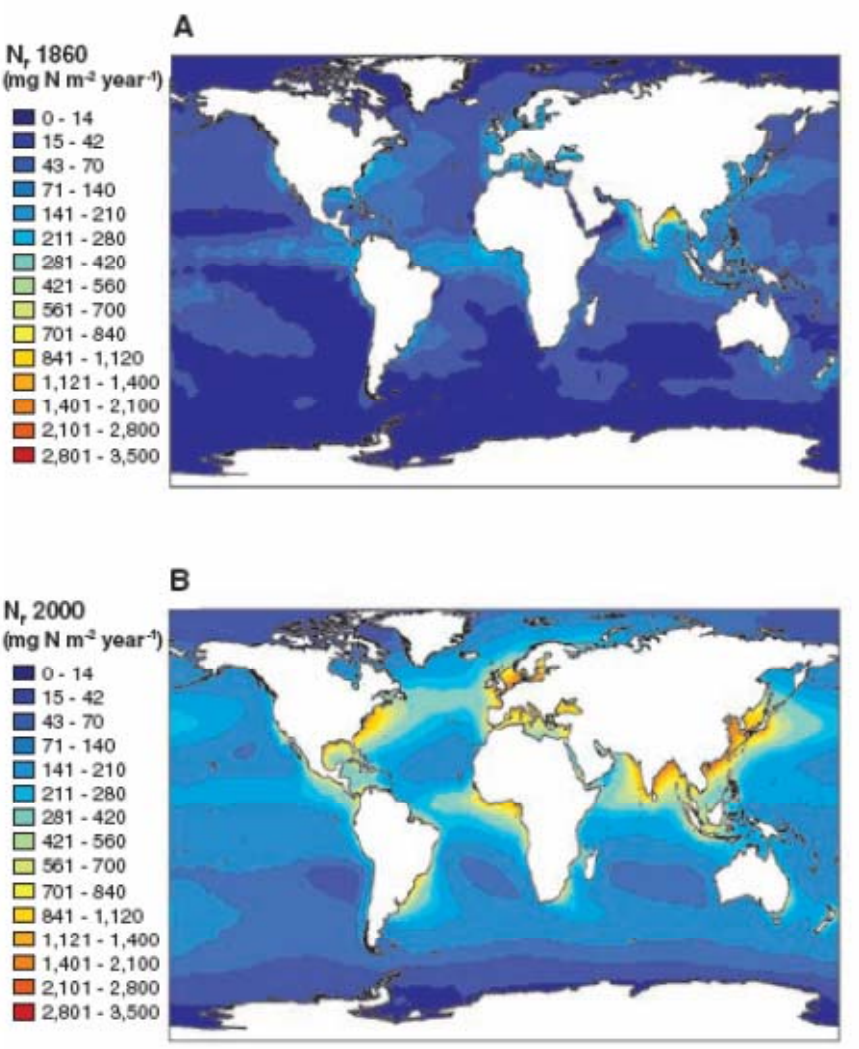

Fig. 1.2. (A) Total atmospheric reactive nitrogen (N_r) deposition in 1860 in mg m^{-2} yr^{-1}. Total atmospheric N_r deposition in 1860 was ~20 Tg N yr^{-1}; of this ~5.7 Tg N yr^{-1} was anthropogenic atmospheric N_r. (B) Total atmospheric N_r deposition in 2000 in mg m^{-2} yr^{-1}. Total atmospheric N_r deposition in 2000 was ~67 Tg N yr^{-1}; of this ~54 Tg N yr^{-1} was anthropogenic atmospheric N_r. The plots are taken from Duce et al. (2008).

References

Baker, A.R., Lesworth, T., Adams, C., Jickells, T.D., Ganzeveld, L., 2010. Estimation of atmospheric nutrient inputs to the Atlantic Ocean from 50°N to 50°S based on large-scale field sampling: fixed nitrogen and dry deposition of phosphorus. Global Biogeochemical Cycles 24(3), GB3006/3001–GB3006/3016.

Baker, A.R., Weston, K., Kelly, S.D., Voss, M., Streu, P., Cape, J.N., 2007. Dry and wet deposition of nutrients from the tropical Atlantic atmosphere: Links to primary productivity and nitrogen fixation. Deep Sea Research Part I 54, 1704–1720.

Benitez-Nelson, C.R., 2000. The biogeochemical cycling of phosphorus in marine systems. Earth-Science Reviews 51, 109–135.

Bergametti, G., Remoudaki, E., Losno, R., Steiner, E., Chatenet, B., Buat-Menard, P., 1992. Source, transport and deposition of atmospheric phosphorus over the northwestern Mediterranean. Journal of Atmospheric Chemistry 14, 501–513.

Brasseur, G.P., Orlando, J.J., Tyndall, G.S., 1999. Atmospheric Chemistry and Global Change, Oxford, New York, pp. 654.

Carrillo, J.H., Hastings, M.G., Sigman, D.M., Huebert, B.J., 2002. Atmospheric deposition of inorganic and organic nitrogen and base cations in Hawaii. Global Biogeochemical Cycles 16, 24/21–24/16.

Clark, H., Kremer, J. N., 2005. Estimating direct and episodic atmospheric nitrogen deposition to a coastal waterbody. Marine Environmental Research 59, 349–366.

Cornell, S.E., Jickells, T.D., Cape, J.N., Rowland, A.P., Duce, R.A., 2003. Organic nitrogen deposition on land and coastal environments: a review of methods and data. Atmospheric Environment 37, 2173–2191.

De Leeuw, G., Cohen, L., Frohn, L.M., Geernaert, G., Hertel, O., Jensen, B., Jickells, T., Klein, L., Kunz, G.J., Lund, S., Moerman, M., Muller, F., Pedersen, B., von Salzen, K., Schlunzen, K.H., Schulz, M., Skjoth, C.A., Sorensen, L.-L., Spokes, L., Tamm, S., Vignati, E., 2001. Atmospheric input of nitrogen into the North Sea: ANICE project overview. Continental Shelf Research 21, 2073–2094.

De Leeuw, G., Skjoth, C.A., Hertel, O., Jickells, T., Spokes, L., Vignati, E., Frohn, L., Frydendall, J., Schulz, M., Tamm, S., Sorensen, L.L., Kunz, G.J., 2003. Deposition of nitrogen into the North Sea. Atmospheric Environment 37, S145–S165.

Dentener, F., Drevet, J., Lamarque, J.F., Bey, I., Eickhout, B., Fiore, A.M., Hauglustaine, D., Horowitz, L.W., Krol, M., Kulshrestha, U.C., Lawrence, M., Galy-Lacaux, C., Rast, S., Shindell, D., Stevenson, D., Van, N.T., Atherton, C., Bell, N., Bergman, D., Butler, T., Cofala, J., Collins, B., Doherty, R., Ellingsen, K., Galloway, J., Gauss, M., Montanaro, V., Muller, J.F., Pitari, G., Rodriguez, J., Sanderson, M., Solmon, F., Strahan, S., Schultz, M., Sudo, K., Szopa, S., Wild, O., 2006. Nitrogen and sulfur deposition on regional and global scales: a multimodel evaluation.

Global Biogeochemical Cycles 20(4), GB4003/4001–GB4003/4021.

Dentener, F. J., Crutzen, P. J., 1994. A three-dimensional model of the global ammonia cycle. Journal of Atmospheric Chemistry 19, 331–369.

Doney, S. C., Mahowald, N., Lima, I., Feely, R. A., Mackenzie, F. T., Lamarque, F., 2007. The impacts of anthropogenic nitrogen and sulfur deposition on ocean acidification and the inorganic carbon system. Proceedings of the National academy of Sciences of the United States of America 104, 14,580–14,585.

Duce, R.A., Liss, P.S., Merrill, J.T., Atlas, E.L., Buat-Menard, P., Hicks, B.B., Miller, J.M., Prospero, J.M., Arimoto, R., et al., 1991. The atmospheric input of trace species to the world ocean. Global Biogeochemical Cycles 5, 193–259.

Duce, R.A., LaRoche, J., Altieri, K., Arrigo, K.R., Baker, A.R., Capone, D.G., Cornell, S., Dentener, F., Galloway, J., Ganeshram, R.S., Geider, R.J., Jickells, T., Kuypers, M.M., Langlois, R., Liss, P.S., Liu, S.M., Middelburg, J.J., Moore, C.M., Nickovic, S., Oschlies, A., Pedersen, T., Prospero, J., Schlitzer, R., Seitzinger, S., Sorensen, L.L., Uematsu, M., Ulloa, O., Voss, M., Ward, B., Zamora, L., 2008. Impacts of Atmospheric Anthropogenic Nitrogen on the Open Ocean. Science 320, 893–897.

Fanning, K. A., 1989. Influence of atmospheric pollution on nutrient limitation in the ocean. Nature 339, 460–463.

Galloway, J.N., 2004. The global nitrogen cycle. Treatise on Geochemistry 8, 557–583.

Gao, Y., Arimoto, R., Zhou, M.Y., Merrill, J.T., Duce, R.A., 1992. Relationships between the dust concentrations over eastern Asia and the remote North Pacific. Journal of Geophysical Research—Atmospheres 97, 9867–9872.

Gilbert, P.M., Garside, C., Fuhrman, J.A., Roman, M.R., 1991. Time-dependent coupling of inorganic and organic nitrogen uptake and regeneration in the plume of the Chesapeake Bay estuary and its regulation by large heterotrophs. Limnology and Oceanography 36, 895–909.

Graham, W.F., Duce, R.A., 1979. Atmospheric pathways of the phosphorus cycle. Geochimica et Cosmochimica Acta 43, 1195–1208.

Graham, W.F., Duce, R.A., 1982. The atmospheric transport of phosphorus to the western North Atlantic. Atmospheric Environment (1967-1989) 16, 1089–1097.

Grubber, N., Galloway, J.N., 2008. An Earth-system perspective of the global nitrogen cycle. Nature 451, 293–296.

Herut, B., Krom, M.D., Pan, G., Mortimer, R., 1999. Atmospheric input of nitrogen and phosphorus to the Southeast Mediterranean: sources, fluxes, and possible impact. Limnology and Oceanography 44, 1683–1692.

Jickells, T., 1995. Atmospheric inputs of metals and nutrients to the oceans: their magnitude and effects. Marine Chemistry 48, 199–214.

Krishnamurthy, A., Moore, J.K., Mahowald, N., Luo, C., Zender, C.S., 2010. Impacts of atmospheric nutrient inputs on marine biogeochemistry. Journal of Geophysical Research—Biogeosciences 115, G01006/01001–G01006/01013.

Levy, H., Moxim, W. J., 1987. Fate of US and Canadian combustion nitrogen emissions. Nature 328, 414–416.

Mahowald, N.M., Artaxo, P., Baker, A.R., Jickells, T.D., Okin, G.S., Randerson, J.T., Townsend, A.R., 2005. Impacts of biomass burning emissions and land use change on Amazonian atmospheric phosphorus cycling and deposition. Global Biogeochemical Cycles 19, GB4030/4031–GB4030/4015.

Mahowald, N., Jickells, T.D., Baker, A.R., Artaxo, P., Benitez-Nelson, C.R., Bergametti, G., Bond, T.C., Chen, Y., Cohen, D.D., Herut, B., Kubilay, N., Losno, R., Luo, C., Maenhaut, W., McGee, K.A., Okin, G.S., Siefert, R.L., Tsukuda, S., 2008. Global distribution of atmospheric phosphorus sources, concentrations and deposition rates, and anthropogenic impacts. Global Biogeochemical Cycles 22, GB4026/4021–GB4026/4019.

Matsumoto, K., Minami, H., Uyama, Y., Uematsu, M., 2009. Size partitioning of particulate inorganic nitrogen species between the fine and coarse mode ranges and its implication to their deposition on the surface ocean. Atmospheric Environment 43(28), 4259–4265.

Nakamura, T., Matsumoto, K., Uematsu, M., 2005. Chemical characteristics of aerosols transported from Asia to the East China Sea: an evaluation of anthropogenic combined nitrogen deposition in autumn. Atmospheric Environment 39, 1749–1758.

Naqvi, S. W. A., Jayakumar, D. A., Narvekar, P. V., Naik, H., Sarma, V. V. S. S., D'Souza, W., Joseph, S., George, M. D., 2000. Increased marine production of N_2O due to intensifying anoxia on the Indian continental shelf. Nature 408, 346– 349.

Nevison, C. D., Lueker, T., Weiss, R. F., 2004. Quantifying the nitrous oxide source from coastal upwelling. Global Biogeochemical Cycles 18, GB1018–GB1034.

Paerl, H.W., 1985. Enhancement of marine primary production by nitrogen-enriched acid rain. Nature 315, 747–749.

Paerl, H.W., 1997. Coastal eutrophication and harmful algal blooms: importance of atmospheric deposition and groundwater as "new" nitrogen and other nutrient sources. Limnology and Oceanography 42, 1154–1165.

Prospero, J.M., Barrett, K., Church, T., Dentener, F., Duce, R.A., Galloway, J.N., Levy, H., II, Moody, J., Quinn, P., 1996. Atmospheric deposition of nutrients to the North Atlantic basin. Biogeochemistry 35, 27–73.

Pryor, S.C., Barthelmie, R.J., 2000. Particle dry deposition to water surfaces: processes and consequences. Marine Pollution Bulletin 41, 220–231.

Rolff, C., Elmgren, R., Voss, M., 2008. Deposition of nitrogen and phosphorus on the Baltic Sea:

seasonal patterns and nitrogen isotope composition. Biogeosciences 5, 1657–1667.

Sandroni, V., Raimbault, P., Migon, C., Garcia, N., Gouze, E., 2007. Dry atmospheric deposition and diazotrophy as sources of new nitrogen to northwestern Mediterranean oligotrophic surface waters. Deep-Sea Research Part I 54, 1859–1870.

Seinfeld, J.H., Pandis, S.N., 1998. Atmospheric Chemistry and Physics: From Air Pollution to Climate Change. John Wiley & Sons, New York, pp. 1326.

Spokes, L.J., Yeatman, S.G., Cornell, S.E., Jickells, T.D., 2000. Nitrogen deposition to the eastern Atlantic Ocean. The importance of south-easterly flow. Tellus, Series B: Chemical and Physical Meteorology 52B, 37–49.

Uematsu, M., Duce, R.A., Prospero, J.M., Chen, L., Merrill, J.T., McDonald, R.L., 1983. Transport of mineral aerosol from Asia over the North Pacific Ocean. Journal of Geophysical Research—Atmospheres 88, 5343–5352.

Uematsu, M., Hattori, H., Nakamura, T., Narita, Y., Jung, J., Matsumoto, K., Nakaguchi, Y., Dileep Kumar, M., 2010. Atmospheric transport and deposition of anthropogenic substances from the Asia to the East China Sea. Marine Chemistry 120, 108–115.

Uno, I., Uematsu, M., Hara, Y., He, Y.J., Ohara, T., Mori, A., Kamaya, T., Murano, K., Sadanaga, Y., Bandow, H., 2007. Numerical study of the atmospheric input of anthropogenic total nitrate to the marginal seas in the western North Pacific region. Geophysical Research Letters 34, L17817–L17822.

2. Methods

2.1. Sample collection

2.1.1. Aerosols

Aerosol samples were collected between 48°N and 55°S during three cruises conducted over the North and South Pacific. The first cruise, KH-08-2, was carried out over the subarctic (Leg 1, 29 July–19 August 2008) and subtropical (Leg 2, 23 August–17 September 2008) western North Pacific aboard R/V *Hakuho Maru* (Fig. 2.1). The second cruise, MR08-06, sailed from Mutsu, Japan to Valparaiso, Chile (15 January–8 April 2009) aboard R/V *Mirai* (Fig. 2.2). During this cruise, aerosol sampling could not be carried out on board heading to southeast between 15 January and 21 January because of influence of strong westerly winds (i.e., the true wind speed was faster than the ship's). The third cruise, KT-09-5 (R/V *Tansei Maru*, 1 May–6 May 2009), was conducted over the semi-pelagic western North Pacific (Fig. 2.3).

During the KH-08-2 and MR08-06 cruises, a high-volume (13 m^3 h^{-1}) virtual impactor air sampler (AS-9, Kimoto Electric Co., Ltd.) was used to collect marine aerosols on a Teflon filter (PF040, 90 mm in diameter, Advantec) for major ionic, inorganic N (NH_4^+ and NO_3^-) species. For the KT-09-5 cruise, a high-volume (11 m^3 h^{-1}) virtual impactor air sampler (AS-900, Kimoto Electric Co., Ltd.) was used to collect marine aerosols on a pre-combusted (at 550°C for 6 h) quartz fiber filter (2500QAT-UP, 90 mm in diameter, PALLFLEX Products Co.). These aerosol samplers allowed to collect fine (D < 2.5 μm) and coarse modes (D > 2.5 μm) aerosols on the same filters (Fig. 2.4) since an inertial force was used to separate atmospheric aerosols according to their aerodynamic diameters (Nakamura et al., 2005).

Prior to use, the filter holders were soaked in detergent (Contaminon B, Wako Pure Chemical Industries) for 24 h to remove organic impurities, then soaked in 1N hydrochloric acid (HCl) for 24 h, then rinsed at least three times with Milli-Q water (>18 MΩ cm^{-1}; Millipore Co.) and finally dried. The Teflon and pre-combusted quartz fiber filters were loaded into the pre-cleaned filter holders under clean (laminar flow) conditions before sampling. In order to collect the enough amount of sample for chemical analysis, aerosol sampling was carried out longer in the open ocean (i.e., the KH-08-2 and MR08-06 cruises) than in the semi-pelagic western North Pacific (i.e., the KT-09-5 cruise). Total aerosol sampling time for the KH-08-2, MR08-06 and KT-09-5 cruises were approximately 1–3 days, 3–5 days and 12–24 h, representing total sampling air volume of 310–930 m^3, 930–1500 m^3 and 130–270 m^3, respectively. The aerosol samplers were put on the front of the upper deck (17 m above sea level for R/V *Hakuho Maru*, 20 m for R/V *Mirai* and 8 m for R/V *Tansei Maru*) of the ship. A wind-sector controller was used to avoid contamination from ship's exhaust during the aerosol sampling. The wind-sector controller system was configured to allow collection of ambient aerosol samples only when the relative wind

directions were within plus or minus 100° relative to the ship's bow and the relative wind speeds were over 1 m s^{-1} during the cruises.

During three cruises, a total of 45 aerosol samples were collected; of these 22 samples were collected from the KH-08-2 cruise, 13 samples from the MR08-06 cruise and 10 samples from the KT-09-5 cruise. When one sampling interval was completed, the holder with the aerosol sample filter was sealed in a polyethylene plastic bag immediately. After sampling, the filter was stored in a freezer at –24ºC for chemical analyses. Deployment blanks (n = 10) were obtained by placing the Teflon and quartz fiber filters in aerosol samplers for 5 min on idle systems (i.e., no airflow through the filters) and processed as other aerosol samples.

During the KH-08-2 and MR08-06 cruises, particle number densities were measured continuously using two different types of optical particle counters (KC-18 and KC-01D, Rion Co., Inc). The KC-18 measured particle number densities in a smaller size range (0.1–0.5 μm in diameter) and the KC-01D in a larger size range (0.3–5.0 μm in diameter). During the KT-09-5 cruise, an optical particle counter, KR-12A, (Rion Co., Inc., D > 0.3, 0.5, 0.7, 1.0, 2.0 and 5.0 μm) was used. These instruments were placed in a watertight aluminum box installed on the front of the upper deck (17 m above sea level for R/V *Hakuho Maru*, 20 m for R/V *Mirai* and 8 m for R/V *Tansei Maru*) of the ship (Sasakawa et al., 2003). Meteorological parameters (i.e., wind speed, wind direction, air temperature, sea temperature, dew point, and relative humidity) were continuously monitored by weather monitoring systems equipped on the research vessels.

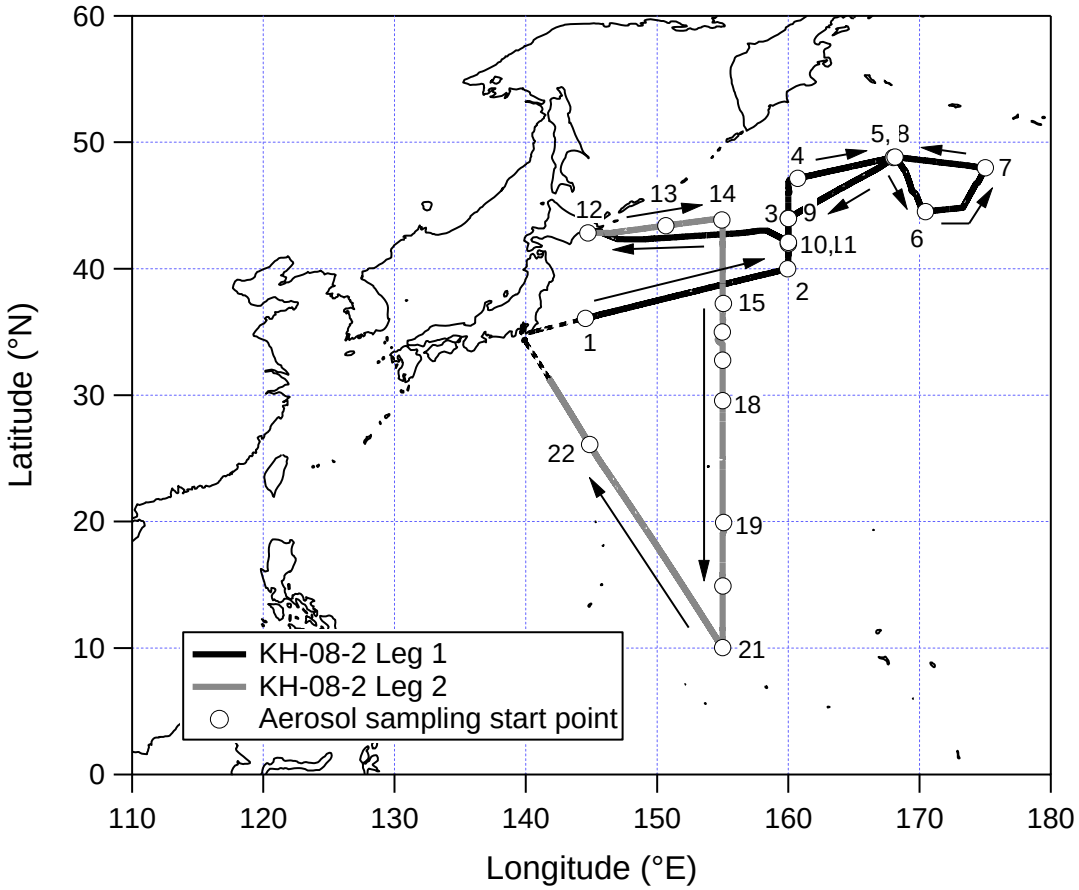

Fig 2.1. Cruise track of the KH-08-2 cruise and aerosol sampling locations. Black and gray lines indicate the cruise tracks of Leg 1 and Leg 2, respectively. White circles and numbers indicate the start point of sampling and sample number of each sample, respectively. Each aerosol sampling start point represents the end of the previous sampling period. Dotted line indicates that no aerosol sampling was conducted.

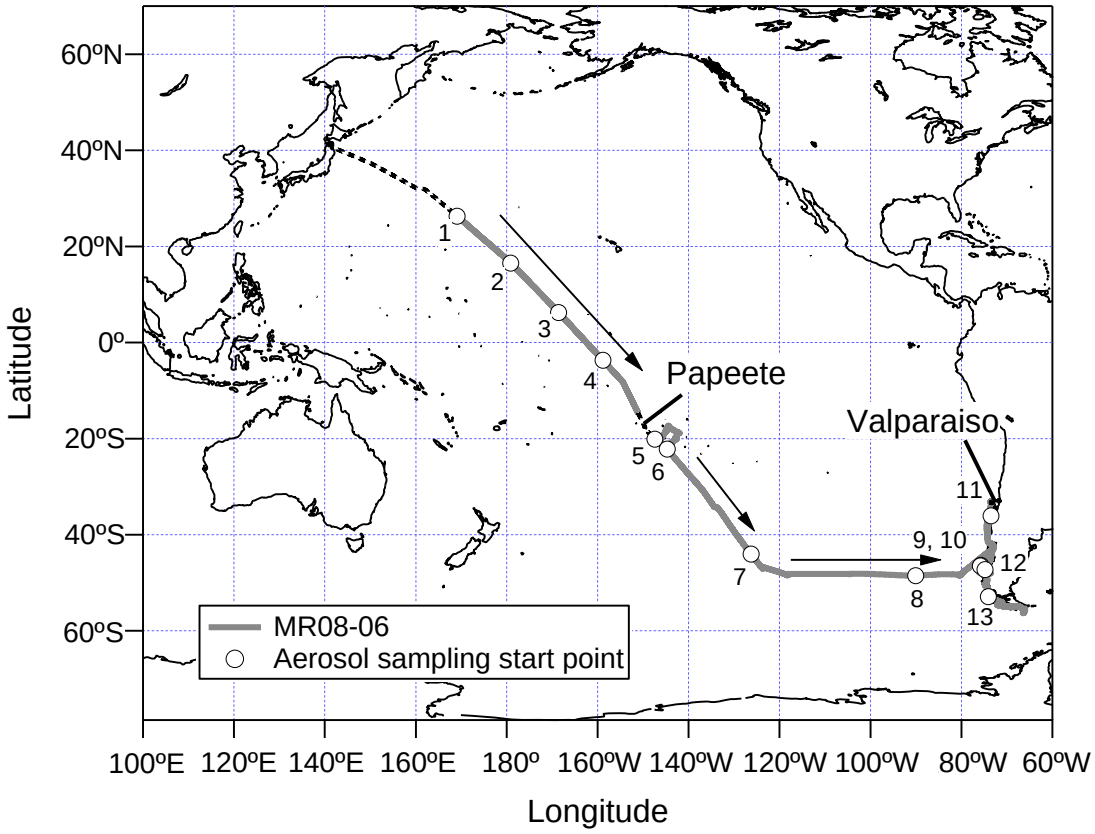

Fig 2.2. Cruise track of the MR08-06 cruise and aerosol sampling locations. White circles and numbers indicate the start point of sampling and sample number of each sample, respectively. Each aerosol sampling start point represents the end of the previous sampling period. Dotted line indicates that no aerosol sampling was conducted.

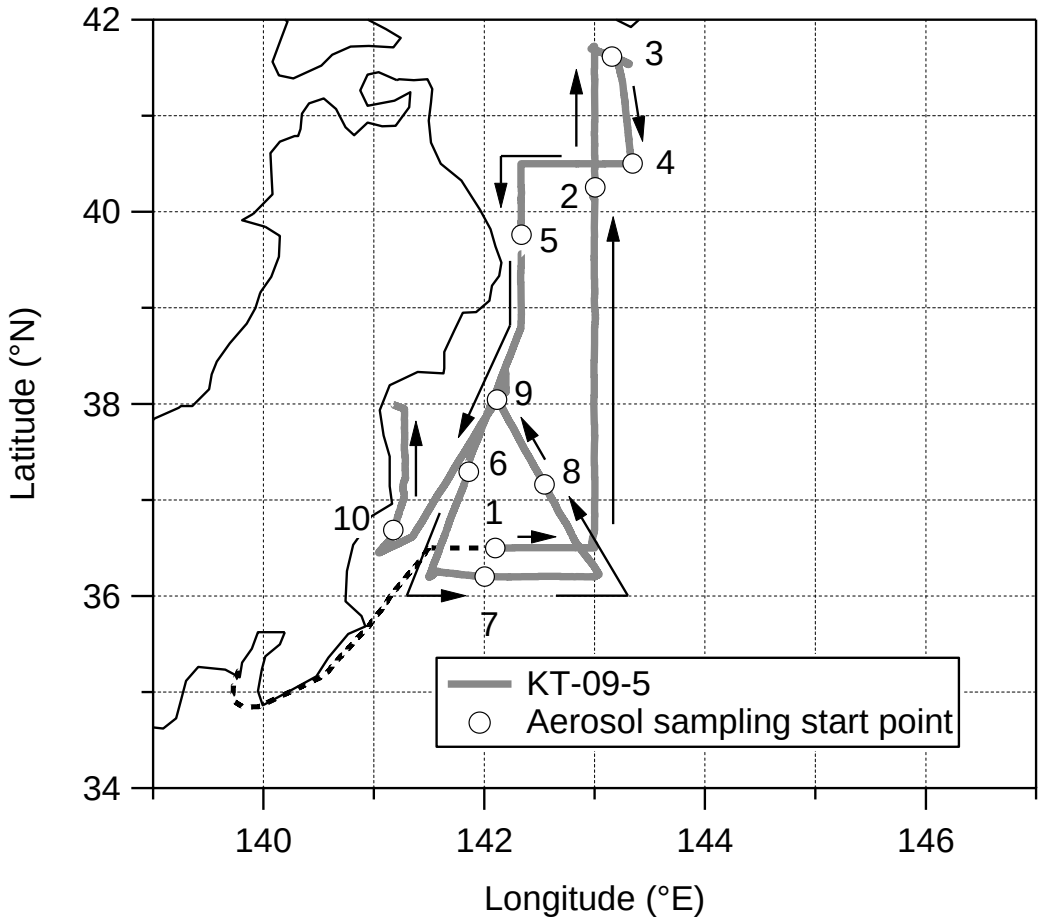

Fig 2.3. Cruise track of the KT-09-5 cruise and aerosol sampling locations. White circles and numbers indicate the start point of sampling and sample number of each sample, respectively. Each sampling starting point represents the end of the previous sampling period. Dotted line indicates that no aerosol sampling was conducted.

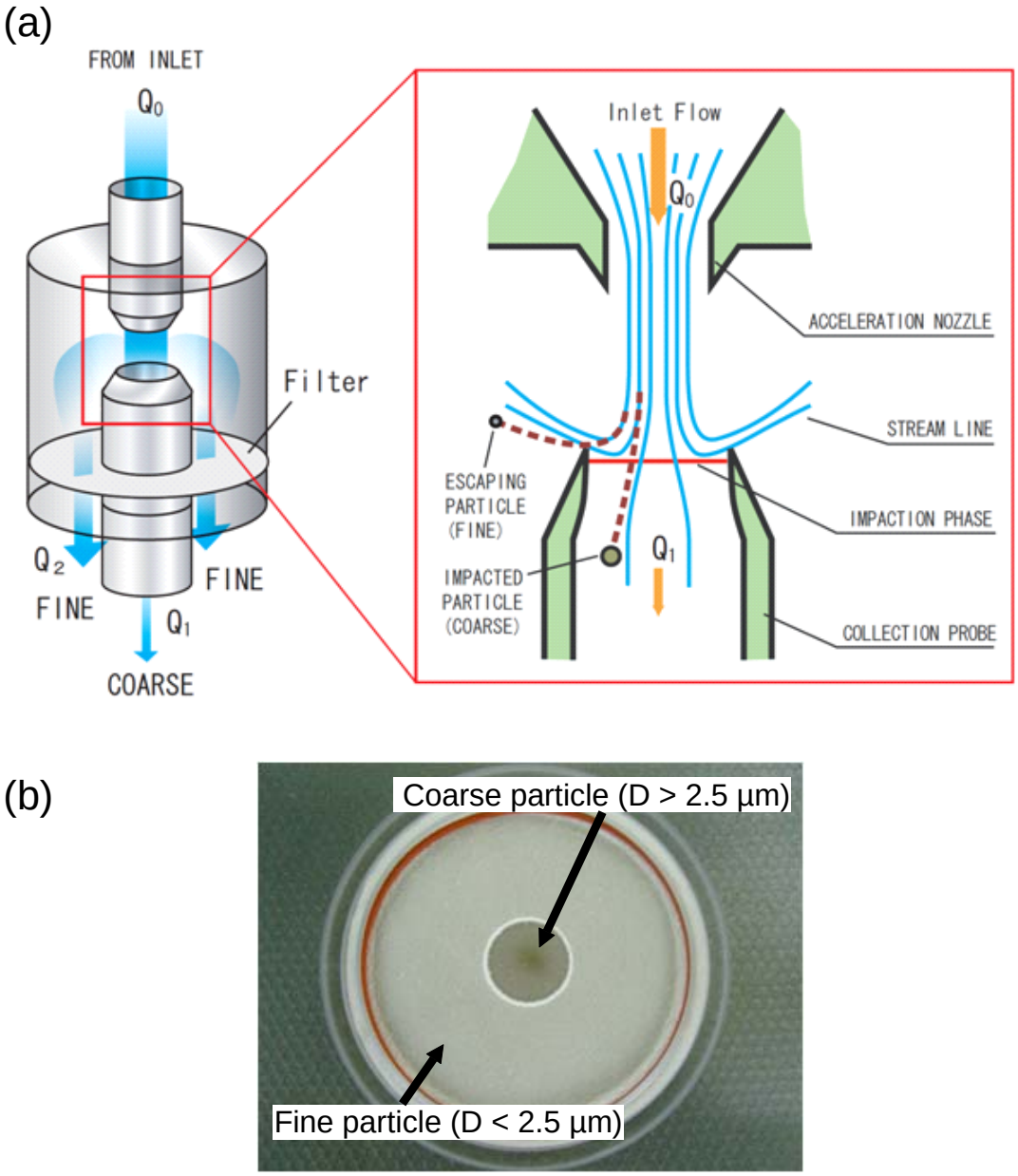

Fig 2.4. (a) Schematic diagram of high-volume virtual impactor air sampler. (b) Photograph of the collected filter containing atmospheric aerosols during the KT-09-5 cruise. The aerosol sampler allows differential aerosol collection between fine (D < 2.5 µm; the outer part) and coarse (D > 2.5 µm; the inner part) fractions on the same filter according to their aerodynamic diameters.

2.1.2. Rainwater

Rainwater sampling was conducted on an event basis during the KH-08-2 (Fig. 2.5) and MR08-06 cruises (Fig. 2.6); no rain occurred during the KT-09-5 cruise. Rain samples were collected with a 36.5 cm diameter polyethylene funnel fitted to a 500 ml polyethylene bottle. Both the funnel and the bottle were first soaked in the detergent for 24 h to remove organic impurities, then soaked in 1N HCl for 24 h, then rinsed at least three times with Milli-Q water (>18 MΩ cm^{-1}; Millipore Co.) and finally dried prior to deployment. The rain sampler was put on the front of the upper deck (17 m above sea level for R/V *Hakuho Maru*, 20 m for R/V *Mirai*) of the ship. The rain sampler was opened just before or as soon as possible after precipitation. After collection, the rain sampler was washed thoroughly with Milli-Q water and closed.

A total of 32 rainwater samples were collected during two cruises; of these 17 samples were collected from the KH-08-2 cruise and 15 samples from the MR08-06 cruise. The rainwater samples were immediately separated into three aliquots. Two of the aliquots were used for measurements of pH (Model 290A, Orion) and conductivity (Model 115, Orion), respectively. When the amount of precipitation was less than 10 ml, pH and conductivity were not measured. The pH and conductivity meters were calibrated before each measurement. Standard pH 4.01 and 7.00 buffer (Thermo Scientific) and conductivity/total dissolved solids (TDS) standard (1413 µS cm^{-1}, Thermo Scientific) solutions were used for calibrations of the pH and conductivity meters, respectively. As the third aliquot, remaining rainwater was filtered through a pre-combusted (at 550ºC for 6 h) glass fiber filter (GF/F, 47 mm in diameter, Whatman). The filtrates and the GF/F filters were sealed in 100 ml high-density polyethylene (HDPE) bottles and in sterile petri dishes (PD-47A, 47 mm in diameter, Advantec), respectively, and stored in a freezer at –24ºC for chemical analyses. Procedural blanks (n = 8) for rainwater were collected by pouring 100 ml of Milli-Q water through the clean funnel-bottle assembly. The procedural blanks were also treated as rainwater samples.

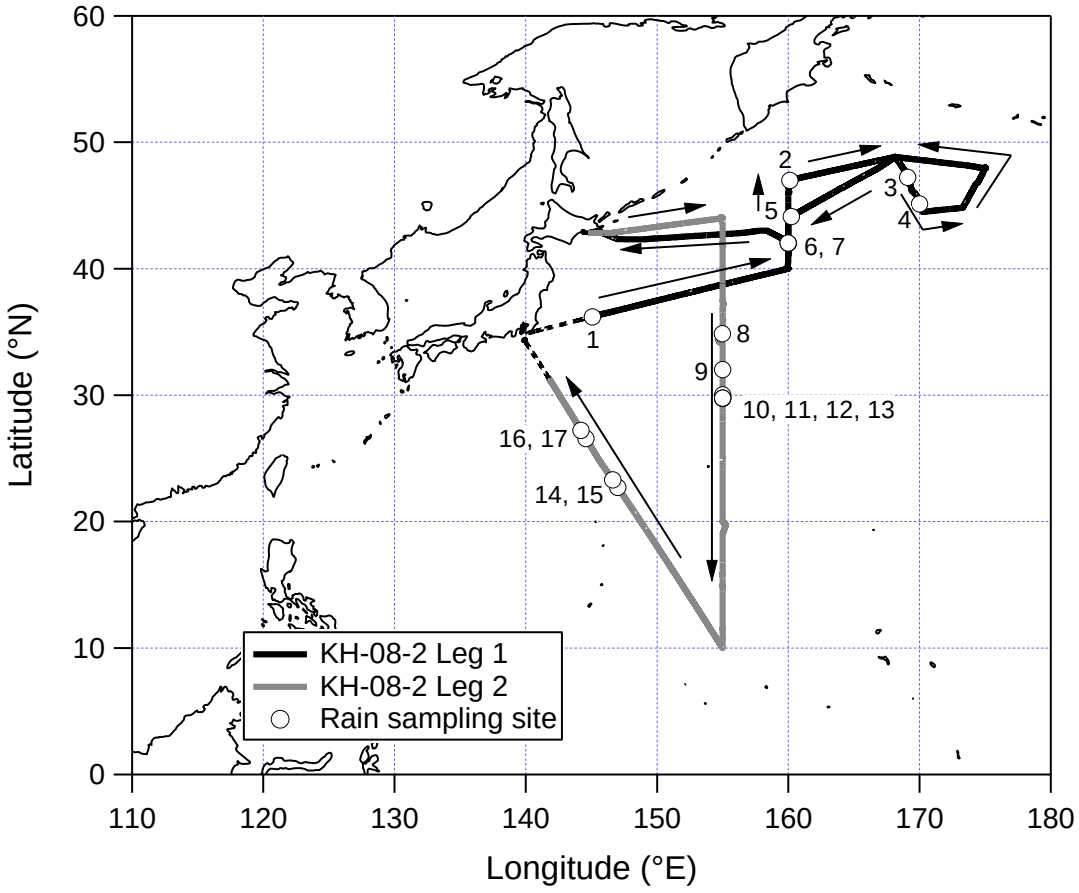

Fig 2.5. Cruise track of the KH-08-2 cruise and rainwater sampling locations. Black and gray lines indicate the cruise tracks of Leg 1 and Leg 2, respectively. White circles and numbers indicate the rainwater sampling sites and sample number, respectively.

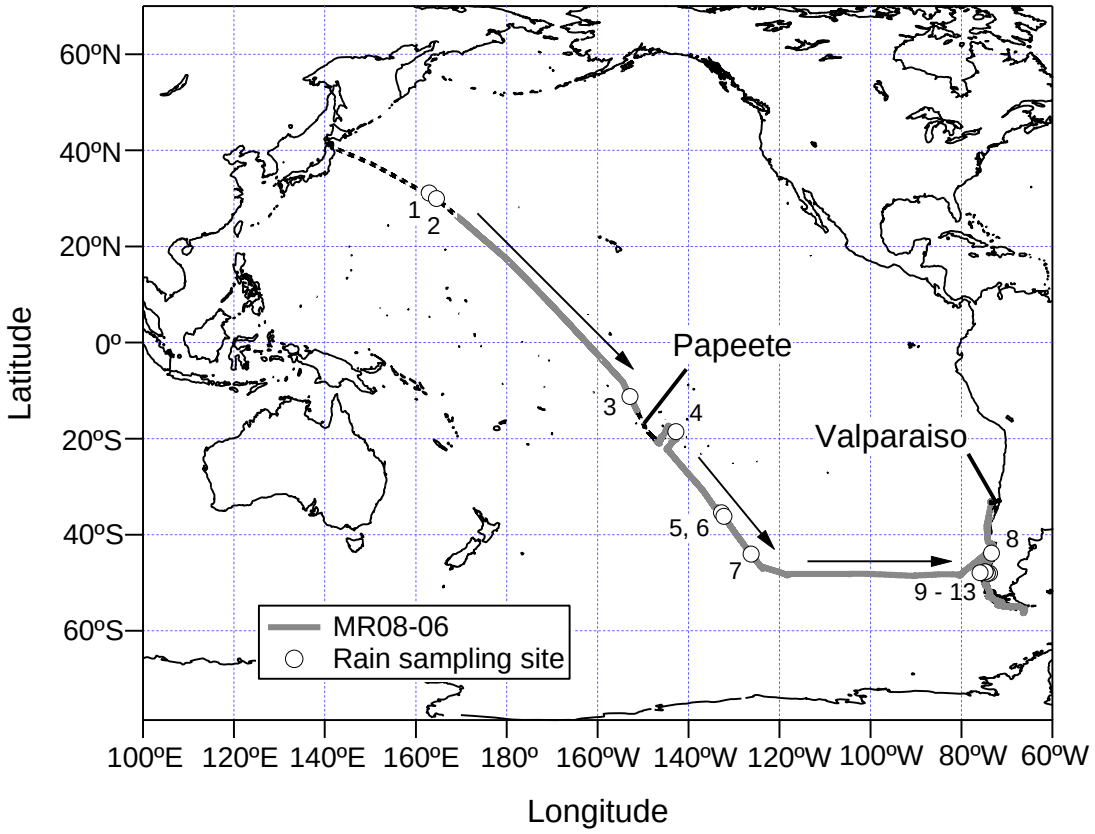

Fig 2.6. Cruise track of the MR08-06 cruise and rainwater sampling locations. White circles and numbers indicate the rainwater sampling sites and sample number, respectively.

2.1.3. Sea fog water

Sea fog water sampling was conducted on an event basis during the KH-08-2 cruise. Sea fog events occurred during the only Leg 1 of this cruise (Fig. 2.7). A fog water sampler (FWG-400, Usui Co. Inc.) was used to collect fog water and put on the front of the upper deck (17 m above sea level for R/V *Hakuho Maru*) of the ship. The fog water sampler is composed of a net of Teflon strings (0.5 mm in diameter), a net holder and a 500 ml low-density polyethylene (LDPE) bottle. Prior to deployment, both the net and the bottle were first soaked in the detergent for 24 h to remove organic impurities, then soaked in a 1N HCl for 24 h, then rinsed at least three times with Milli-Q water (>18 MΩ cm^{-1}; Millipore Co.) and finally dried. The net of Teflon strings and the LDPE bottle were set only during the sea fog occurrence and put back to be washed with Milli-Q water. When the ship sails the fog occurrence zone, fog droplets collide with the strings and drop along the strings into the 500 ml LDPE bottle beneath the strings (Sasakawa et al., 2003).

A total of 16 sea fog water samples were collected during the Leg 1 of KH-08-2 cruise. After collection, sea fog water samples were immediately separated into three aliquots. Two of the aliquots were used for measurements of pH (Model 290A, ORION) and conductivity (Model 115, ORION), respectively. The pH and conductivity meters were calibrated before each measurement. Standard pH 4.01 and 7.00 buffer (Thermo Scientific) and conductivity/total dissolved solids (TDS) standard (1413 μS cm^{-1}, Thermo Scientific) solutions were used for calibrations of the pH and conductivity meters, respectively. As the third aliquot, remaining fog water was filtered through a pre-combusted (at 550ºC for 6 h) glass fiber filter (GF/F, 47 mm in diameter, Whatman). The filtrates and the GF/F filters were sealed in 100 ml high-density polyethylene (HDPE) bottles and in sterile petri dishes (PD-47A, 47 mm in diameter, Advantec), respectively, and stored in the freezer at –24ºC for chemical analyses. Procedural blanks (n = 5) for sea fog water samples were collected by pouring 100 ml of Milli-Q water through the clean net-bottle assembly. The procedural blanks were also treated as fog water samples.

Size distributions of fog droplets were measured with a fog monitor (model FM-100; Droplet Measurement Technologies). The fog monitor detects the number and size of individual fog droplets with a diameter from 2 μm up to 50 μm by the forward scattering principle, and can classify droplets in up to 40 size classes (Burkard et al., 2002). Liquid water content (LWC) for each of the 40 droplet size classes was computed based on an idealized mean volume of spherical droplets with aerodynamic diameter. Total LWC was obtained from the sum of LWC for all size.

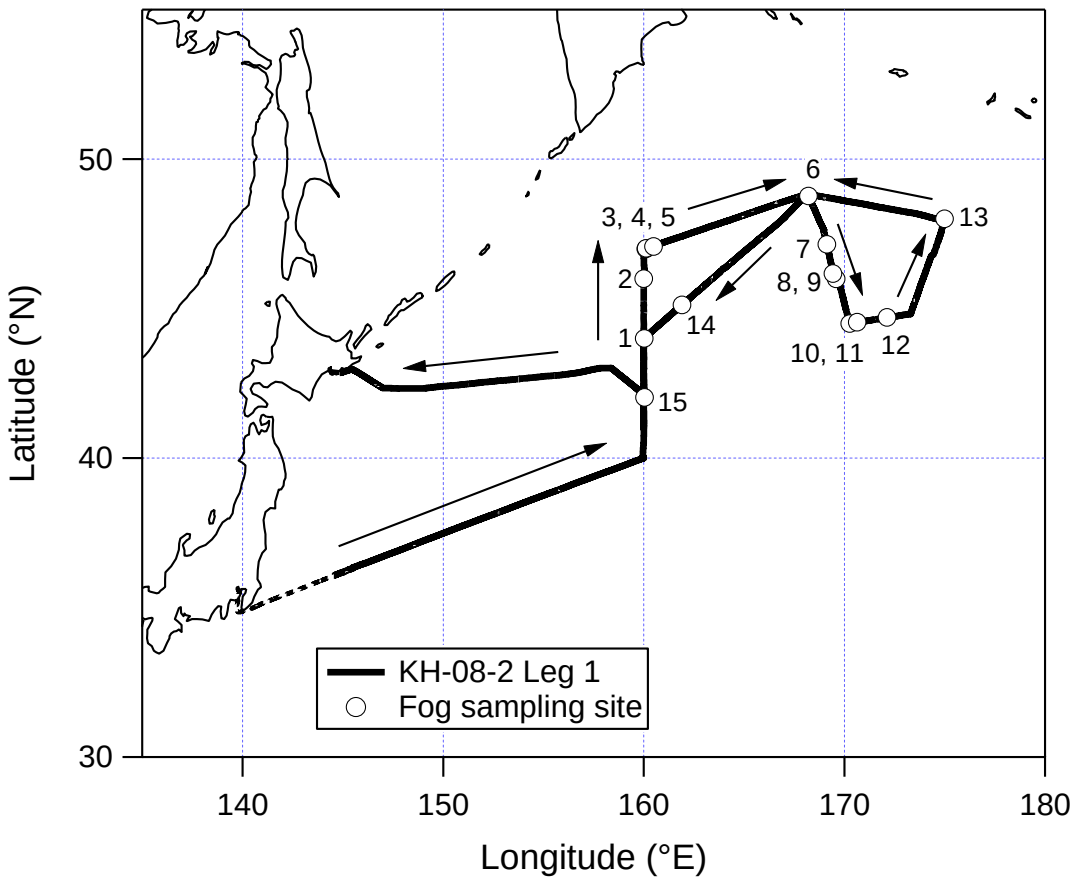

Fig 2.7. Cruise track of Leg 1 of the KH-08-2 cruise and fog water sampling locations. Black line indicates the cruise track of Leg 1. White circles and numbers indicate the fog water sampling sites and sample number, respectively.

2.2. Chemical analysis

The Teflon and quartz fiber filters, on which aerosols were collected, were cut into four equivalent subsamples. The subsamples of Teflon filters for the KH-08-2 and MR08-06 cruises and quartz fiber filters for the KT-09-5 cruise were used to analyze water-soluble inorganic N (NH_4^+ and NO_3^-) and major ionic species.

For each of the analyses described below, procedural blanks were obtained by carrying out identical analysis procedures. These procedural blanks were subtracted from the results for each batch. In addition, concentrations in aerosol extracts were converted into atmospheric concentrations by calculating the total quantity of analyte on each filter, after appropriate blank correction, and dividing by the known volume of air for each sample.

2.2.1. Water-soluble inorganic nitrogen and dissolved inorganic nitrogen

The subsamples of Teflon filters for the KH-08-2 and MR08-06 cruises (or quartz fiber filters for the KT-09-5 cruise) were placed in acid-cleaned polypropylene bottles with the dusty side facing up. Fifty ml of Milli-Q water (>18 MΩ cm^{-1}; Millipore Co.) was added to the bottles, and the bottles were covered using polypropylene screw caps. The subsamples were sonicated for 30 min to resuspend the aerosol particles into the solutions. The extraction solutions were then filtered, as were the rain and fog water samples, through 13-mm diameter, 0.45-μm pore-size membrane filters (PTFE syringe filter, Millipore Co.) prior to analysis. The filtrates of aerosol extracts, rain and fog water samples were analyzed by ion chromatography (IC; Dionex-320, Thermo Scientific Dionex) for water-soluble inorganic N in aerosols or dissolved inorganic N in rain and fog water. Nitrate (NO_3^-) was analyzed using an AS17 anion exchange column with an AG17 guard column (Thermo Scientific Dionex). An EG40 eluent generator equipped with an EGC-KOH cartridge was used to produce potassium hydroxide eluent. Ammonium (NH_4^+) was separated and quantified using a CS16 cation exchange column with a CG16 guard column (Thermo Scientific Dionex). A solution of methanesulfonic acid (MSA) served as the eluent. Standard stock solutions for NH_4^+ (in 0.02 mol L^{-1} HNO_3) and NO_3^- (in H_2O) were obtained from Wako Pure Chemical Industries. The instrumental detection limits were 0.10 μM for NO_3^- and 0.17 μM for NH_4^+. The procedural mean blanks of aerosols, rain and fog water for inorganic N were 0.16 ± 0.093, 0.12 ± 0.078, 0.11 ± 0.10 μM for NO_3^- and 3.4 ± 0.16, 2.3 ± 0.15, 2.2 ± 0.43 μM for NH_4^+, respectively. The detection limits calculated as three times of the standard deviation of the procedural blanks of aerosols, rain and fog water were 0.28, 0.23, 0.30 μM for NO_3^-, and 0.48, 0.45, 1.3 μM for NH_4^+, respectively. The relative standard deviations of the NO_3^- and NH_4^+ analyses for reproducibility tests were less than 3% and 6%, respectively.

2.2.2. Major ionic species

The subsamples of Teflon filters (quartz fiber filters for the KT-09-5 cruise) were ultrasonically extracted and filtered, as were the rain and fog water samples, with the membrane filters. The filtrates of aerosol extracts, rain and fog water were analyzed by ion chromatography (IC; Dionex-320, Thermo Scientific Dionex) for anions (F^-, Cl^-, Br^-, MSA and SO_4^{2-}) and cations (Na^+, K^+, Mg^{2+}, and Ca^{2+}). Anions were analyzed using an AS17 anion exchange column with an AG17 guard column (Thermo Scientific Dionex). An EG40 eluent generator equipped with an EGC-KOH cartridge was used to produce potassium hydroxide eluent. Cations were separated and quantified using a CS16 cation exchange column with a CG16 guard column (Thermo Scientific Dionex). A solution of methanesulfonic acid (MSA) served as the eluent. Standard stock solutions for cations (in 0.02 mol L^{-1} HNO_3) and anions (in H_2O) were obtained from Wako Pure Chemical Industries. For MSA, standard solution was prepared by diluting MSA (98%, Wako Pure Chemical Industries). The relative standard deviations of both the anions and cations analyses for reproducibility tests were less than 10%.

The instrumental detection limits were 0.066 μM for F^-, 0.035 μM for Cl^-, 0.078 μM for Br^-, 0.031 μM for MSA, 0.065 μM for SO_4^{2-}, 0.11 μM for Na^+, 0.16 μM for K^+, 0.15 μM for Mg^{2+} and 0.16 μM for Ca^{2+}. The procedural mean blanks of aerosols for ionic components were: F^- 0.17 ± 0.022 μM, Cl^-: 2.1 ± 0.15 μM, SO_4^{2-}: 1.1 ± 0.040 μM, Na^+: 3.5 ± 0.96 μM, K^+: 0.22 ± 0.015 μM, Mg^{2+}: 0.15 ± 0.026 μM, Ca^{2+}: 0.094 ± 0.0020 μM. The procedural mean blanks of aerosols for Br^- and MSA were below the instrumental detection limits. The detection limits calculated as three times of the standard deviations of the procedural blanks of aerosols for ionic components were 0.066 μM for F^-, 0.45 μM for Cl^-, 0.12 μM for SO_4^{2-}, 2.9 μM for Na^+, 0.045 μM for K^+, 0.078 μM for Mg^{2+} and 0.0060 μM for Ca^{2+}.

The procedural mean blanks of rain (fog water) for ionic components were 2.2 ± 0.69 (0.10 ± 0.011) μM for F^-, 7.8 ± 1.9 (9.8 ± 3.4) μM for Cl^-, 1.1 ± 0.040 (3.0 ± 0.17) μM for SO_4^{2-}, 5.2 ± 1.3 (7.5 ± 2.5) μM for Na^+, 1.2 ± 0.16 (1.8 ± 0.15) μM for K^+, 2.0 ± 0.23 (1.8 ± 0.20) μM for Mg^{2+} and 0.098 ± 0.011 (1.7 ± 0.13) μM for Ca^{2+}. The procedural mean blanks of rain and fog water for Br^- and MSA were below the instrumental detection limits. The detection limits calculated as three times of the standard deviations of the procedural blanks of rain (fog water) for ionic components were 2.1 (0.033) μM for F^-, 5.7 (10) μM for Cl^-, 0.12 (0.51) μM for SO_4^{2-}, 3.9 (7.5) μM for Na^+, 0.48 (0.45) μM for K^+, 0.69 (0.60) μM for Mg^{2+} and 0.033 (0.39) μM for Ca^{2+}.

Non sea-salt (nss-) concentrations of some ionic components were calculated by subtracting the component's sea-salt-derived (ss-) concentration from its total concentration. In this study, it was assumed that all Na^+ in aerosols, rainwater and sea fog water were derived from sea salt. Contributions from sea-salt were calculated from the Na^+ concentration in aerosols, rainwater or sea fog water using the mole ratio of the component of interest to Na^+ in seawater (Savoie et al., 1987). Uncertainties of non sea-salt ionic components were calculated by standard error propagation methods as mentioned above.

2.3. Backward trajectory analysis

Air mass backward trajectories (AMBTs) provide a better understanding of air flow and long-range transport of aerosols. In particular, AMBTs have been used to identify the origin of primary aerosols collected far away from their source region (Chiapello et al., 1997). In this study, 7-day AMBTs were calculated from the National Oceanic and Atmospheric Administration (NOAA) GDAS (Global Data Assimilation System) database using the Hybrid Single-Particle Lagrangian Integrated Trajectories (HY-SPLIT) model (NOAA Air Resources Laboratory, http://www.arl.noaa.gov/ready/hysplit4.html). AMBTs were performed at 500, 1000, and 1500 m above ground level to represent the airflow trajectories at surface, middle and high altitudes, respectively. Chen and Siefert (2004) reported that atmospheric aerosols may not follow the resulting trajectories because of scavenging processes and gravitational settling; however, the AMBTs provide useful background data on airstreams and the potential origins of the source of the sampled air mass.

References

Burkard, R., Eugster, W., Wrzesinsky, T., Klemm, O., 2002. Vertical divergence of fogwater fluxes above a spruce forest. Atmospheric Research 64, 133–145.

Chen, Y., Siefert, R.L., 2004. Seasonal and spatial distributions and dry deposition fluxes of atmospheric total and labile iron over the tropical and subtropical North Atlantic Ocean. Journal of Geophysical Research—Atmospheres 109, D09305–D09318.

Chiapello, I., Bergametti, G., Chatenet, B., Bousquet, P., Dulac, F., Soares, E.S., 1997. Origins of African dust transported over the northeastern tropical Atlantic. Journal of Geophysical Research—Atmospheres 102, 13701–13709.

Nakamura, T., Matsumoto, K., Uematsu, M., 2005. Chemical characteristics of aerosols transported from Asia to the East China Sea: an evaluation of anthropogenic combined nitrogen deposition in autumn. Atmospheric Environment 39, 1749–1758.

Sasakawa, M., Ooki, A., Uematsu, M., 2003. Aerosol size distribution during sea fog and its scavenge process of chemical substances over the northwestern North Pacific. Journal of Geophysical Research—Atmospheres 108, AAC13/11-AAC13/19.

Savoie, D.L., Prospero, J.M., Nees, R.T., 1987. Nitrate, non-sea-salt sulfate, and mineral aerosol over the northwestern Indian Ocean. Journal of Geophysical Research—Atmospheres 92, 933–942.

3. Characteristics of marine aerosols over the semi-pelagic western North Pacific (KT-09-5)

3.1. Introduction

Atmospheric inputs of nutrients and trace elements are an important consideration in the science of climate change (Zhang et al., 2011). Biogeochemical cycles of atmospheric N and interactions between the atmosphere, the continents, and the ocean are strong sources of feedback in the evolution of climate (Duce et al., 2008; Krishnamurthy et al., 2010). Previous studies have highlighted the significance of the atmosphere as a pathway for transport of nutrients from continents to marine surface waters and their critical role in oceanic biogeochemical cycling (Duce et al., 1991; Prospero et al., 1996; Paerl, 1997).

Considerable effort has been devoted to quantifying the deposition fluxes of atmospheric N and its impact on biogeochemical cycles (Paerl, 1985; Spokes et al., 2000; Carrillo et al., 2002; Duce et al., 2008; Rolff et al., 2008; Krishnamurthy et al., 2010). Although the global flux of N has been simulated in several models (Dentener et al. 2006; Duce et al., 2008), the details of atmospheric depositions in marine recipient environments are still not well understood due to measurement difficulties and thus a lack of data (Zhang et al., 2011).

The western North Pacific Ocean is an important receptacle of mineral particles and anthropogenic substances because of its proximity to the Gobi Desert in Central East Asia and rapid Asian economic growth (Uematsu et al., 1983; Gao et al., 1992; Nakamura et al., 2005; Uno et al., 2007; Uematsu et al., 2010; Zhang et al., 2011). Accordingly, estimating deposition fluxes of atmospheric N and its impacts on biogeochemical cycles over the western North Pacific have become increasingly important. Nevertheless, few studies have been carried out over this region to estimate the deposition fluxes of atmospheric N in marine aerosols. This study therefore aims to (1) investigate general characteristic of atmospheric inorganic N, (2) estimate fractions of atmospheric inorganic N species from specific sources, (3) estimate dry deposition flux of atmospheric inorganic N, and (4) evaluate its impact on the ocean marine ecosystem.

3.2. Variations of major ionic species and particle number density

Concentrations obtained for water-soluble major ionic species are shown in Fig. 3.1. These data show strong variations related to different aerosol sources and this relationship may play a key role in distinguishing potential sources such as sea salt, crustal material, biomass burning, and the combustion of fossil fuel (Wang et al., 2006). In this study, nss-SO_4^{2-}, nss-K^+, nss-Ca^{2+} and Na^+ were used as tracers of fossil fuel combustion, biomass burning, crustal and marine origin, respectively (Gabriel et al., 2002; Kocak et al., 2004).

Mean concentrations of nss-SO_4^{2-}, nss-K^+, nss-Ca^{2+} and Na^+ were 68 ± 21 nmol m^{-3}, 2.5 ± 1.3 nmol m^{-3}, 3.1 ± 1.3 nmol m^{-3} and 62 ± 35 nmol m^{-3}, respectively. Non-sea-salt SO_4^{2-} and nss-K^+ existed predominantly in fine mode, while nss-Ca^{2+} and Na^+ were largely associated with the coarse mode. Mean percentages of total concentrations in the fine mode for these species were: nss-SO_4^{2-} 87%, nss-K^+ 94%, nss-Ca^{2+} 18% and Na^+ 40%. The highest concentrations of nss-SO_4^{2-} and nss-K^+ were observed on the morning of 2 May (sample number 2), and then gradually decreased. The variation trends of nss-SO_4^{2-} and nss-K^+ were also similar, suggesting that they experienced the same transport and removal processes. On the other hand, nss-Ca^{2+} and Na^+ showed different variation trends from those of nss-SO_4^{2-} and nss-K^+. The maximum concentrations of nss-Ca^{2+} and Na^+ were observed on the afternoon of 4 May (sample number 7), under the dominant influence of crustal and oceanic-derived aerosols.

During the cruise, air masses were largely classified into two types. As shown in Fig. 3.2, the first type of air mass originated from the Asian continent and thereafter swept over large regions of the Korean Peninsula and the Japanese Islands, indicating that these air masses were most likely affected by strong anthropogenic and crustal sources (Fig. 3.2a). The second type of air mass originated from Siberia and circulated around the western North Pacific, permitting input of both crustal and marine origin aerosols with relatively little anthropogenic input (Fig. 3.2b).

The temporal variations of particle number densities in the range of 0.3–2.0 μm showed similar trends to those of nss-SO_4^{2-} and nss-K^+ which were predominantly associated with fine mode aerosols, whereas the variation of particle number density with diameters larger than 5.0 μm, was related to the trend of Na^+ (Figs. 3.3 and 3.1). Particle number densities drastically decreased during sea fog events (Fig. 3.3), suggesting that particles with diameters larger than 0.5 μm could act preferentially as condensation nuclei for sea fog droplets and were more efficiently scavenged by sea fog (Sasakawa et al., 2003). The results of water-soluble major ionic species were consistent with those of particle number densities and backward trajectory analyses, indicating that marine aerosols collected during the cruise were influenced by both source and meteorological factors.

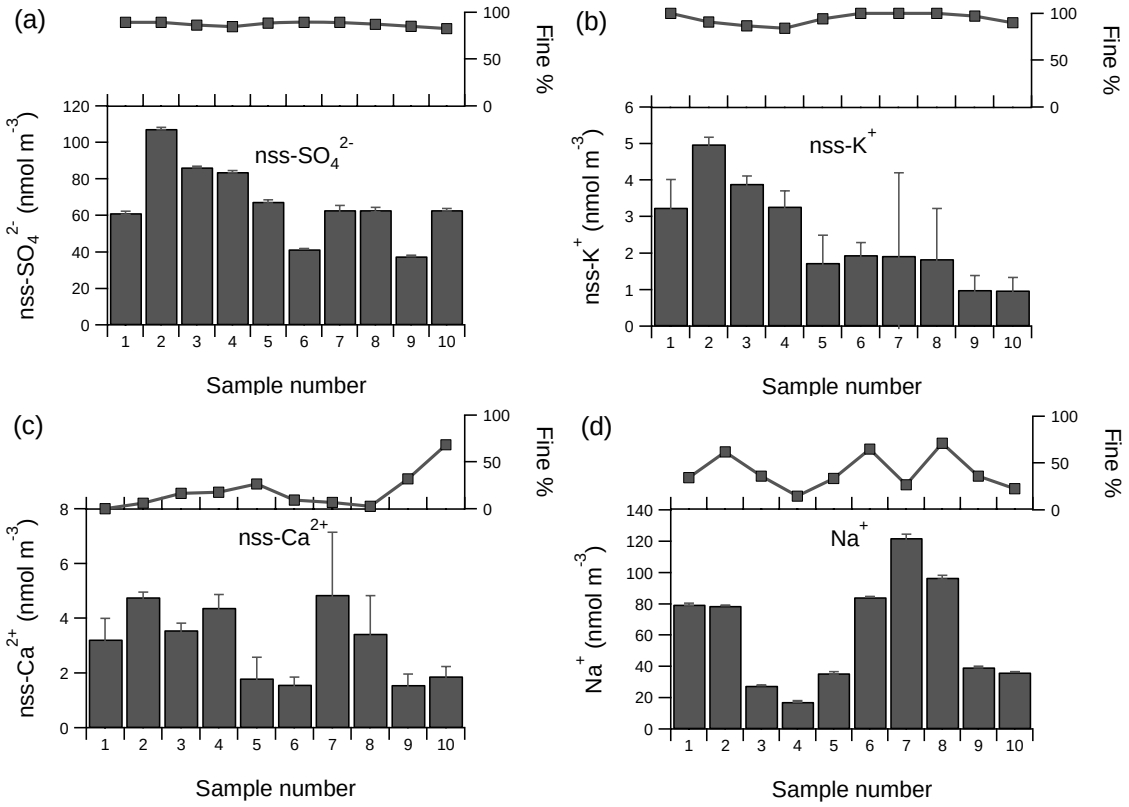

Fig. 3.1. Concentrations of water-soluble (a) nss-SO_4^{2-}, (b) nss-K^+, (c) nss-Ca^{2+} and (d) Na^+ during the KT-09-5 cruise. Upper sections in every panel shows the percentage of each component in fine (D < 2.5 μm) aerosol particles.

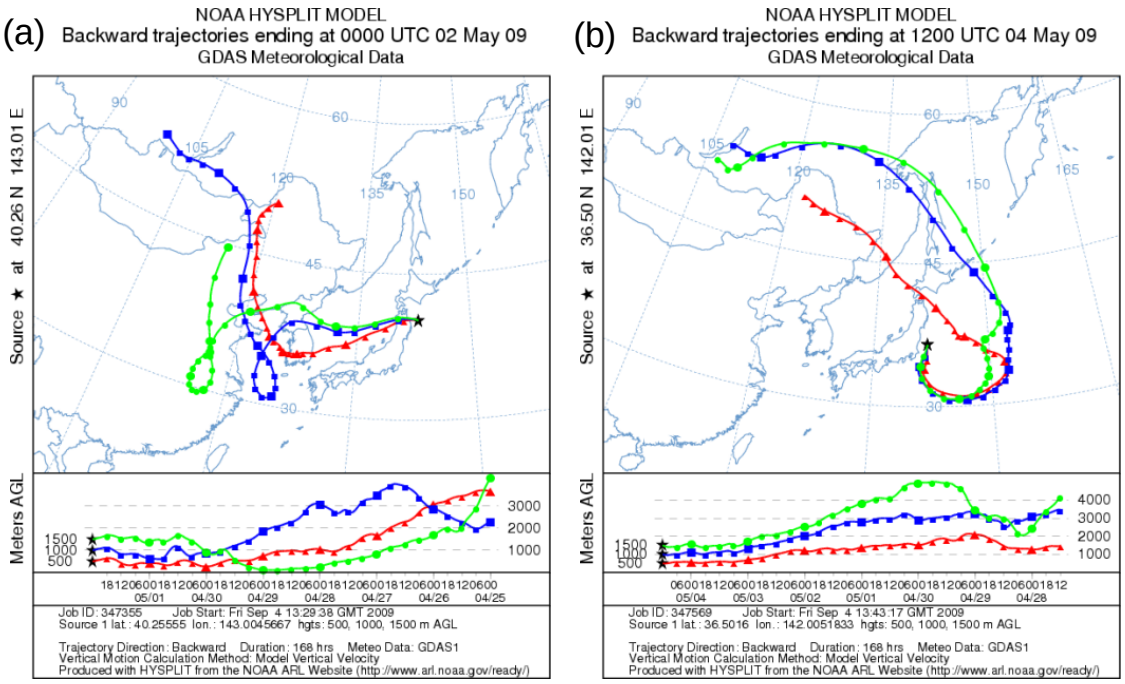

Fig. 3.2. The 168 h (7 days) air mass backward trajectories for starting altitudes of 500, 1000 and 1500 m above ground level (AGL) were calculated from the GDAS database of the National Ocean and Atmospheric Administration (NOAA) and simulated by using the Hybrid Single-Particle Langrangian Integrated Trajectory (HY-SPLIT) model: (a) May 2, 2009; (b) May 4, 2009.

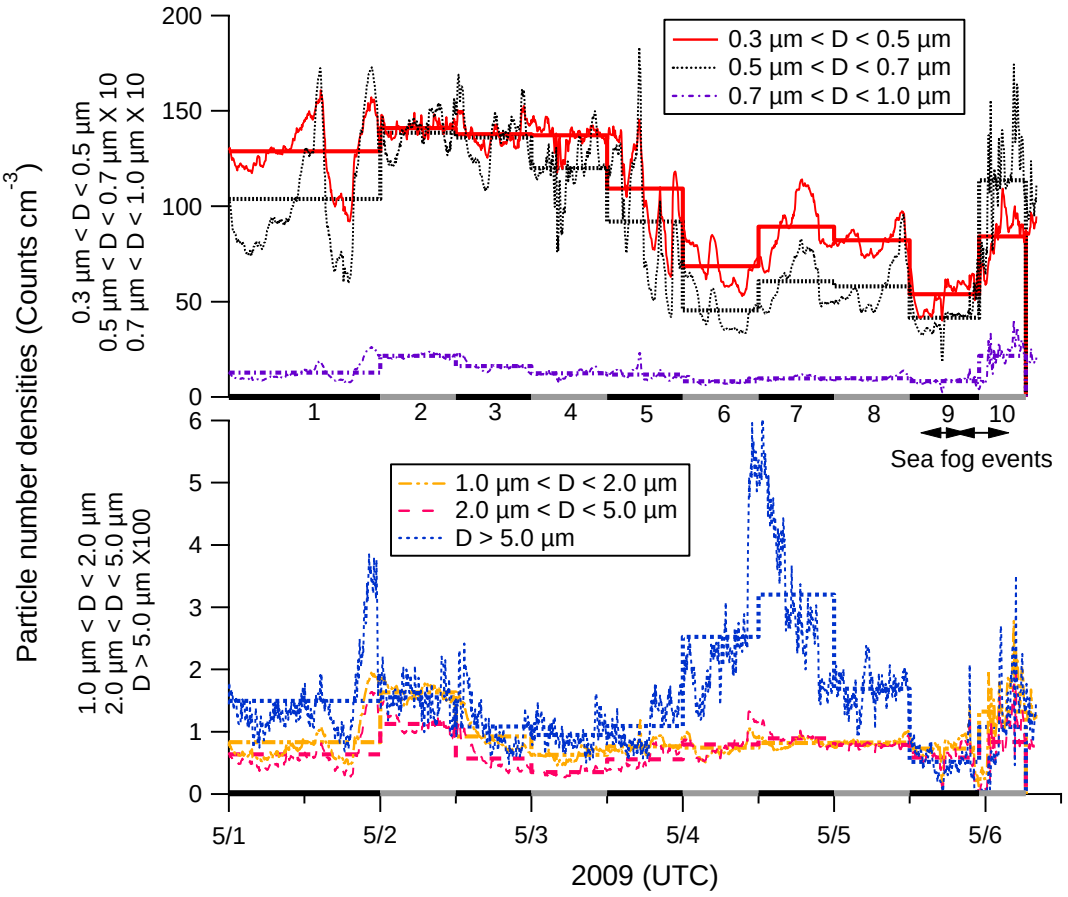

Fig. 3.3. Temporal variations (thin lines) and mean values (bold lines) of particle number densities along the cruise track for aerosols in six size groups. Horizontal gray and black bars and numbers indicate aerosol sampling duration and aerosol sample number of each sample, respectively. Arrows indicate occurrence of sea fog events.

3.3. General characteristics of atmospheric particulate N species

Inorganic N in aerosols collected over the semi-pelagic western North Pacific Ocean was composed of ~77% NH_4^+ and 23% NO_3^- (median values for all data). Concentrations of NH_4^+ and NO_3^- varied from 59–182 nmol m^{-3} and 13–86 nmol m^{-3}, with averages of 117 ± 42 nmol m^{-3} and 36 ± 22 nmol m^{-3}, respectively (Fig. 3.4 and Table 3.1). The NH_4^+ and NO_3^- concentrations were about 29% and 72% lower than the results of Nakamura et al. (2005), who reported that mean concentrations of NH_4^+ and NO_3^- in marine aerosols collected over the East China Sea from 26 September 2002–9 October 2002, were 164 ± 136 nmol m^{-3} and 129 ± 86 nmol m^{-3}, respectively, reflecting the strong influence of terrestrial-derived NH_4^+ and NO_3^- in the East China Sea.

Nitrate mainly existed in coarse mode aerosols, while NH_4^+ was largely associated with the fine mode. Mean percentages of total aerosol concentration in the fine mode for NO_3^- and NH_4^+ were ~45% and ~90%, respectively. Seinfeld and Pandis (1998) indicated that NO_3^- is an end product of a series of gas-phase photochemical and heterogeneous reactions involving NO_x primarily derived from fossil fuel combustion. Nitrate is predominantly associated with coarse mode aerosol as a result of a chemical reaction between HNO_3 and sea-salt/crustal aerosols in the marine atmosphere (Graedel and Keene, 1995; Andreae and Crutzen, 1997). It is also known that NH_4^+ is primarily associated with fine mode aerosol and produced by heterogeneous reactions involving NH_3 derived from intensive agricultural activity (Aneja et al., 2001), biomass burning (Andreae and Merlet, 2001) and a relatively weak marine source (Jickells et al., 2003).

While examining aerosol data sets, a high correlation coefficient between two species usually indicates similar production and/or removal mechanisms and/or similar transport patterns (Kocak et al., 2004). Both NH_4^+ and NO_3^- showed strong relationships with nss-SO_4^{2-} and nss-K^+ (r = 0.73–0.96, Table 3.2), suggesting that fossil fuel combustion and biomass burning are significant sources of NH_4^+ and NO_3^-, and/or that they experienced similar transport and removal mechanisms.

3.4. Sources of atmospheric particulate N species

In order to estimate the fractions of observed NH_4^+ and NO_3^- derived from a specific source, nss-SO_4^{2-}, nss-K^+, nss-Ca^{2+} and Na^+ were used as tracers of fossil fuel combustion, biomass burning, crustal and marine origins, respectively. Non sea-salt SO_4^{2-} is derived from biomass burning as well as fossil fuel combustion (Baker et al., 2006). It is therefore necessary to estimate the nss-SO_4^{2-} derived from biomass burning (nss-$SO_4^{2-}{}_{biomass}$). Shen et al. (2009) reported that SO_4^{2-}/K^+ ratio in total suspended particulate (TSP) samples collected in Xi'an, China from October 2006 to September 2007 during biomass burning (straw combustion), was 4.4, which is useful for distinguishing biomass burning from other sources. In order to estimate the nss-$SO_4^{2-}{}_{biomass}$, it was assumed that all nss-K^+ was derived from

biomass burning, and the ratio (nss-SO_4^{2-}/nss-K^+ = 4.4) was multiplied by nss-K^+ concentrations observed during the cruise. As a result, it was estimated that 7–23% (mean 16%) of nss-SO_4^{2-} was derived from biomass burning. The nss-SO_4^{2-} derived from fossil fuel combustion (nss-$SO_4^{2-}{}_{fossil}$) calculated by subtracting nss-$SO_4^{2-}{}_{biomass}$ from nss-SO_4^{2-} was estimated to be 77–93% (mean 84%) of the total nss-SO_4^{2-}.

Shen et al. (2009) also reported that NH_4^+/K^+ and NO_3^-/K^+ ratios in TSP samples during biomass burning, were 1.2 and 2.2, respectively. In order to estimate what fraction of the observed atmospheric N species is from biomass burning, the ratios (NH_4^+/K^+ = 1.2 and NO_3^-/K^+ = 2.2) were multiplied by the concentrations of nss-K^+ and divided by the concentrations of atmospheric N species. As a result, it was estimated that 1.3–3.4% (mean 2.5%) of NH_4^+ ($NH_4^+{}_{biomass}$), 12–22% (mean 16%) of NO_3^- ($NO_3^-{}_{biomass}$) were derived from biomass burning. It is then assumed that the other fractions of NH_4^+ (NH_4^+ – $NH_4^+{}_{biomass}$) and NO_3^- (NO_3^- – $NO_3^-{}_{biomass}$) were derived from agricultural activity and fossil fuel combustion, respectively. Consequently, it was estimated that 97–99% (mean 98%) of NH_4^+ and 78–88% (mean 84%) of NO_3^- were derived from agricultural activity and fossil fuel combustion, respectively.

In this study, the fractions of atmospheric N species derived from specific sources were roughly estimated due to limited sampling period and simplified calculation (e.g. using assumptions and major ionic species only as tracers), but are useful in contributing to the understanding of atmospheric N sources. Further studies, however, are required to understand the sources of atmospheric N more clearly and should focus on long-term monitoring of atmospheric N species with simultaneous measurements of N isotope and/or single-particle size and composition using an Aerosol-Time-Of-Flight Mass Spectrometer (ATOFMS).

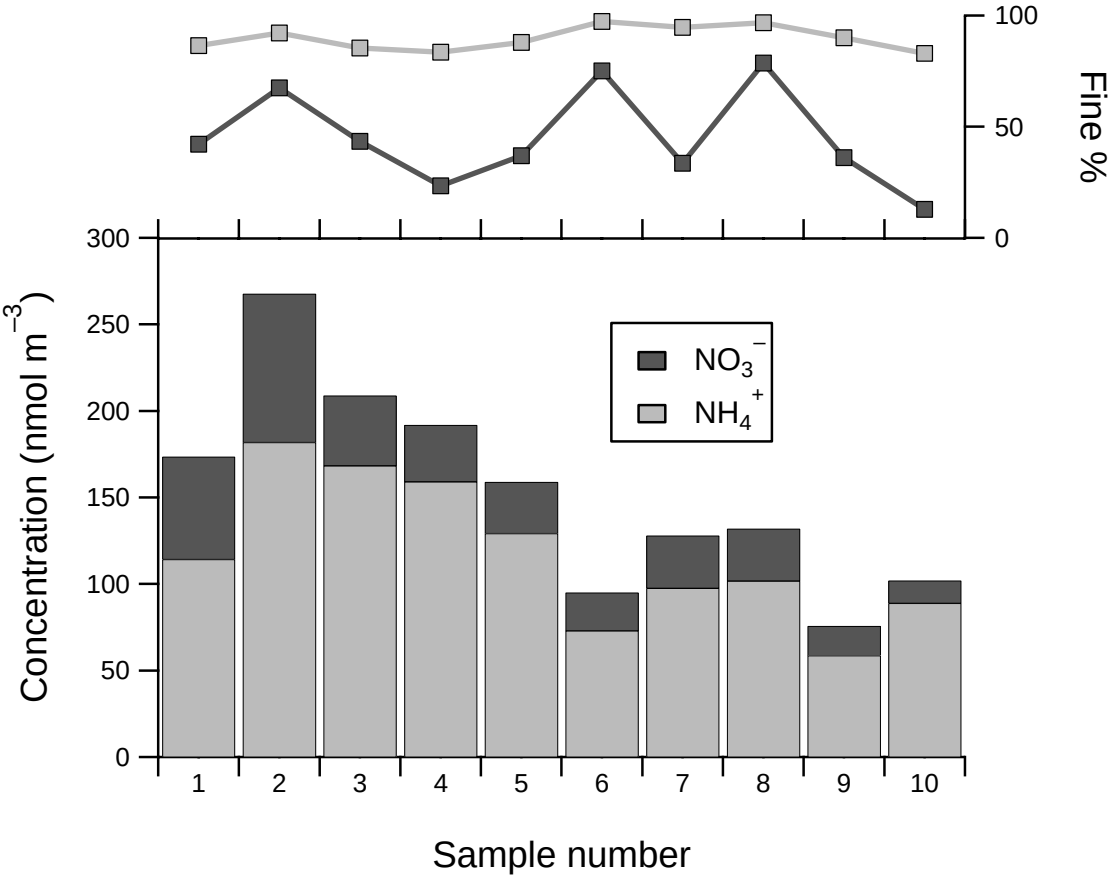

Fig. 3.4. Concentrations of NO_3^- and NH_4^+ against sample number in aerosols collected during the cruise. Upper section of panel shows the percentage of each component in fine (D < 2.5 μm) aerosol particles.

Table 3.1 Mean concentrations of atmospheric inorganic N species in aerosols during the KT-09-5 cruise[a]

Sample number	Atmospheric inorganic N species (nmol m^{-3})	
	NH_4^+	NO_3^-
1	114 (0.649)	59.2 (0.297)
2	182 (0.194)	85.9 (0.652)
3	168 (1.08)	40.5 (0.117)
4	159 (1.12)	32.7 (0.229)
5	129 (1.01)	29.7 (0.0569)
6	72.9 (0.151)	22.1 (0.0559)
7	97.5 (1.22)	30.4 (0.166)
8	102 (0.933)	30.2 (0.218)
9	58.6 (1.10)	17.0 (0.118)
10	88.8 (1.02)	13.2 (0.112)
Average	117 (41.5)	36.1 (21.7)

[a]Mean with (standard deviations).

Table 3.2 The correlation coefficients (r) between atmospheric inorganic N and major ionic species[a]

r	nss-SO_4^{2-}	nss-$SO_4^{2-}{}_{biomass}$	nss-$SO_4^{2-}{}_{fossil}$	nss-K^+	nss-Ca^{2+}	Na^+
NH_4^+	**0.96**	**0.88**	**0.91**	**0.88**	0.65	-0.27
NO_3^-	**0.73**	**0.89**	0.62	**0.89**	0.62	0.23

[a]Statistically significant correlations ($p < 0.05$) are shown in bold print.

3.5. Dry deposition flux of atmospheric particulate N

Dry deposition fluxes (F_d) were calculated from aerosol concentrations (C_a) in the coarse (c) and fine (f) modes and dry deposition velocities (V_d) for each size mode (Duce et al., 1991; Yeatman et al., 2001; Baker et al., 2007):

$$F_d = C_a^c \times V_d^c + C_a^f \times V_d^f \quad (1)$$

Here, V_d of 2 cm s^{-1} for coarse mode and 0.1 cm s^{-1} for fine mode were used since these two values are known to be best estimates based on experimental and model studies (Duce et al., 1991; Baker et al., 2003; Nakamura et al., 2005). Estimated F_d of atmospheric inorganic N species varied from 9.6–57 μmol m^{-2} d^{-1} for NH_4^+ and 11–61 μmol m^{-2} d^{-1} for NO_3^-during the sampling period (Table 3.3). Mean F_d for NH_4^+ and NO_3^- were estimated to be 31 ± 17 μmol m^{-2} d^{-1} and 33 ± 17 μmol m^{-2} d^{-1}, respectively. Although the mean concentration of NH_4^+ was 3 times higher than that of NO_3^-, F_d of both were approximately the same since fluxes to the ocean are dominated by the coarse mode, resulting in NO_3^- being deposited much more rapidly.

Nakamura et al. (2005) reported that mean dry deposition flux of inorganic N over the East China Sea was 83 μmol m^{-2} d^{-1}; with 32 μmol m^{-2} d^{-1} of this being contributed by dry deposition of NH_4^+ and 51 μmol m^{-2} d^{-1} from NO_3^-. The dry deposition flux for NH_4^+ was comparable to the result of this study, whereas the dry deposition flux for NO_3^- was 1.5 times higher than the estimate for NO_3^- in this study. This difference is likely due to strong influences of NO_x emission from China (Uno et al., 2007) and/or higher deposition velocity of NO_3^- than that of NH_4^+ since NO_3^- is largely associated with coarse mode particles in the marine atmosphere (Graedel and Keene, 1995; Andreae and Crutzen, 1997).

While dry deposition is a continuous process occurring at all times over all surfaces, wet deposition is highly episodic occurring only when precipitation (i.e., rain, snow and fog) falls to the ground or the sea surface. The relative importance of wet and dry deposition fluxes varies between locations since wet deposition is intermittent and primarily a function of the rainfall frequency and amount in the region (Spokes et al., 2000). In this study, wet deposition fluxes of atmospheric N could not be estimated since no rain event occurred and sea fog water was collected during the sampling period. Iwamoto et al. (2011) reported that mineral dust aerosols observed over the semi-pelagic northwestern North Pacific (40°N–44°N, 140°E–146°E) from 18 April–29 April 2007, were scavenged by sea fog, and that their deposition to the ocean increased the particle concentration in surface seawater, suggesting that sea fog can increase air-to-sea transfer mineral matter into the ocean surface. This result raises the question of whether sea fog plays an important role in supplying atmospheric N to the ocean. The northern North Pacific region (> 40°N), however, has a probability of sea fog occurrence of 5–30% in the spring (March–May), with a high sea fog frequency (~50%) during the summertime period from June to August (Wang 1985). Thus,

the atmospheric N input via sea fog deposition over the western North Pacific in the spring periods may not an important transfer process for atmospheric N to the ocean, because of the low frequency of sea fog occurrence. Moreover, Uematsu et al. (2003) reported that dry deposition is the dominant process removing the mineral dust particles over the western North Pacific region (5–60°N, 75–165°E) because there is little precipitation in the spring, and that more than 60% of mineral dust was removed over the western North Pacific by dry deposition during March 1994–Feburuary 1995. Considering this study was conducted in the spring of 2009, dry deposition is most likely the dominant process in supplying atmospheric N to the ocean during the sampling period, although further research on wet deposition is required to estimate the deposition fluxes of atmospheric N by precipitation and by sea fog in the western North Pacific.

In order to evaluate the impact of atmospheric N on marine ecosystem, potential primary production was estimated using our results for dry deposition fluxes of N and the Redfield C/N ratio of 6.6. The impact of atmospheric deposition on marine ecosystems depends on the nutrient status of the receiving waters, and is related to both the total amount and ratio of nutrients supplied atmospherically and to the limiting nutrient for the existing local water column (Baker et al., 2006). Assuming that phytoplankton can take up all the N coming from atmospheric deposition with no losses, and that there is no co-limitation by other nutrients (i.e., P and Fe), atmospheric bioavailable N deposition flux (64 ± 31 μmol m^{-2} d^{-1}) was found to be maximally responsible for the carbon uptake of 420 ± 210 μmol C m^{-2} d^{-1} (139–669 μmol C m^{-2} d^{-1}) by using the Redfield C/N ratio of 6.6. Wong et al. (2002) reported that the annual new primary production at the sea surface over the region off south-east Japan (35°–42°N, 140°–160°E) from 1995–1996 was estimated to be 33 g C m^{-2} yr^{-1}. To facilitate evaluation, g C m^{-2} yr^{-1} unit for the annual new primary production was converted to the μmol C m^{-2} d^{-1} unit used in this study. Based on this, the result of this study suggests that inorganic N deposited to the semi-pelagic western North Pacific Ocean from the atmosphere can support 1.9–8.9% of the new primary production. If co-limitation by other nutrient is considered, the contribution of atmospheric N deposition to primary production would be lower; however, episodic deposition events such as dust storms provide a large amount of nutrients to the surface ocean over a very short period. These events can change and improve the nutrient structures of surface seawater and may even induce blooms of phytoplankton (Prospero and Savoie, 1989; Zhang et al., 2007). Atmospheric N deposition therefore could be an important in the ocean where the sporadic atmospheric N deposition events caused by the transport of continental dust are affected and the supply of deep nutrient rich water is restricted by the stratification of the surface ocean that is enhanced by global warming.

Table 3.3 Dry deposition fluxes of atmospheric inorganic N species during the KT-09-5 cruise

Sample	Dry deposition flux (μmol m^{-2} d^{-1})		
number	Bioavailable N[a]	NH_4^+	NO_3^-
1	96	35	61
2	92	39	53
3	96	55	41
4	101	57	44
5	70	37	33
6	21	9.6	11
7	53	17	36
8	27	14	13
9	34	15	19
10	52	32	20
Average	64	31	33
Std	31	17	17

[a]Bioavailable N represents the sum of NH_4^+ and NO_3^-.

3.6. Conclusions

Atmospheric bioavailable N input to the semi-pelagic western North Pacific has been determined during the spring time. Aerosol inorganic N was composed of ~77% NH_4^+ and 23% NO_3^-. Ammonium existed mainly in the fine mode, and tends to deposit more slowly from the atmosphere than coarse mode aerosol. Since NO_3^- is mainly associated with rapidly depositing coarse mode, it may dominate atmospheric N deposition to the ocean. It is concluded that agricultural activity and fossil fuel combustion are significant sources of atmospheric inorganic N in the investigated region.

Nutrient inputs via atmospheric deposition can be significant over large and remote areas of the oceans. In this study, the contribution of atmospheric bioavailable N deposited to the semi-pelagic western North Pacific to primary production was estimated to be 1.9–8.9%. Although the contribution of atmospheric bioavailable N deposition to primary production in the study was not significant, the sporadic atmospheric deposition events caused by dust storms can supply a large amount of N to the surface ocean over a very short period (Prospero and Savoie, 1989; Zhang et al., 2007). In addition, since the emissions of anthropogenic atmospheric reactive N (e.g., NH_3 and NO_x) by rapid growth in human population and industrial activity are increasing (Akimoto, 2003; Uno et al. 2007; Galloway et al. 2008; Duce et al., 2008), atmospheric deposition could become an important source of nutrients in the ocean where the supply of deep nutrient rich water is restricted by the stratification of the surface ocean that is enhanced by global warming. To properly understand the contribution of atmospheric nutrient deposition to primary production in the western North Pacific, future work should therefore include other nutrients such as phosphorus and iron, and focus on long-term monitoring of atmospheric nutrients.

References

Akimoto, H., 2003. Global air quality and pollution. Science 302, 1716–1719.

Andreae, M.O., Crutzen, P.J., 1997. Atmospheric aerosols: biogeochemical sources and role in atmospheric chemistry. Science 276, 1052–1058.

Andreae, M.O., Merlet, P., 2001. Emission of trace gases and aerosols from biomass burning. Global Biogeochemical Cycles 15, 955–966.

Aneja, V.P., Roelle, P.A., Murray, G.C., Southerland, J., Erisman, J.W., Fowler, D., Asman, W.A.H., Patni, N., 2001. Atmospheric nitrogen compounds II: emissions, transport, transformation, deposition and assessment. Atmospheric Environment 35, 1903–1911.

Baker, A.R., Kelly, S.D., Biswas, K.F., Witt, M., Jickells, T.D., 2003. Atmospheric deposition of nutrients to the Atlantic Ocean. Geophysical Research Letters 30, OCE 11/11–OCE 11/14.

Baker, A.R., Jickells, T.D., Biswas, K.F., Weston, K., French, M., 2006. Nutrients in atmospheric aerosol particles along the Atlantic Meridional Transect. Deep Sea Research Part II 53, 1706–1719.

Baker, A.R., Weston, K., Kelly, S.D., Voss, M., Streu, P., Cape, J.N., 2007. Dry and wet deposition of nutrients from the tropical Atlantic atmosphere: Links to primary productivity and nitrogen fixation. Deep Sea Research Part I 54, 1704–1720.

Carrillo, J.H., Hastings, M.G., Sigman, D.M., Huebert, B.J., 2002. Atmospheric deposition of inorganic and organic nitrogen and base cations in Hawaii. Global Biogeochemical Cycles 16, 24/21–24/16.

Dentener, F., Drevet, J., Lamarque, J.F., Bey, I., Eickhout, B., Fiore, A.M., Hauglustaine, D., Horowitz, L.W., Krol, M., Kulshrestha, U.C., Lawrence, M., Galy-Lacaux, C., Rast, S., Shindell, D., Stevenson, D., Van, N.T., Atherton, C., Bell, N., Bergman, D., Butler, T., Cofala, J., Collins, B., Doherty, R., Ellingsen, K., Galloway, J., Gauss, M., Montanaro, V., Muller, J.F., Pitari, G., Rodriguez, J., Sanderson, M., Solmon, F., Strahan, S., Schultz, M., Sudo, K., Szopa, S., Wild, O., 2006. Nitrogen and sulfur deposition on regional and global scales: a multimodel evaluation. Global Biogeochemical Cycles 20(4), GB4003/4001–GB4003/4021.

Duce, R.A., Liss, P.S., Merrill, J.T., Atlas, E.L., Buat-Menard, P., Hicks, B.B., Miller, J.M., Prospero, J.M., Arimoto, R., et al., 1991. The atmospheric input of trace species to the world ocean. Global Biogeochemical Cycles 5, 193–259.

Duce, R.A., LaRoche, J., Altieri, K., Arrigo, K.R., Baker, A.R., Capone, D.G., Cornell, S., Dentener, F., Galloway, J., Ganeshram, R.S., Geider, R.J., Jickells, T., Kuypers, M.M., Langlois, R., Liss, P.S., Liu, S.M., Middelburg, J.J., Moore, C.M., Nickovic, S., Oschlies, A., Pedersen, T., Prospero, J., Schlitzer, R., Seitzinger, S., Sorensen, L.L., Uematsu, M., Ulloa, O., Voss, M., Ward, B., Zamora, L., 2008. Impacts of Atmospheric Anthropogenic Nitrogen on the Open Ocean. Science 320, 893–897.

Gabriel, R., Mayol-Bracero, O.L., Andreae, M.O., 2002. Chemical characterization of submicron aerosol particles collected over the Indian Ocean. Journal of Geophysical Research—Atmospheres 107, INX2/4/1–INX2/4/12.

Galloway, J.N., Townsend, A.R., Erisman, J.W., Bekunda, M., Cai, Z., Freney, J.R., Martinelli, L.A., Seitzinger, S.P., Sutton, M.A., 2008. Transformation of the Nitrogen Cycle: Recent Trends, Questions, and Potential Solutions. Science 320, 889–892.

Gao, Y., Arimoto, R., Zhou, M.Y., Merrill, J.T., Duce, R.A., 1992. Relationships between the dust concentrations over eastern Asia and the remote North Pacific. Journal of Geophysical Research—Atmospheres 97, 9867–9872.

Graedel, T.E., Keene, W.C., 1995. Tropospheric budget of reactive chlorine. Global Biogeochemical Cycles 9, 47–77.

Iwamoto, Y., Yumimoto, K., Toratani, M., Tsuda, A., Miura, K., Uno, I., Uematsu, M. 2011. Biogeochemical implications of increased mineral particle concentrations in surface waters of the northwestern North Pacific during an Asian dust event. Geophysical Research Letters 38, L01604–L01608.

Jickells, T.D., Kelly, S.D., Baker, A.R., Biswas, K., Dennis, P.F., Spokes, L.J., Witt, M., Yeatman, S.G., 2003. Isotopic evidence for a marine ammonia source. Geophysical Research Letters 30, 27/21–27/24.

Kocak, M., Kubilay, N., Mihalopoulos, N., 2004. Ionic composition of lower tropospheric aerosols at a Northeastern Mediterranean site: implications regarding sources and long-range transport. Atmospheric Environment 38, 2067–2077.

Krishnamurthy, A., Moore, J.K., Mahowald, N., Luo, C., Zender, C.S., 2010. Impacts of atmospheric nutrient inputs on marine biogeochemistry. Journal of Geophysical Research—Biogeosciences 115, G01006/01001–G01006/01013.

Nakamura, T., Matsumoto, K., Uematsu, M., 2005. Chemical characteristics of aerosols transported from Asia to the East China Sea: an evaluation of anthropogenic combined nitrogen deposition in autumn. Atmospheric Environment 39, 1749–1758.

Paerl, H.W., 1985. Enhancement of marine primary production by nitrogen-enriched acid rain. Nature 315, 747–749.

Paerl, H.W., 1997. Coastal eutrophication and harmful algal blooms: importance of atmospheric deposition and groundwater as "new" nitrogen and other nutrient sources. Limnology and Oceanography 42, 1154–1165.

Prospero, J.M., Barrett, K., Church, T., Dentener, F., Duce, R.A., Galloway, J.N., Levy, H., II, Moody, J., Quinn, P., 1996. Atmospheric deposition of nutrients to the North Atlantic basin. Biogeochemistry 35, 27–73.

Prospero, J.M., Savoie, D.L., 1989. Effect of continental sources on nitrate concentrations over the Pacific Ocean. Nature 339(6227), 687–689.

Rolff, C., Elmgren, R., Voss, M., 2008. Deposition of nitrogen and phosphorus on the Baltic Sea: seasonal patterns and nitrogen isotope composition. Biogeosciences 5, 1657–1667.

Sasakawa, M., Ooki, A., Uematsu, M., 2003. Aerosol size distribution during sea fog and its scavenge process of chemical substances over the northwestern North Pacific. Journal of Geophysical Research—Atmospheres 108, AAC13/11-AAC13/19.

Seinfeld, J.H., Pandis, S.N., 1998. Atmospheric Chemistry and Physics: From Air Pollution to Climate Change, John Wiley & Sons, New York, pp. 1326.

Shen, Z., Cao, J., Arimoto, R., Han, Z., Zhang, R., Han, Y., Liu, S., Okuda, T., Nakao, S., Tanaka, S., 2009. Ionic composition of TSP and PM2.5 during dust storm and air pollution episodes at Xi'an, China. Atmospheric Environment 43, 2911–2918.

Spokes, L.J., Yeatman, S.G., Cornell, S.E., Jickells, T.D., 2000. Nitrogen deposition to the eastern Atlantic Ocean. The importance of south-easterly flow. Tellus, Series B: Chemical and Physical Meteorology 52B, 37–49.

Uematsu, M., Duce, R.A., Prospero, J.M., Chen, L., Merrill, J.T., McDonald, R.L., 1983. Transport of

mineral aerosol from Asia over the North Pacific Ocean. Journal of Geophysical Research—Atmospheres 88, 5343–5352.

Uematsu, M., Wang, Z., Uno, I., 2003. Atmospheric input of mineral dust to the western North Pacific region based on direct measurements and a regional chemical transport model. Geophysical Research Letters 30, 1342.

Uematsu, M., Hattori, H., Nakamura, T., Narita, Y., Jung, J., Matsumoto, K., Nakaguchi, Y., Dileep Kumar, M., 2010. Atmospheric transport and deposition of anthropogenic substances from the Asia to the East China Sea. Marine Chemistry 120, 108–115.

Uno, I., Uematsu, M., Hara, Y., He, Y.J., Ohara, T., Mori, A., Kamaya, T., Murano, K., Sadanaga, Y., Bandow, H., 2007. Numerical study of the atmospheric input of anthropogenic total nitrate to the marginal seas in the western North Pacific region. Geophysical Research Letters 34, L17817–L17822.

Wang, B.-H., 1985. Distributions and variations of sea fog in the world, in Sea Fog. China Ocean Press, Beijing, pp. 51–90.

Wang, Y., Zhuang, G., Zhang, X., Huang, K., Xu, C., Tang, A., Chen, J., An, Z., 2006. The ion chemistry, seasonal cycle, and sources of PM2.5 and TSP aerosol in Shanghai. Atmospheric Environment 40, 2935–2952.

Wong, C.S., Waser, N.A.D., Nojiri, Y., Whitney, F.A., Page, J.S., Zeng, J. 2002. Seasonal cycles of nutrients and dissolved inorganic carbon at high and mid latitudes in the North Pacific Ocean during the Skaugran cruise: determination of new production and nutrient uptake ratios. Deep-Sea Research Part II 49, 5317–5338.

Yeatman, S.G., Spokes, L.J., Jickells, T.D., 2001. Comparisons of coarse-mode aerosol nitrate and ammonium at two polluted coastal sites. Atmospheric Environment 35, 1321–1335.

Zhang, G., Zhang, J., Liu, S., 2007. Characterization of nutrients in the atmospheric wet and dry deposition observed at the two monitoring sites over Yellow Sea and East China Sea. Journal of Atmospheric Chemistry 57(1), 41–57.

Zhang, J., Zhang, G.S., Bi, Y.F., Liu, S.M., 2011. Nitrogen species in rainwater and aerosols of the Yellow and East China seas: Effects of the East Asian monsoon and anthropogenic emissions and relevance for the NW Pacific Ocean. Global Biogeochemical Cycles 25, GB3020–GB3033.

4. Atmospheric inorganic nitrogen input via dry, wet and sea fog deposition to the subarctic western North Pacific Ocean

4.1. Introduction

Fogs and clouds form when air becomes supersaturated with respective to liquid water. There is no difference between fogs and clouds other than altitude (Wallace and Hobbs, 2006). A necessary condition for fog or cloud formation is the increase in the relative humidity of an air parcel to a value exceeding 100%. Isobaric cooling and adiabatic cooling are major mechanisms by which air parcels can cool in the atmosphere (Seinfeld and Pandis, 1998). Isobaric cooling is the cooling of an air parcel under constant pressure. It is usually the result of radiative losses of energy or horizontal movement of an air mass over a colder land or water surface. If an air parcel ascends in the atmosphere, its pressure decreases. And then the parcel expands, and its temperature drops (i.e., adiabatic cooling) (Seinfeld and Pandis, 1998). Uplift is more effective in cooling air than other physical mechanisms, such as adiabatic cooling, so that this is the common cause of cloud formation (Brasseur et al., 1999). Under these conditions, the relative humidity of an air parcel increases and water condenses on aerosol particles that serve as condensation nuclei in accordance with water vapor equilibrium. When the relative humidity of the air parcel reaches a critical supersaturation, the particles become activated, and fogs or clouds form (Pandis and Seinfeld, 1990; Wallace and Hobbs, 2006).

Fog and clouds are characterized by their droplet size distribution as well as their liquid water content (i.e., grams of H_2O per cubic meter of air; LWC). Fog droplets typically have diameters in the range from a few μm to ~30–40 μm and LWCs in the range of 0.05–0.1 g m^{-3}. Clouds, on the other hand, generally have droplet diameters from 5 μm up to ~100 μm, with typical LWCs of ~0.05–2.5 g m^{-3} (Finlayson-Pitts and Pitts, 2000). Raindrops are much larger than fog or cloud droplets, with diameters of ~0.2–3 mm and correspondingly large LWCs. Because of their size, rain drops remain suspended in the atmosphere for only minutes en route to the earth's surface (Finlayson-Pitts and Pitts, 2000).

Chemical constituents of the atmosphere are removed or reduced by three processes: dry deposition, wet deposition and fog deposition. Dry deposition is determined by the factors including meteorological conditions, atmospheric concentrations and surface type/condition. The latter two refer to incorporation of the chemical of interest into precipitation or cloud/fog water, respectively. Wet deposition removes chemicals from the atmosphere either by in-cloud scavenging where gases and particles are incorporated into cloud droplets, and below-cloud scavenging where gases and particles are removed by falling rain or snow (Pryor and Barthelmie, 2000). While numerous studies dealt with the input of substances via atmospheric deposition, especially dry and wet deposition, relatively little is known about the deposition flux of atmospheric constituent by fog (Lange et al., 2003).

Scavenging processes of water-soluble gases and aerosols in the atmosphere by fog events are

determined by the properties of ionic compositions in fog water and by the growth rate of fog droplets during fog events (Aikawa et al., 2007). The chemical compositions of the particles acting as condensation nuclei determine the initial compositions of the fog droplets, which can be further altered by uptake of water-soluble gases (e.g., HNO_3, NH_3 and SO_2) and by aqueous phase chemical reactions (Sasakawa et al., 2003; Raja et al., 2008). The physico-chemical interactions among water-soluble gases, particles and fog droplets can influence the composition of fog droplets (Pandis and Seinfeld 1989; Pandis et al., 1990). In fog, the condensation of water vapor on pre-existent particles in the boundary layer shifts the aerosol size distribution towards larger sizes and accelerates their removal from the atmosphere (Jacob et al., 1984; Sasakawa et al., 2003; Herckes et al., 2007; Li et al., 2011). The deposition of fog can contribute significantly to the hydrologic, pollutant and nutrient cycles in coastal and mountainous regions, since it is an important transfer process for water and various inorganic and organic substances from the atmosphere to the biosphere (Lovett et al., 1982; Jacob et al., 1984; Collett et al., 2001; Zhang and Anastasio, 2001; Klemm and Wrzesinsky, 2007). However, quantifying fog deposition flux for atmospheric substances and assessing its impact are still a challenge in atmospheric science and ecosystem research (Klemm and Wrzesinsky, 2007).

Considerable effort has been devoted to investigating the chemical and physical properties of fog in valleys, mountains and urban areas (e.g., Collett et al., 2001; Burkard et al., 2002; Collett et al., 2002; Moore et al, 2004; Lu et al., 2010; Li et al., 2011). However, sea fog has not been extensively investigated (e.g., Sasakawa and Uematsu, 2002; Sasakawa et al., 2003; Sasakawa and Uematsu, 2005); although it may stimulate phytoplankton growth over the oceanic regions where sea fog occurs frequently and atmospheric nutrients derived from natural and anthropogenic sources are transported and/or affected (Sasakawa et al., 2003). It is therefore necessary to clarify the scavenging process of atmospheric nutrients by sea fog and quantify their deposition flux to the sea surface.

Rapid growth in human population and industrial activity has led to increases in the concentrations of reactive N species throughout the environment (Galloway et al. 2008). In particular, the increase in NO_x emissions in eastern Asia has been dramatic over the last decade (Akimoto, 2003; Uno et al. 2007). The western North Pacific receives a large influx of mineral particles and pollutants from the Asian continent through atmospheric long-range transport (Uematsu et al., 1983; Gao et al., 1992; Nakamura et al., 2005; Uematsu et al., 2010). Accordingly, estimating deposition flux of atmospheric N and evaluating its impact on marine biogeochemical cycles over the western North Pacific have become increasingly important. In addition, the subarctic western North Pacific (> 40°N) has a high sea fog frequency with a maximum of ~50% during the summertime period from June to August (Wang 1985). Nevertheless, no study has been carried out over this region to estimate atmospheric inorganic N input via dry, wet and sea fog deposition simultaneously. In order to improve the understanding of the biogeochemical cycle of N between the ocean and the atmosphere, simultaneous sampling of aerosols, rainwater and sea fog water was carried out over the subarctic western North Pacific during Leg 1 of the

KH-08-2 cruise (Fig. 4.1). The aims of this study are to (1) investigate general characteristics of sea fog, (2) estimate the fluxes of atmospheric inorganic N via dry, wet and sea fog deposition, (3) estimate the contribution of each deposition to total atmospheric inorganic N input, and (4) evaluate the impact of atmospheric inorganic N deposition on the ocean marine ecosystem.

4.2. Meteorological conditions associated with sea fog occurrences

Sea fog typically occurs as a result of warm marine air advection over a region where a cold ocean current affects (Lewis et al., 2004). During the sampling period, sea fog occurred predominantly when the dominant wind direction was southerly and air temperature dropped to its dew point (Fig. 4.2). This result indicates that the warm and humid air masses form the low and middle latitudes of the North Pacific Ocean passed over the cold sea surface of the northwestern North Pacific Ocean and they were cooled down to a saturation temperature. Sea fog events, however, did not occur when sea surface temperature was higher than air temperature, although the dominant wind direction was southerly, suggesting that the difference between the air and sea surface temperatures is a key factor controlling sea fog formation (Cho et al., 2000).

According to previous studies (Cho et al., 2000; Fu et al., 2006; Tokinaga and Xie, 2009), the difference between air and sea surface temperatures is often observed to be positive in frequent sea fog occurrence regions, since the relatively cold sea surface temperature stabilizes the lower atmosphere, making a favorable condition for sea fog formation. Therefore, the meteorological conditions during the sea fog sampling period show that advection of warm and humid air masses from the subtropical North Pacific Ocean and the positive difference between air and sea surface temperatures make favorable conditions for sea fog occurrence over the subarctic western North Pacific Ocean.

4.3. Effect of sea fog on particle number density

Temporal variations of total LWC, particle number densities for aerosols in the range of 0.3–2.0 μm and fog droplet size distribution for each of the 40 droplet size classes during Leg 1 of the KH-08-2 cruise are shown in Fig. 4.3. The total LWC varied from < 0.2–140 mg m^{-3}. Mean particle number densities during non sea fog events were 25 ± 31 cm^{-3} for aerosols in the range of 0.3 < D < 0.5 μm, 2.6 ± 3.0 cm^{-3} for 0.5 < D < 1.0 μm, 0.53 ± 0.70 cm^{-3} for 1.0 < D < 2.0 μm, and 0.17 ± 0.27 cm^{-3} for D > 2.0 μm. In comparison, the mean particle number densities during sea fog events decreased by 4% (mean particle number density 24 ± 20 cm^{-3}) for aerosols in the range of 0.3 < D < 0.5 μm, 12% (2.3 ± 3.1 cm^{-3}) for 0.5 < D < 1.0 μm, 55% (0.24 ± 0.52 cm^{-3}) for 1.0 < D < 2.0 μm, and 78% (0.038 ± 0.091 cm^{-3}) for D > 2.0 μm. This result suggests that the growth of aerosol particles to liquid droplets leads to the acceleration of particle removal from the atmosphere (Pandis and Seinfeld, 1990), and that particles

with diameters larger than 0.5 μm could act preferentially as condensation nuclei for sea fog droplets and were more efficiently scavenged by sea fog (Sasakawa et al., 2003).

During the initial formation of sea fog, larger particles (D > 0.5 μm) preferentially became activated and the fog droplet size distribution was shifted towards the larger droplet sizes (Fig. 4.3) because of the condensation of water vapor on pre-existent particles (Jacob et al., 1984). After a few hours, the fog droplets reached a size starting to settle gravitationally and deposited to the sea surface, suggesting that sea fog can enhance deposition of atmospheric substances since fogs are effective scavengers of both particles and water-soluble gases (Collett et al., 2001).

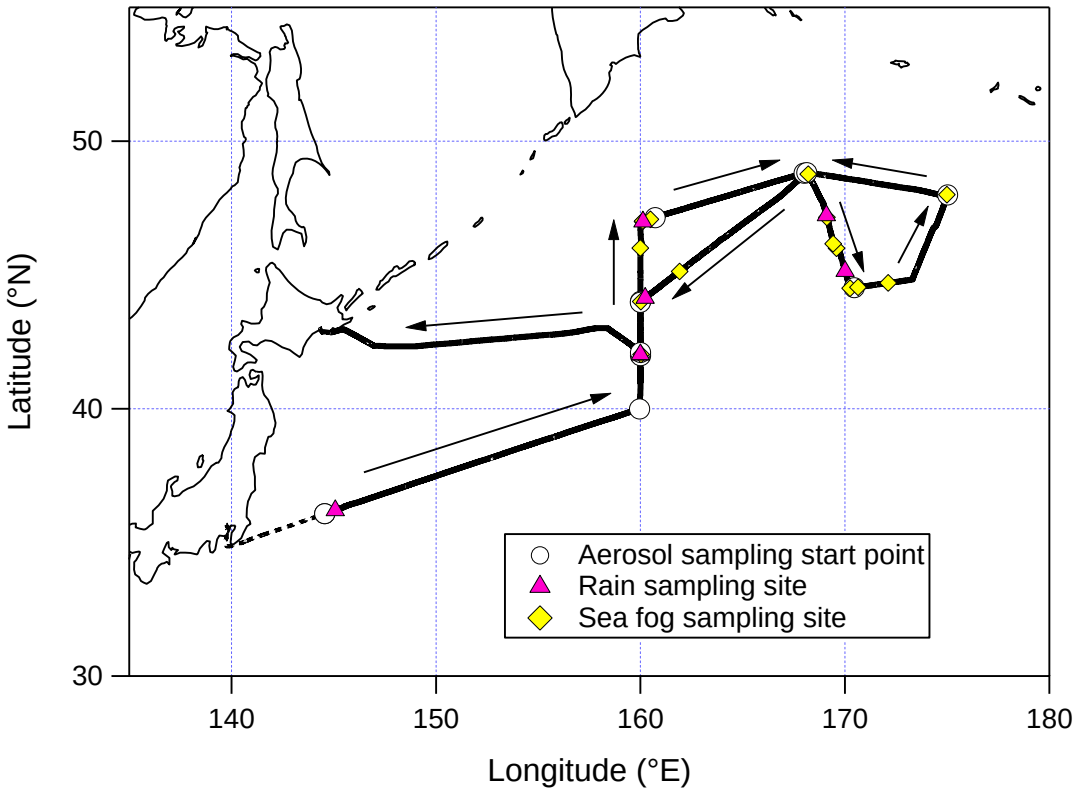

Fig. 4.1. Cruise track of Leg 1 of the KH-08-2. White circles, pink triangles and yellow diamonds indicate aerosol, rain and sea fog sampling locations during the cruise. Each aerosol sampling start point represents the end of the previous sampling period. Dotted line indicates that no aerosol sampling was conducted.

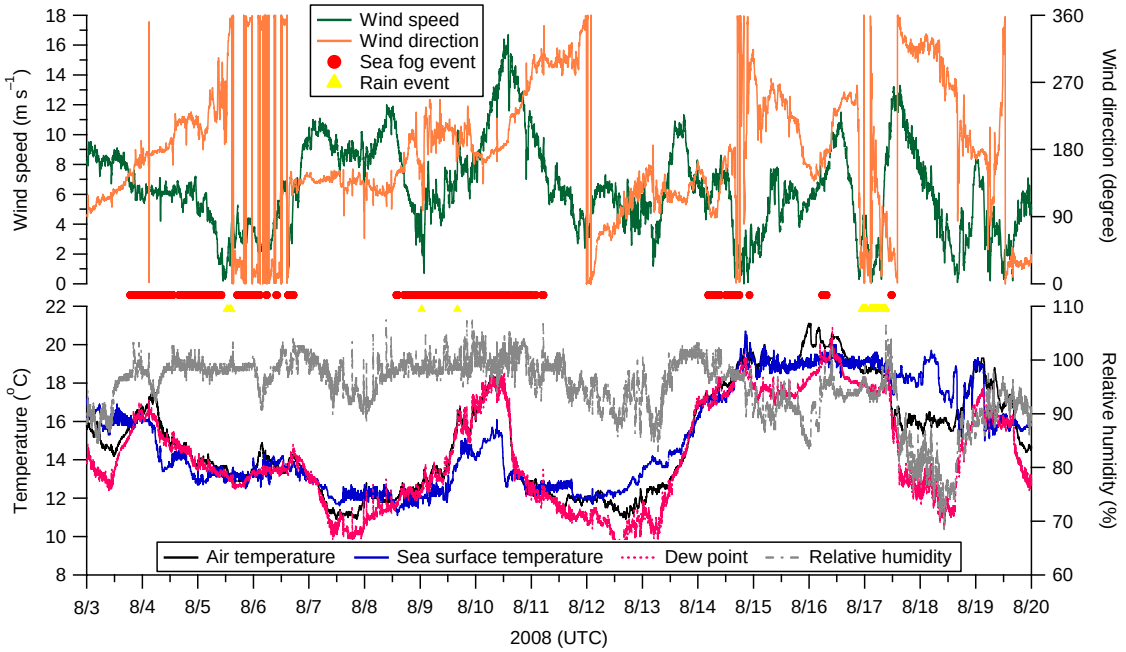

Fig. 4.2. Temporal variations of wind speed, wind direction, air temperature, sea surface temperature, dew point and relative humidity during Leg 1 of the KH-08-2 cruise. Sea fog and rain events indicate the occurrences of observed sea fog and rain events, respectively.

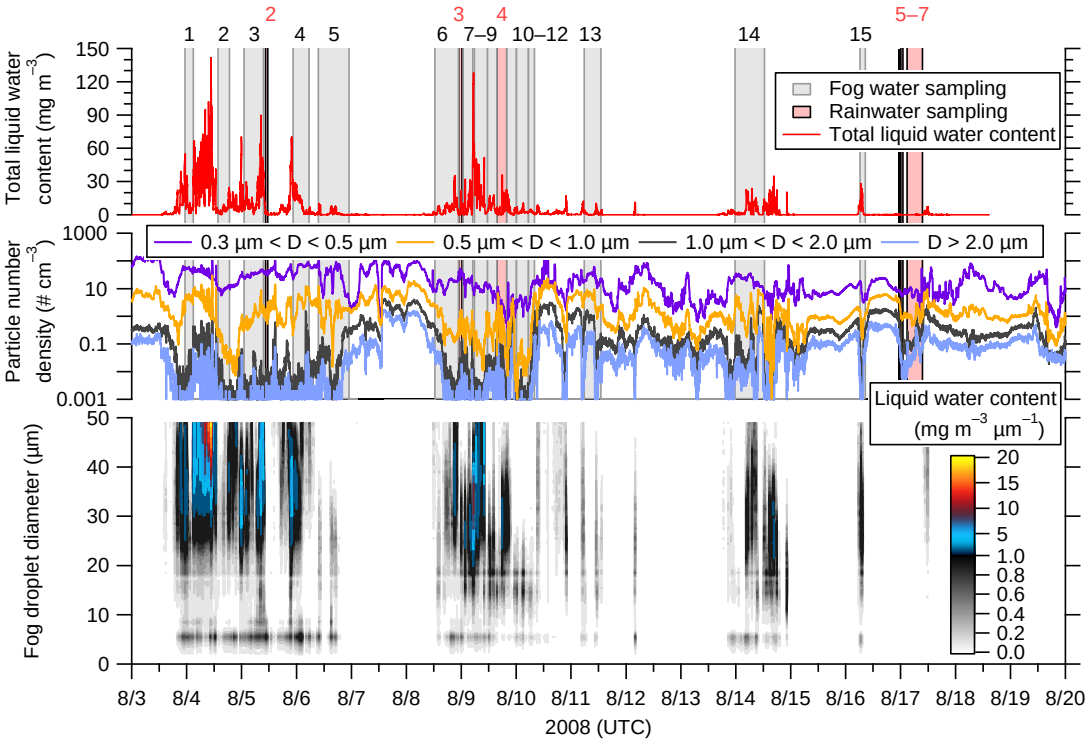

Fig. 4.3. Temporal variations of total LWC, particle number densities for aerosols in four size groups, and LWC for each of the 40 droplet size classes along the KH-08-2 cruise track (Leg 1). The gray and pink shaded areas indicate sea fog water and rainwater sampling durations, respectively. The black and pink numbers indicate sea fog and rainwater sample number of each sample, respectively. When sea fog and rain events occurred simultaneously, only rainwater sample was collected. Then that sample was considered as a rainwater sample (i.e., rainwater samples 3 and 4). Since rainwater sample number 1 was collected on 30 July, it was not present here.

4.4. Chemical composition of aerosols, rainwater and sea fog water

Aerosol (n = 11), rainwater (n = 7) and sea fog water (n = 17) samples were collected during Leg 1 of the KH-08-2 cruise conducted over the subarctic western North Pacific Ocean from 29 July–19 August 2008. Sea salt ions (Na^+, Cl^- and ss-ions) were the dominant components in aerosols, rainwater and sea fog water, representing approximately 72%, 61% and 86% of total ionic concentration, respectively (Fig. 4.4 and Table 4.1). In aerosols and sea fog water, the mole equivalent ratios of Cl^-/Na^+ were slightly lower than that in seawater (Table 4.2), suggesting that Cl^- depletion occurred through the volatilization of hydrogen chloride (HCl) from sea-salt particles that became acidified by the incorporation of nitric (HNO_3) and/or sulfuric (H_2SO_4) acids in the marine atmosphere (Graedel and Keene 1995; Andreae and Crutzen 1997), and that the acidified sea salt particles acted as condensation nuclei of sea fog droplets (Sasakawa and Uematsu, 2002; Raja et al., 2008). Furthermore, the Mg^{2+}/Na^+, K^+/Na^+ and Ca^{2+}/Na^+ ratios in aerosols and sea fog water were similar or slightly higher than those in seawater, suggesting that most of Mg^{2+}, K^+ and Ca^{2+} in aerosols and sea fog water were derived from sea salt particles.

Two volcanoes on the Aleutians erupted during Leg 1 of the KH-08-2 cruise. The eruption at Okmok volcano (53.40°N, 168.17°W) started on 12 July 2008 and ended in late August 2008 (Larsen et al., 2009; Lu and Dzurisin, 2010), and Kasatochi volcano (52.18°N, 175.51°W) became active on 7 August 2008 (Schmale et al., 2010). During the sampling period, air masses originated from the Asian continent and the Kamchatka Peninsula, indicating that these air masses were likely affected by anthropogenic and crustal sources as well as the eruptions of two volcanoes (Figs. 4.5a–4.5c).

Unlike aerosol and sea fog water samples, the Cl^-/Na^+, Mg^{2+}/Na^+, K^+/Na^+ and Ca^{2+}/Na^+ ratios in rainwater were much higher than those in seawater (Table 4.2). Atmospheric HCl are derived from sea salt particles, volcanoes and anthropogenic activities (e.g., fossil fuel combustion and incineration) (Graedel and Keene, 1995). Gioda et al. (2011) observed high Cl^-/Na^+ ratios in rainwater (2.2) and cloud water (3.2), collected in Puerto Rico from December 2004 to March 2007, when ash from the Soufriere Hills volcano reached the sampling site. During the collection of rainwater samples, air masses originated from the Asian continent/subtropical western North Pacific Ocean and thereafter swept over large regions of the Korean Peninsula and/or the Japanese Islands, indicating that these air masses were most likely affected by strong anthropogenic and crustal sources rather than by the influences of two volcanoes (Fig. 4.5b). The high Cl^-/Na^+ ratio in rainwater thus is likely due to scavenging of HCl derived from sea salt particles and/or anthropogenic source by rainwater. Sasakawa and Uematsu (2002) reported that NH_4^+/nss-Ca^{2+} ratio in rainwater (0.53) collected over the northwestern North Pacific from 15–29 July 1998, was two orders of magnitude lower than that in sea fog water (11), reflecting that mineral particles, such as calcium carbonate ($CaCO_3$), mainly existed over higher altitudes than those where sea fog appeared. While sea fog occurs near the sea surface (Fu et al., 2006) and scavenges only

lower atmospheric substances (Ali et al., 2004), precipitation removes the substances existing in the whole air column below clouds (Deboudt et al., 2004). The high Mg^{2+}/Na^{+}, K^{+}/Na^{+} and Ca^{2+}/Na^{+} ratios in rainwater therefore suggest that most of these ionic species in rainwater were derived from crustal sources, and that scavenging processes of aerosols by sea fog are different to those by rain.

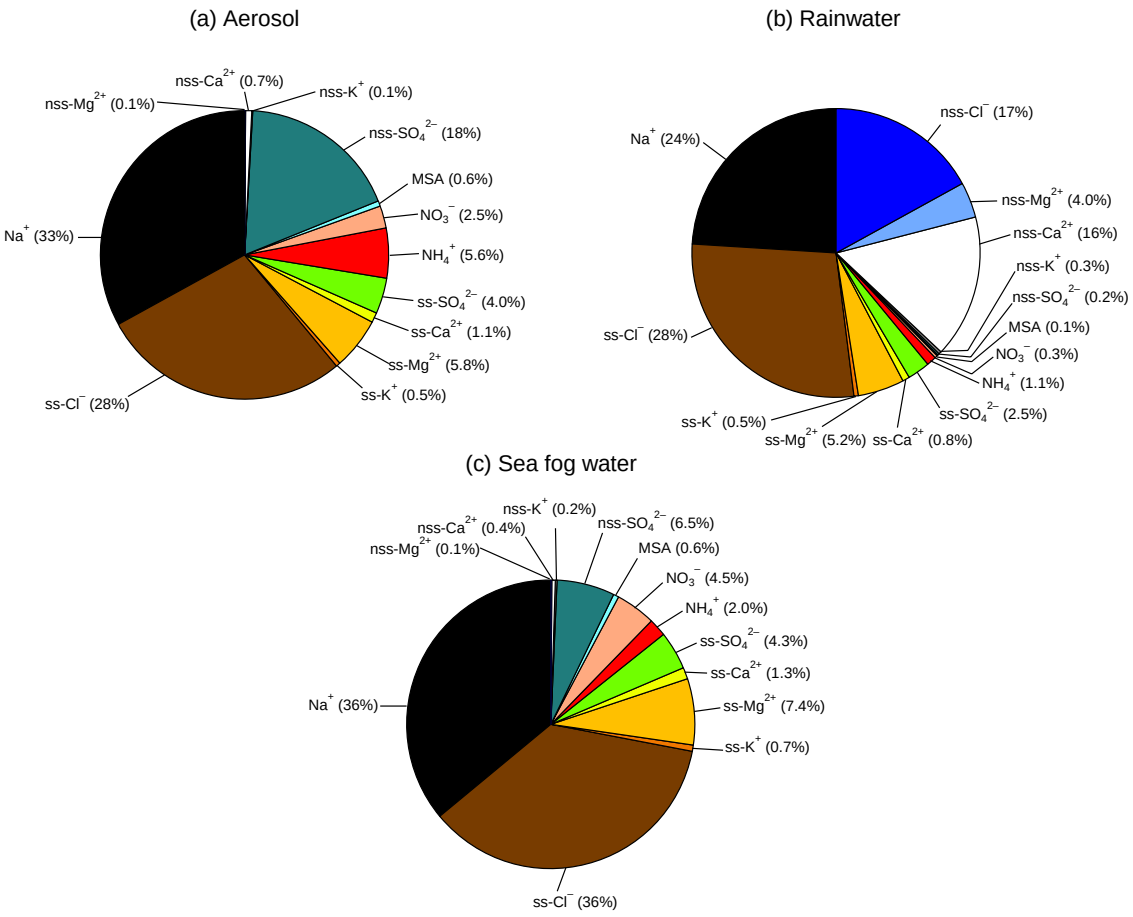

Fig. 4.4. Mean contributions of each major ionic component to total ionic concentration in (a) aerosols (n = 11), (b) rainwater (n = 7), and (c) sea fog water (n = 15) collected over the subarctic western North Pacific Ocean during Leg 1 of the KH-08-2 cruise.

Table 4.1 Mean concentrations of major ionic species in aerosols, rainwater and sea fog water collected over the subarctic western North Pacific during the KH-08-2 cruise (Leg 1)[a]

		Concentration												
	pH	Na^+	NH_4^+	K^+	Mg^{2+}	Ca^{2+}	Cl^-	NO_3^-	SO_4^{2-}	MSA	nss-SO_4^{2-}	nss-K^+	nss-Ca^{2+}	nss-Mg^{2+}	nss-Cl^-
Aerosol (n = 11)							Unit: neq m^{-3}								
Average	-	33	5.6	0.59	5.9	1.8	28	2.5	22	0.62	18	0.068	0.66	0.12	-
Std[b]	-	22	1.9	0.46	4.3	1.2	25	1.4	8.3	0.50	9.0	0.10	0.57	0.35	-
n[c]	-	11	11	11	11	11	11	11	11	11	11	9	11	2	-
Rain (n = 7)							Unit: μeq L^{-1}								
Average	4.1	580	25	19	220	400	1100	7.9	66	0.42	5.5	7.0	380	95	420
Std[b]	0.37	820	20	20	290	540	1200	6.9	82	0.69	6.9	7.8	520	160	610
n[c]	5	7	7	7	7	7	7	7	7	6	5	7	7	5	7
Sea fog (n = 15)							Unit: μeq L^{-1}								
Average	4.2	390	22	9.3	83	20	400	50	120	6.2	72	1.7	4.6	1.1	-
Std[b]	0.64	570	13	13	130	27	580	40	71	6.7	58	1.5	5.2	2.3	-
n[c]	15	15	15	15	15	15	15	15	15	15	14	14	12	5	-

[a]Negative values that arise for non-sea salt ionic species as a result of analytical uncertainty and samples where concentration of each ionic component was below the detection limit have been included in the calculation of the average as 0.

[b]Std represents standard deviation.

[c]Sample number of each ionic component detected (or calculated) in aerosols, rainwater and sea fog water.

Table 4.2 Mole equivalent ratios for major ionic species in aerosols, rainwater and sea fog water[a]

	Aerosol	Rain	Sea fog	Seawater[b]
Cl^-/Na^+	0.79	2.7	1.0	1.17
Mg^{2+}/Na^+	0.19	0.42	0.19	0.22
K^+/Na^+	0.021	0.051	0.031	0.021
Ca^{2+}/Na^+	0.073	1.2	0.069	0.044
SO_4^{2-}/Na^+	1.4	0.15	0.92	0.12
nss-SO_4^{2-}/Na^+	1.3	0.047	0.86	-
NO_3^-/Na^+	0.099	0.029	0.43	-
NH_4^+/Na^+	0.34	0.10	0.16	-
NO_3^-/nss-SO_4^{2-}	0.19	0.81	0.57	-
NH_4^+/nss-Ca^{2+}	12	0.14	28	-
NH_4^+/nss-Mg^{2+}	17	0.82	11	-

[a]The samples with negative value of non-sea salt ionic component were excluded.

[b]Seawater ratios from Keene et al. (1986).

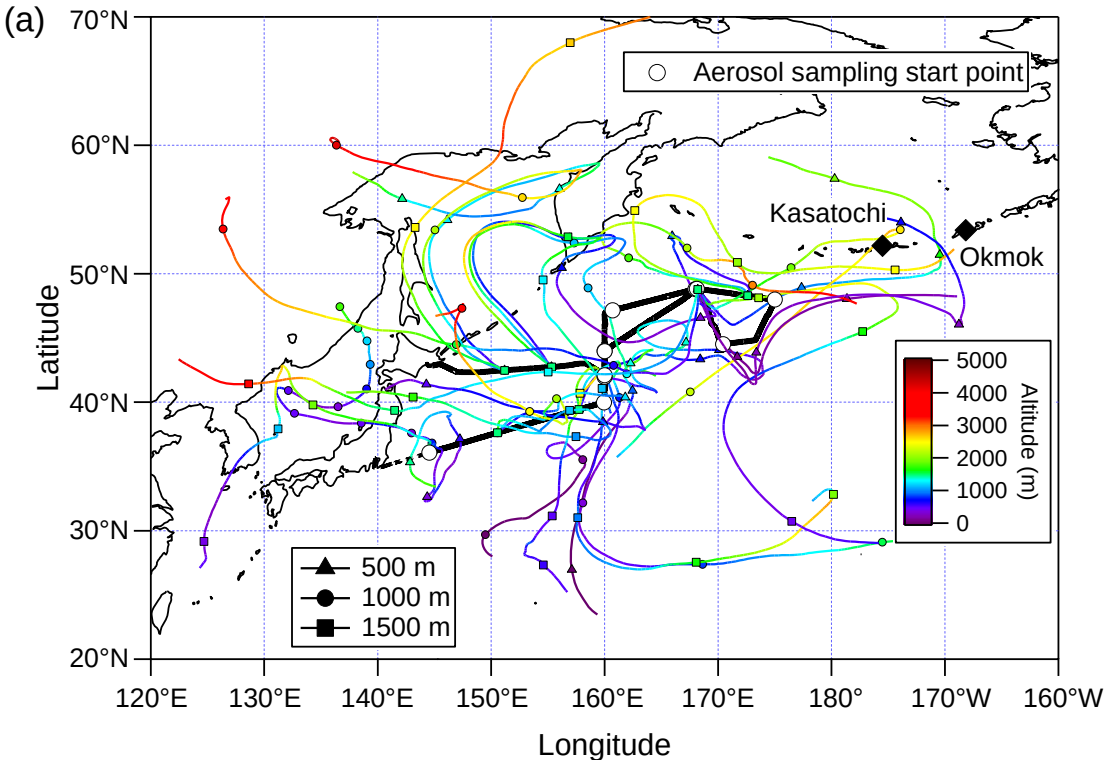
(a)
70°N
60°N
50°N
40°N
30°N
20°N
Latitude
120°E
130°E
140°E
150°E
160°E
170°E
180°
170°W
160°W
Longitude
Aerosol sampling start point
Kasatochi
Okmok
500 m
1000 m
1500 m
5000
4000
3000
2000
1000
0
Altitude (m)

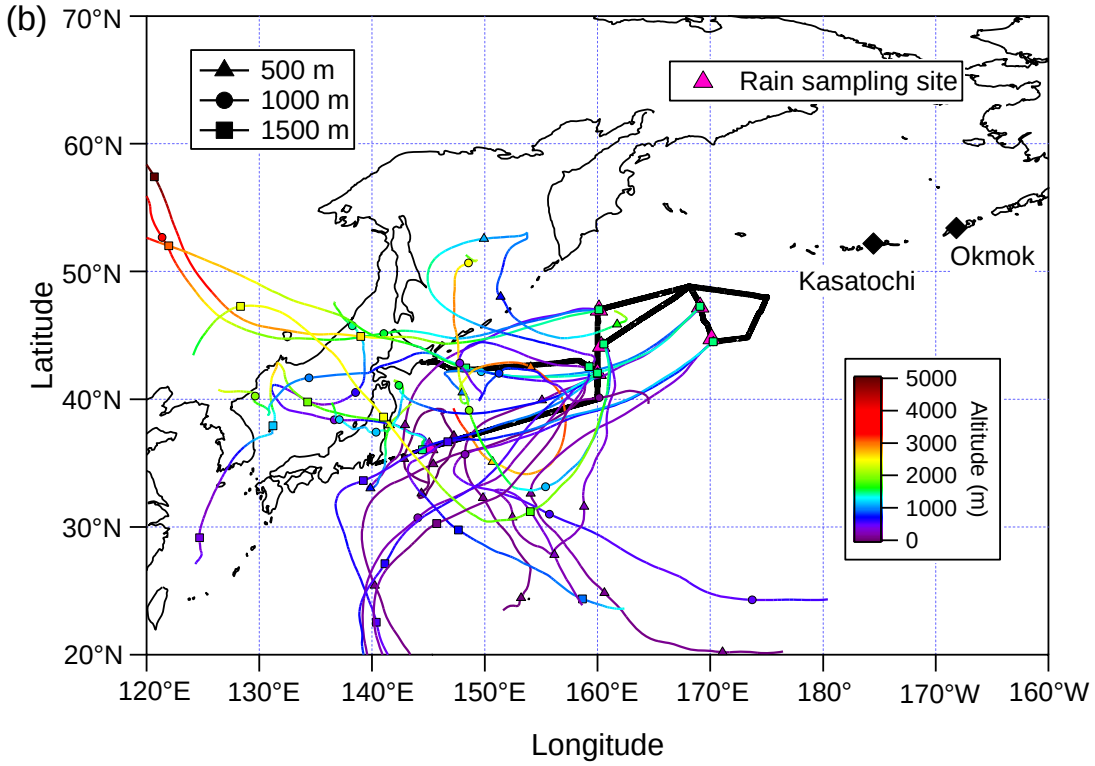
(b)
70°N
60°N
50°N
40°N
30°N
20°N
Latitude
120°E
130°E
140°E
150°E
160°E
170°E
180°
170°W
160°W
Longitude
500 m
1000 m
1500 m
Rain sampling site
Okmok
Kasatochi
5000
4000
3000
2000
1000
0
Altitude (m)

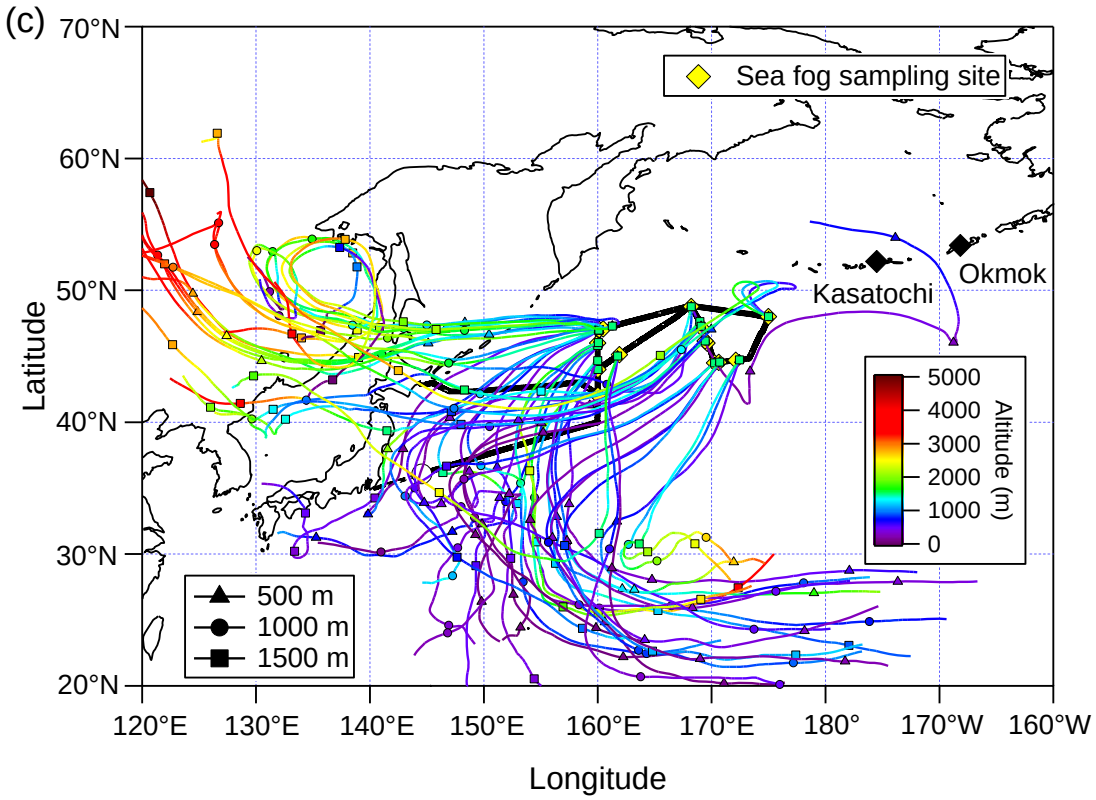

Fig. 4.5. The 168 h (7 days) air mass backward trajectories for starting altitudes of 500 (triangle symbols), 1000 (circle symbols) and 1500 m (square symbols) above ground level (AGL) during the collections of aerosol (a), rain (b) and sea fog (c) samples (Leg 1 of the KH-08-2 cruise) were calculated from the GDAS database of the National Ocean and Atmospheric Administration (NOAA) and simulated by using the Hybrid Single-Particle Langrangian Integrated Trajectory (HY-SPLIT) model (web site http://www.arl.noaa.gov/ready/hysplit4.html). White circles, pink triangles and yellow diamonds indicate aerosol, rain and sea fog sampling locations during the cruise, respectively. Kasatochi and Okmok volcanoes are black diamonds.

4.5. The pH of rainwater and sea fog water

The pH values of rainwater and sea fog water varied from 3.5–4.5 and 3.4–5.9, with averages of 4.1 ± 0.37 and 4.2 ± 0.64, respectively (Table 4.1). Several compounds, such as H_2SO_4, HNO_3, HCl, NH_3 and $CaCO_3$, contribute to the acid-base balance of rainwater and fog water (Millet et al., 1996).

The mean nss-Cl^- concentration in rainwater was two orders of magnitude greater than those of nss-SO_4^{2-} and NO_3^- (Table 4.1), suggesting that nss-Cl^- exerted a larger influence on acidity of rainwater collected over the subarctic western North Pacific Ocean. Assuming the nss-SO_4^{2-}, NO_3^- and nss-Cl^- in rainwater existed in the form of free acids, the expected pH of rainwater was 3.4. This discrepancy indicates that rainwater had experienced some neutralization. From the difference between the sum of nss-SO_4^{2-}, NO_3^-, nss-Cl^- and the mean H^+ concentration obtained from the mean pH value, it was estimated that approximately 61% of these acidic substances was in neutralized forms. The mean concentrations of nss-Ca^{2+} and nss-Mg^{2+}, tracers of crustal origin (Wang et al., 2005), in rainwater were 15 times and 3.8 times higher than that of NH_4^+, respectively (Table 4.1). Moreover, the mole equivalent ratios of NH_4^+/nss-Ca^{2+} and NH_4^+/nss-Mg^{2+} in rainwater were lower than 1, suggesting that nss-Ca^{2+} and nss-Mg^{2+} played key roles in neutralization of rainwater acidity.

In sea fog water, nss-SO_4^{2-} and NO_3^- were the dominant acidic species (Fig. 4.4 and Table 4.1). The mole equivalent ratio of NO_3^-/nss-SO_4^{2-} in sea fog water was 0.57 (Table 4.2). This result suggests that nss-SO_4^{2-} was the major component to lower the pH of sea fog, and that the pH of sea fog water was controlled by nss-SO_4^{2-} derived mainly from marine biological activity than that of rainwater since mean concentrations of MSA and nss-SO_4^{2-} in sea fog water were an order of magnitude greater than those in rainwater (Table 4.1 and see section 4.7). For sea fog water, it was estimated that approximately 48% of nss-SO_4^{2-} and NO_3^- was in neutralized forms. While nss-Ca^{2+} and nss-Mg^{2+} were the dominant neutralization substances in rainwater, NH_4^+ was the major basic component in sea fog water (Fig. 4.4 and Table 4.2), suggesting that neutralization of sea fog water was predominantly caused by NH_4^+, and that nss-SO_4^{2-} and NO_3^- in sea fog water were probably in fully or partially neutralized forms, such as ammonium sulfate ($(NH_4)_2SO_4$), ammonium bisulfate (NH_4HSO_4) and ammonium nitrate (NH_4NO_3).

4.6. Concentrations of NH_4^+ and NO_3^- in aerosols, rainwater and sea fog water

4.6.1. Aerosols

Total concentrations of NH_4^+ and NO_3^- in bulk (fine + coarse) aerosols ranged from 2.9–9.8 neq m^{-3} and 0.64–5.6 neq m^{-3}, respectively (Figs. 4.6a and 4.6b). Mean concentrations of aerosol inorganic N species were 5.6 ± 1.9 neq m^{-3} for NH_4^+ and 2.5 ± 1.4 neq m^{-3} for NO_3^-, accounting for ~70% by NH_4^+ and ~30% by NO_3^- of aerosol total inorganic N (i.e., TIN = NH_4^+ + NO_3^-) (Table 4.1). Sasakawa and

Uematsu (2002) reported that mean concentrations of NH_4^+ and NO_3^- in aerosols collected over the Northwestern North Pacific Ocean from 15–29 July 1998, were 11 ± 2.9 neq m^{-3} and 3.7 ± 2.2 neq m^{-3}, respectively. In comparison, the results for NH_4^+ and NO_3^- in this study were about 49% and 33% lower than their results, respectively. During the sampling period, over a dozen sea fog events occurred and aerosol samples, A03–A06 and A08–A09, were largely affected by these fog appearance. As shown in Figs. 4.6a and 4.6b, NO_3^-, which mainly existed in coarse mode aerosols, was more efficiently scavenged by sea fog than NH_4^+. The low mean NH_4^+ and NO_3^- concentrations thus are likely due to the influences of sea fog.

Ammonium is primarily associated with fine mode aerosol and produced by heterogeneous reactions involving NH_3 derived from intensive agricultural activity (Aneja et al., 2001), biomass burning (Andreae and Merlet, 2001) and a relatively weak marine source (Jickells et al., 2003). It is also known that NO_3^- in the marine atmosphere is predominantly associated with coarse mode aerosol as a result of a chemical reaction between HNO_3 derived primarily from NO_x emissions from combustion processes and sea-salt (Andreae and Crutzen, 1997). Mean percentages of total aerosol concentration in the fine mode for NH_4^+ and NO_3^- were ~84% and ~36%, respectively. These values were similar to the results of Nakamura et al. (2005), who reported the size distributions of NH_4^+ and NO_3^- in aerosols collected over the East China Sea.

4.6.2. Rainwater

When sea fog and rain events occurred simultaneously, only rainwater was collected (Fig. 4.3). That sample was then considered as a rainwater sample (i.e., rainwater samples 3 and 4), although the rainwater sample contains sea fog water as well as rainwater, since sea fog water is deposited by rainwater during that time. Concentrations of NH_4^+ and NO_3^- in rainwater ranged from 4.1–55 μeq L^{-1} and 1.2–18 μeq L^{-1}, respectively (Figs. 4.6c and 4.6d). Mean concentrations of inorganic N species were 25 ± 20 μeq L^{-1} for NH_4^+ and 7.9 ± 6.9 μeq L^{-1} for NO_3^- (Table 4.1). These values were in the range of the observed NH_4^+ (1.7–67 μeq L^{-1}) and NO_3^- (2.4–26 μeq L^{-1}) concentrations in rainwater collected over the Northwestern North Pacific Ocean from 15–29 July 1998 (Sasakawa and Uematsu, 2002). Inorganic N in rainwater was composed of ~77% NH_4^+ and ~23% NO_3^- (mean values), suggesting that NH_4^+ is more abundant in rainwater collected over the subarctic western North Pacific Ocean, and that it is a more important inorganic N species supplied by wet deposition.

4.6.3. Sea fog water

Concentrations of NH_4^+ and NO_3^- in sea fog water ranged from 4.2–45 μeq L^{-1} and 1.8–139 μeq L^{-1}, respectively (Figs. 4.6e and 4.6f). Contributions of NH_4^+ and NO_3^- to TIN in sea fog water were found

to represent ~39% (mean concentration 22 ± 13 μeq L^{-1}) and ~61% (mean concentration 50 ± 40 μeq L^{-1}), respectively (Table 4.1). Sasakawa and Uematsu (2002) reported that mean NH_4^+ and NO_3^- concentrations in sea fog water collected over the Northwestern North Pacific Ocean from 15–29 July 1998, were 25 ± 17 μeq L^{-1} and 25 ± 22 μeq L^{-1}, respectively. The mean NH_4^+ concentration observed in this study was comparable to their result; however, the mean concentration of NO_3^- was a factor of 2 higher than their result for NO_3^-. This different concentration may be related to the duration, frequency of sea fog events and changes in the quality of air mass.

If the fog solute concentration is predominantly controlled by condensation and evaporation processes, it is inversely proportional to LWC (Minami and Ishizaka, 1996). Elbert et al. (2000) observed an inverse relationship between the measured ion concentrations and the LWC of fog, and reported that LWC level is the primary control on the concentration of water-soluble species in fog. In this study, Na^+ concentration in sea fog water showed an inverse relationship with mean total LWC (Figs. 4.7a and 4.7b), except sea fog samples, F02, F05 and F11, indicating that sea salt particles acted predominantly as condensation nuclei of sea fog droplets. As shown in Fig. 4.3, these sea fog samples, F02, F05 and F11, were collected after large sea fog droplets were deposited, suggesting that the Na^+ concentration and LWC of these samples were affected by deposition process. In contrast, no pronounced inverse relationships were found between NH_4^+, NO_3^- concentrations and mean total LWC (Figs. 4.7c and 4.7d). In some of sea fog water samples, the concentrations of NH_4^+ and NO_3^- in sea fog water did not decrease when mean total LWC increased and vice versa (Figs. 4.6e and 4.6f). Minami and Ishizaka (1996) found that during the mature stage of a fog event, LWC could not always explain the temporal variation in fog solute concentrations because of dissolution of water-soluble gases. Raja et al. (2008) reported that the chemical composition of fog droplets is determined by nucleation of droplets on a subset of particles that act as condensation nuclei, scavenging of other non-activated aerosol particles, uptake of water-soluble gases, aqueous phase chemical reactions occurring inside the droplets and dilution of fog solutes by condensational droplet growth. The relationships between NH_4^+, NO_3^- concentrations in sea fog water and mean total LWC therefore are likely affected by many factors mentioned by Raja et al. (2008), which may result in the unclear relationships between NH_4^+, NO_3^- and LWC.

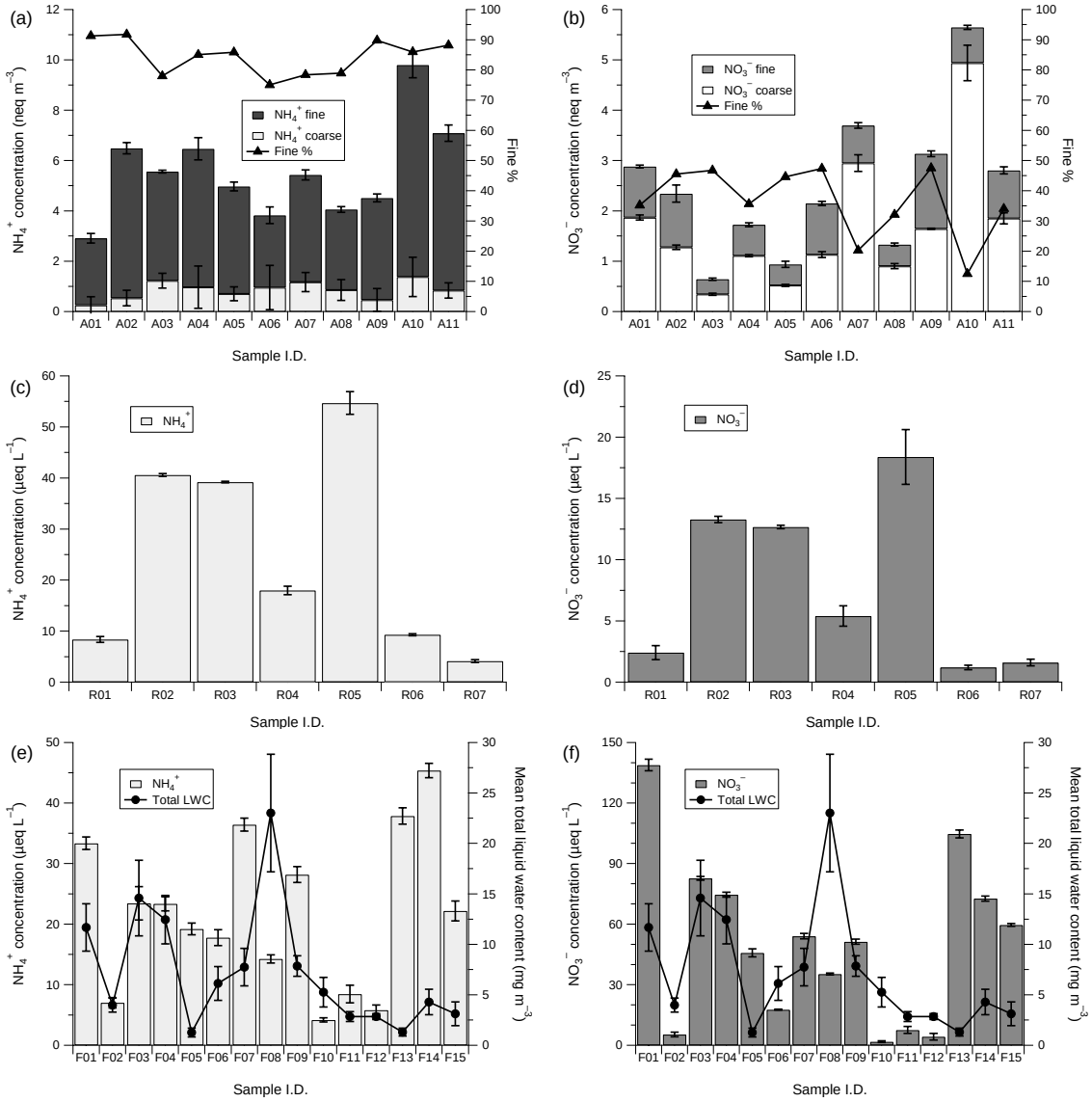

Fig. 4.6. Concentrations of NH_4^+ and NO_3^- against sample I.D in aerosols (a, b), rainwater (c, d) and sea fog water (e, f) collected during Leg 1 of the KH-08-2 cruise. Solid triangle lines in (a) and (b) and solid circle lines in (e) and (f) show the percentage of NH_4^+ and NO_3^- in fine (D < 2.5 μm) aerosol particles and the mean total LWC of each sea fog water sample, respectively.

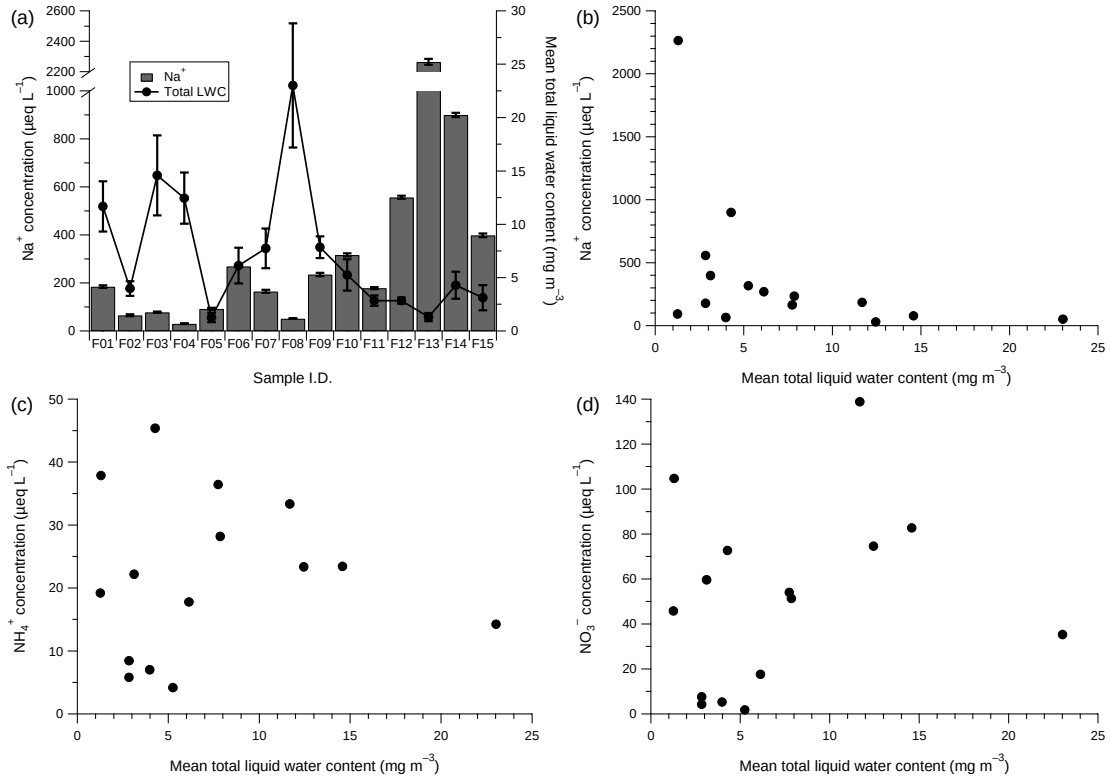

Fig. 4.7. Concentration of Na^+ against sample I.D in sea fog water (a) collected during Leg 1 of the KH-08-2 cruise, and the relationships between (b) Na^+, (c) NH_4^+, (d) NO_3^- concentrations in sea fog water and mean total LWC. Solid circle line in (a) shows the mean total LWC of each sea fog water sample.

4.7. Difference of scavenging process between rain and sea fog

Mean concentrations of NO_3^-, MSA and nss-SO_4^{2-} in sea fog water were higher than those in rainwater (Tables 4.1 and 4.3), suggesting that they were more effectively scavenged by sea fog droplets with their higher surface-to-volume ratios and longer atmospheric residence times (Sasakawa and Uematsu, 2002; Sasakawa and Uematsu, 2005; Gioda et al., 2011).

The sea fog water/rainwater ratio for NH_4^+ was 0.88 (Table 4.3), suggesting that NH_4^+ was not scavenged by sea fog as efficiently as NO_3^-, MSA and nss-SO_4^{2-}. The mean NO_3^- concentration in sea fog water was 6.3 times higher than that in rainwater, whereas the mean NH_4^+ concentration in sea fog water was similar to that in rainwater. Sasakawa et al. (2003) reported that coarse particles (e.g., sea salt particles and $NaNO_3$) act predominantly as condensation nuclei of sea fog droplets rather than NH_4^+ and nss-SO_4^{2-} particles, such as $(NH_4)_2SO_4$ and NH_4HSO_4 since aerosol NH_4^+ and nss-SO_4^{2-} are largely associated with the fine mode ($D < 2.5$ μm) particles (Nakamura et al., 2005). In addition, NH_3 readily reacts with acids in the atmosphere to form NH_4^+ aerosols that can act as cloud condensation nuclei (Spokes et al., 2000). In this study, it was observed that larger particles ($D > 0.5$ μm) preferentially became activated and the fog droplet size distribution was shifted towards the larger droplet sizes (Fig. 4.3), and that NH_4^+ and NO_3^- were largely associated with fine and coarse mode aerosols, respectively (Figs. 4.6a and 4.6b). Therefore, higher NO_3^- concentration in sea fog water than in rainwater is likely due to preferential behaviors of coarse particles as condensation nuclei in sea fog.

While MSA is formed exclusively from dimethylsulfide (DMS) produced by phytoplankton in the ocean, non sea-salt SO_4^{2-} has a variety of sources, including DMS oxidation, volcanic and industrial sulfur emissions (Gondwe et al., 2003). Dimethylsulfide is emitted into the atmosphere, where it undergoes chemical transformation to eventually form gaseous (e.g., MSA and SO_2) and/or particulate (e.g., MSA and nss-SO_4^{2-}) sulfur species (e.g., Charlson et al., 1987; Bardouki et al., 2003). Mean concentrations of MSA and nss-SO_4^{2-} in sea fog water were 15 times and 13 times higher than those in rainwater, respectively (Tables 4.1 and 4.3). During the sampling period, SeaWiFS satellite images revealed high chlorophyll a levels (http://oceancolor.gsfc.nasa.gov) in the subarctic western North Pacific Ocean (Fig. 4.8). Considering sea fog occurs near the sea surface where DMS is emitted, these results suggest that sea fog scavenged biogenic sulfur species more effectively than rain (Sasakawa and Uematsu, 2005).

If aerosol particles exert the primary influence as condensation nuclei of sea fog droplets, there would be no difference in the mole equivalent ratios between aerosols and sea fog water (Sasakawa and Uematsu, 2002; Gioda et al., 2011). The mole equivalent ratio of NO_3^-/Na^+ in sea fog water was higher than that in aerosols (Table 4.2), whereas the NO_3^-/Na^+ ratio in rainwater was lower than in aerosols. These results suggest that not only aerosol NO_3^-, but also gaseous HNO_3 was scavenged by sea fog water, and that scavenging of sea salt particle by rain via inertial impaction exerted a larger influence on

the ratio. Nitric acid is highly soluble in water. Once a large amount of liquid water has amassed, the gas phase HNO_3 is rapidly dissolved (Fahey et al., 2005). In order to estimate the fraction of HNO_3 scavenged by sea fog water, the NO_3^-/Na^+ ratios in aerosols was compared to those in sea fog water (Fig. 4.9a). In 8 sea fog samples, the higher NO_3^-/Na^+ ratios than in aerosols were observed when sea fogs were in growth periods, and air masses originated from the subtropical western North Pacific Ocean circulated around the vicinity of the Japanese Islands and thereafter reached the sea fog sampling sites (Figs. 4.3 and 4.5c). In this study, it was estimated that 25–94% (mean 74%) of NO_3^- in the 8 sea fog water samples was derived from the dissolution of HNO_3, suggesting that sea fog over the subarctic western North Pacific Ocean is an important removal mechanism for gas phase HNO_3.

Ammonia is emitted into the atmosphere from the ocean as a result of biological activity (Quinn et al., 1988). As shown in Fig. 4.8, chlorophyll a concentrations were high over the subarctic western North Pacific Ocean during the sampling period. It is therefore expected that, likewise MSA, NH_3 derived from marine biological activity could be scavenged by sea fog. The NH_4^+/Na^+ ratios in sea fog water for all periods, however, were lower than those in aerosols (Fig. 4.9b). This result suggests that aerosol NH_4^+ was affected by strong terrestrial-derived NH_4^+ in addition to NH_4^+ produced by marine biota over the subarctic western North Pacific Ocean, and that sea salt particles exerted a greater influence on the NH_4^+/Na^+ ratios in sea fog water due to condensation occurred preferably on coarse particles.

Table 4.3 Sea fog water/rainwater ratios for major ionic species[a]

	Sea fog water/Rainwater
Na^+	0.67
NH_4^+	0.88
ss-K^+	0.63
ss-Mg^{2+}	0.66
ss-Ca^{2+}	0.77
ss-Cl^-	0.59
NO_3^-	6.3
ss-SO_4^{2-}	0.79
MSA	15
nss-SO_4^{2-}	13
nss-K^+	0.24
nss-Ca^{2+}	0.012
nss-Mg^{2+}	0.012

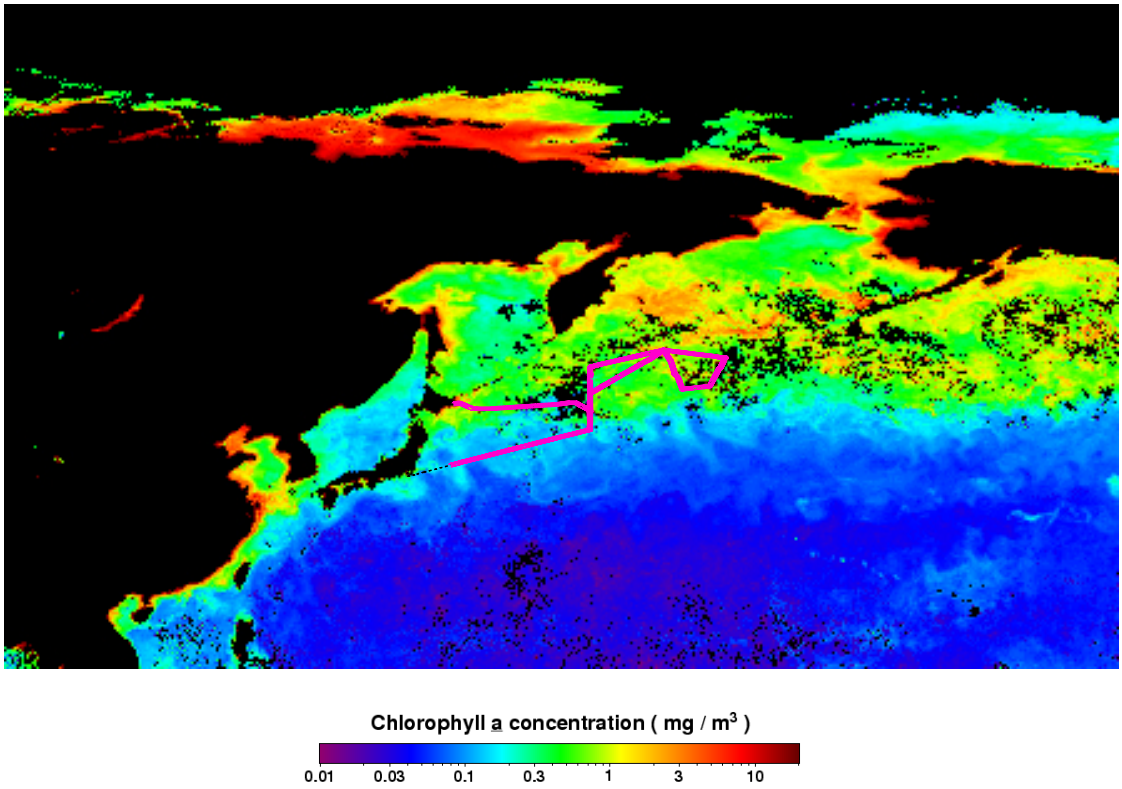

Fig. 4.8. SeaWiFS chlorophyll a image of the subarctic western North Pacific Ocean in August 2008 (web site: http://oceancolor.gsfc.nasa.gov) and cruise track (pink line) of Leg 1 of the KH-08-2 cruise.

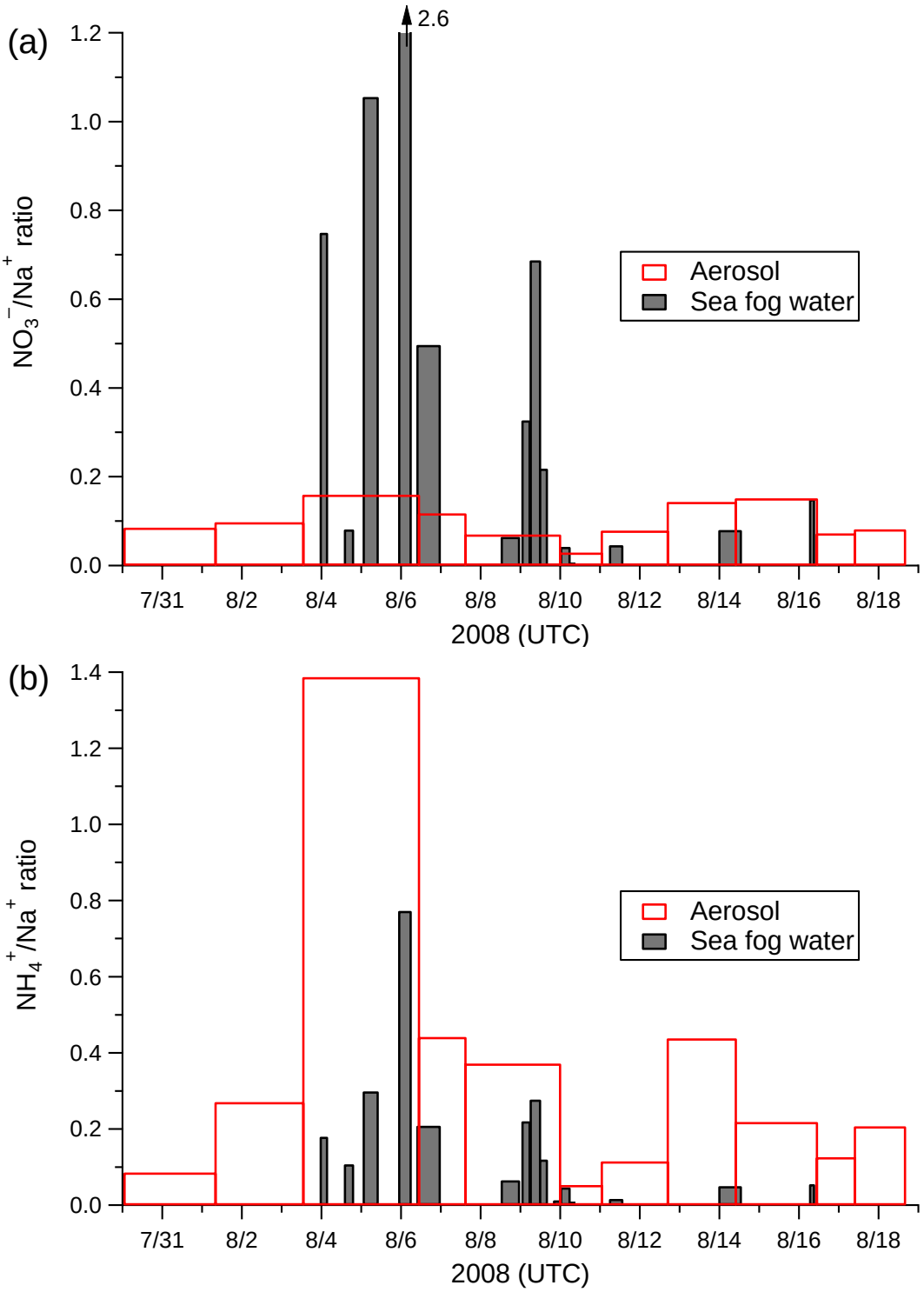

Fig. 4.9. The ratios of NO_3^-/Na^+ (a) and NH_4^+/Na^+ (b) in aerosols and sea fog water during Leg 1 of the KH-08-2. The widths of red open and gray bars indicate the sampling duration of aerosol and sea fog water samples, respectively.

4.8. Deposition flux estimates

4.8.1. Dry deposition

Dry deposition fluxes (F_d) were calculated from aerosol concentrations (C_a) in the coarse (c) and fine (f) modes and dry deposition velocities (V_d) for each size mode (Duce et al., 1991; Baker et al., 2007):

$$F_d = C_a^c \times V_d^c + C_a^f \times V_d^f \qquad (1)$$

Here, V_d of 2 cm s^{-1} for coarse mode and 0.1 cm s^{-1} for fine mode were used since these two values are known to be best estimates based on experimental and model studies (Duce et al., 1991; Baker et al., 2003; Nakamura et al., 2005). This estimate results in an uncertainty of a factor of 2–3 in the calculated flux, since deposition velocity includes terms for gravitational settling, impaction and diffusion of particles, all of which vary in complex functions of particle size and meteorological conditions (e.g., wind speed and relative humidity) (Duce et al., 1991).

4.8.2. Wet deposition

Wet deposition fluxes (F_w) were estimated from the concentration of the species of interest in rainwater (C_r) and the precipitation rate (P) (Baker et al., 2010):

$$F_w = C_r \times P \qquad (2)$$

The precipitation rate was calculated from the monthly averaged precipitation rate (mm d^{-1}) using the CMAP model output (http://www.cdc.noaa.gov/cdc/data.cmap.html) (Xie and Arkin 1997). Similar to estimates for dry deposition flux, the choice of precipitation rates based on limited data causes the greatest uncertainty in wet deposition flux estimates, particularly in the open ocean (Spokes et al., 2000). Baker et al. (2010 and references therein), who used the same method for estimating wet deposition flux, argued that the uncertainty arising from selection of precipitation rate is minor since the precipitation rate data agreed relatively well with other studies in terms of total rainfall amount.

4.8.3. Sea fog deposition

Sea fog deposition fluxes (F_f) were estimated by multiplying sea fog water flux (F_{fw}) of each event by the concentration of the species of interest in each sea fog water sample (C_f) (Thalmann et al., 2002):

$$F_f = F_{fw} \times C_f \quad (3)$$

The F_{fw} was estimated according to equation 4, where $LWC(D_p)$ represents the mean LWC for each of the 40 droplet size classes during each sea fog event and $V(D_p)$ the deposition velocity for sea fog droplets with an aerodynamic diameter. The sum of sea fog water flux for all size classes then yielded the F_{fw}.

$$F_{fw} = \sum LWC(D_p) \times V(D_p) \quad (4)$$

Size distribution of mean LWC for each sea fog event is shown in Fig. 4.10. For $V(D_p)$, the modeled values reported by Matsumoto et al. (2011), who calculated the deposition velocities for the particles with diameters larger than 3 μm, were used (i.e., 4.69 cm s^{-1} for 3 μm < D < 5 μm, 10.1 cm s^{-1} for 5 μm < D < 10 μm, 13.5 cm s^{-1} for 10 μm < D < 20 μm, 15.6 cm s^{-1} for 20 μm < D < 30 μm and 19.0 cm s^{-1} for 30 μm < D < 50 μm). This ambiguity in values used for sea fog deposition velocities leads to the greatest uncertainty in sea fog flux estimates.

In this study, it was assumed that all sea fog droplets measured with the fog monitor were deposited to the sea surface without changes in size distribution of LWC; however, due to evaporation and coalescence of sea fog droplets, their size and deposition velocities are subject to change, suggesting that the deposition velocities used here leads to the uncertainty in sea fog deposition flux estimates. The fog water sampler used in this study has a 50% efficiency collection diameter of 6 μm under flow rate 3 m s^{-1} (Minami and Ishizaka, 1996). It is difficult, however, to calculate the precise collection efficiency of this fog sampler in this study, because the relative wind directions and the relative wind speeds change extremely with the movements of the ship (Sasakawa and Uematsu, 2005). Hence, the estimates of sea fog deposition fluxes in this study contain the uncertainties that are related to the changes in size distribution of LWC and the collection efficiency.

4.9. Contributions of dry, wet and sea fog deposition to atmospheric inputs of nitrogen to the subarctic western North Pacific Ocean

Temporal variations of dry, wet and sea fog deposition fluxes for NH_4^+ and NO_3^- during the sampling period are shown in Fig. 4.11. The estimated dry deposition fluxes for atmospheric inorganic N species ranged from 0.67–3.1 μmol m^{-2} d^{-1} for NH_4^+ and from 0.62–8.6 μmol m^{-2} d^{-1} for NO_3^-, contributing ~43% by NH_4^+ and ~57% by NO_3^- to the dry deposition flux for TIN. Mean dry deposition fluxes for NH_4^+ and NO_3^- were estimated to be 1.9 ± 0.67 μmol m^{-2} d^{-1} and 3.0 ± 2.2 μmol m^{-2} d^{-1}, respectively. Although the mean concentration of total NH_4^+ in aerosols collected over the subarctic western North Pacific Ocean was approximately 2 times higher than that of total NO_3^- (Table 4.1), inorganic N supplied to

surface waters by atmospheric dry deposition was mainly from NO_3^-, which was largely associated with coarse mode particles, since fluxes to the ocean are dominated by the coarse mode, resulting in NO_3^- being deposited much more rapidly (Figs. 4.6a and 4.6b).

Wet deposition of atmospheric inorganic N was highly variable from one event to the next depending on the concentrations of NH_4^+ and NO_3^- in the precipitation as well as the frequency and amount of precipitation. Wet deposition fluxes of atmospheric inorganic N species ranged from 3.5 to 98 (mean 25 ± 35) μmol m^{-2} d^{-1} for NH_4^+ and from 1.0 to 32 (mean 8.0 ± 12) μmol m^{-2} d^{-1} for NO_3^-, accounting for ~77% by NH_4^+ and ~23% by NO_3^- of TIN from wet deposition flux. While NO_3^- was the dominant inorganic N species in dry deposition, inorganic N supplied to surface waters by atmospheric wet deposition was predominantly by NH_4^+ (72–89% of the wet deposition fluxes for TIN).

Likewise wet deposition, sea fog deposition of atmospheric inorganic N was highly variable depending on the size distribution of LWC, the amount of LWC and the duration of sea fog event as well as the concentrations of NH_4^+ and NO_3^- in the sea fog water. The estimated sea fog deposition fluxes for atmospheric inorganic N species ranged from 0.18–5.2 μmol m^{-2} d^{-1} for NH_4^+ and from 0.13–22 μmol m^{-2} d^{-1} for NO_3^-, contributing ~39% by NH_4^+ and ~61% by NO_3^- to the sea fog deposition flux for TIN. Mean sea fog deposition fluxes for NH_4^+ and NO_3^- were estimated to be 2.1 ± 1.9 μmol m^{-2} d^{-1} and 5.7 ± 6.9 μmol m^{-2} d^{-1}, respectively, indicating that inorganic N supplied to surface waters by sea fog deposition was mainly from NO_3^-, since aerosol NO_3^- and HNO_3 were scavenged more effectively by sea fog as mentioned in section 4.7.

While dry deposition is a continuous process occurring at all times over all surfaces, wet and sea fog deposition are highly episodic. The relative importance of dry, wet and sea fog deposition obviously varies greatly on short time scales, and varies spatially on longer time scales with global rainfall patterns (Jickells, 2006) and trends in fog frequency (Gultepe et al., 2007). Mean total (dry + wet + sea fog) deposition flux of atmospheric TIN in the subarctic western North Pacific Ocean was estimated to be 46 ± 48 μmol m^{-2} d^{-1}, with 72% of this in the form of wet deposition (Table 4.4). This indicates that wet deposition plays an important role in the supply of atmospheric inorganic N to the subarctic western North Pacific Ocean compared to dry and sea fog deposition, although the relative contributions are highly variable. The estimate of the proportion of atmospheric N input via wet deposition were comparable to previously published values: the Pacific 86% (Duce et al., 1991), the Atlantic 78–85% (Baker et al., 2010), and the world oceans 71% (Duce et al., 1991).

Fog can lead to substantial N deposition if the event persists long enough (several hours) with sufficient LWC (dense fog), particularly for those formed in continental air masses (Jordan and Talbot, 2000). Although the mean contribution of sea fog deposition to total atmospheric TIN input to the subarctic western North Pacific Ocean was ~17% (Table 4.4), in some cases, atmospheric TIN deposition flux via sea fog exceeded the combined dry and wet deposition flux of TIN (Fig. 4.11), suggesting that sea fog can deposit as much N as a high N deposited by rain event, and that sea fog is an

important transfer process for atmospheric inorganic N from the marine atmosphere to the subarctic western North Pacific Ocean.

Table 4.4 Mean dry, wet, sea fog, and total deposition fluxes of NH_4^+ and NO_3^-, and the contribution of each deposition to total inorganic N input in the subarctic western North Pacific Ocean during Leg 1 of the KH-08-2 cruise

	Dry deposition flux ($\mu mol\ m^{-2}\ d^{-1}$)	Wet deposition flux ($\mu mol\ m^{-2}\ d^{-1}$)	Sea fog deposition flux ($\mu mol\ m^{-2}\ d^{-1}$)	Total deposition flux ($\mu mol\ m^{-2}\ d^{-1}$)
NH_4^+	1.9 ± 0.67 (4.1%)	25 ± 35 (54%)	2.1 ± 1.9 (4.6%)	29 ± 35 (63%)
NO_3^-	3.0 ± 2.2 (6.5%)	8.0 ± 12 (17%)	5.7 ± 6.9 (12%)	17 ± 14 (37%)
TIN[a]	4.9 ± 2.6 (11%)	33 ± 47 (72%)	7.8 ± 8.7 (17%)	46 ± 48 (100%)

[a]TIN represents total inorganic nitrogen. In this study, total inorganic nitrogen is defined as including NH_4^+ and NO_3^-; i.e., TIN = NH_4^+ + NO_3^-.

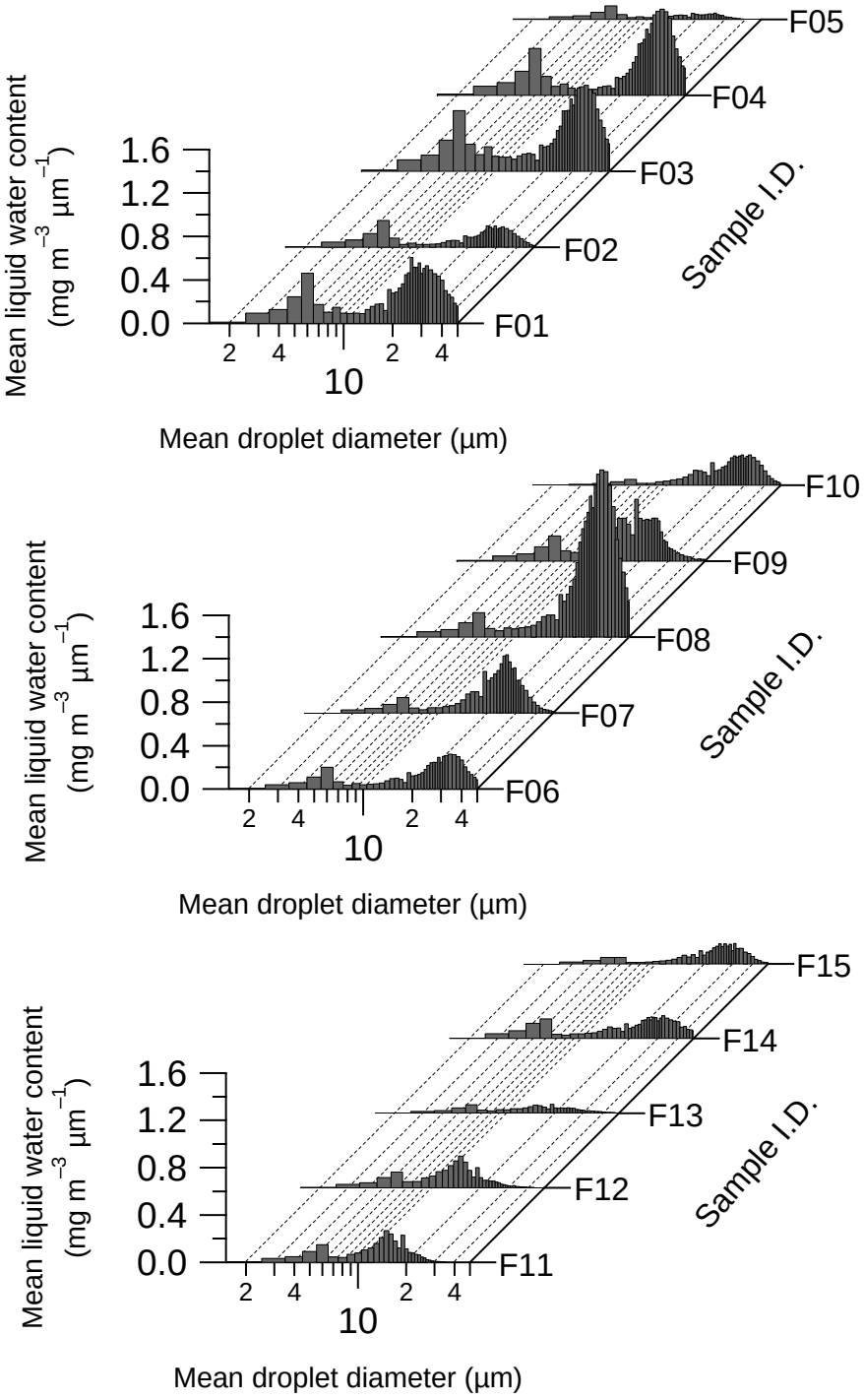

Fig. 4.10. Variations of mean LWC for each sea fog event as a function of mean droplet diameter during Leg 1 of the KH-08-2 cruise.

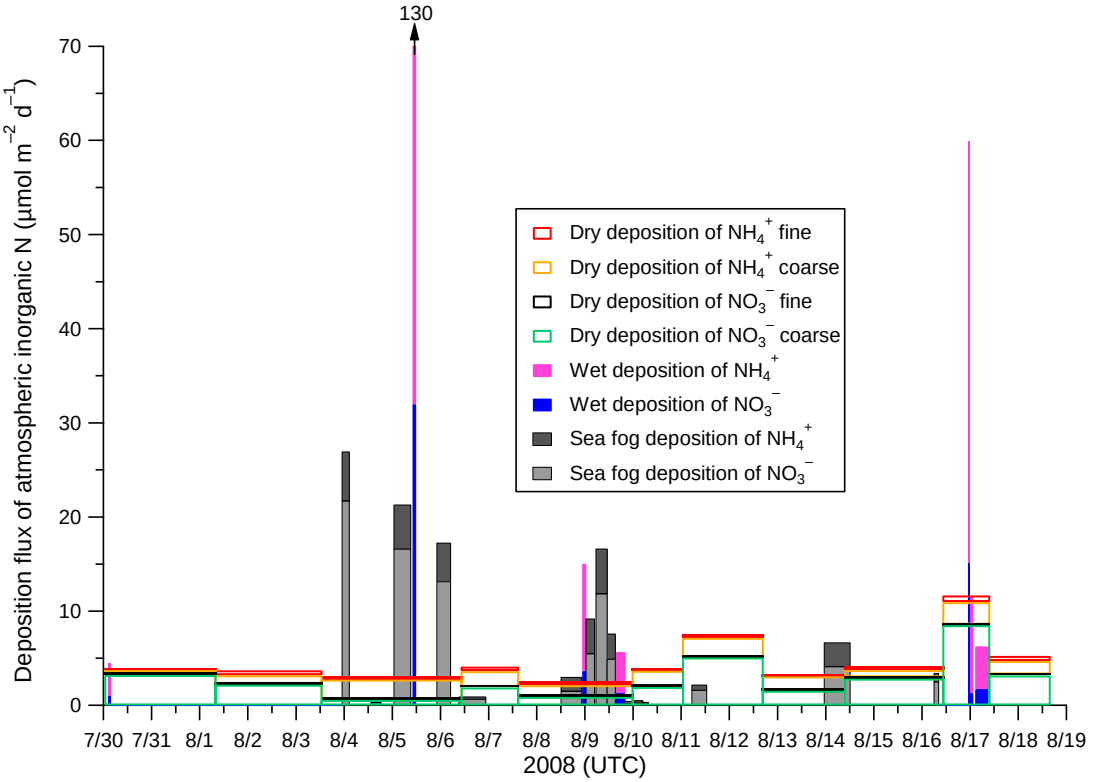

Fig. 4.11. Temporal variations of dry, wet and sea fog deposition fluxes for NH_4^+ and NO_3^- over the subarctic western North Pacific Ocean during Leg 1 of the KH-08-2 cruise.

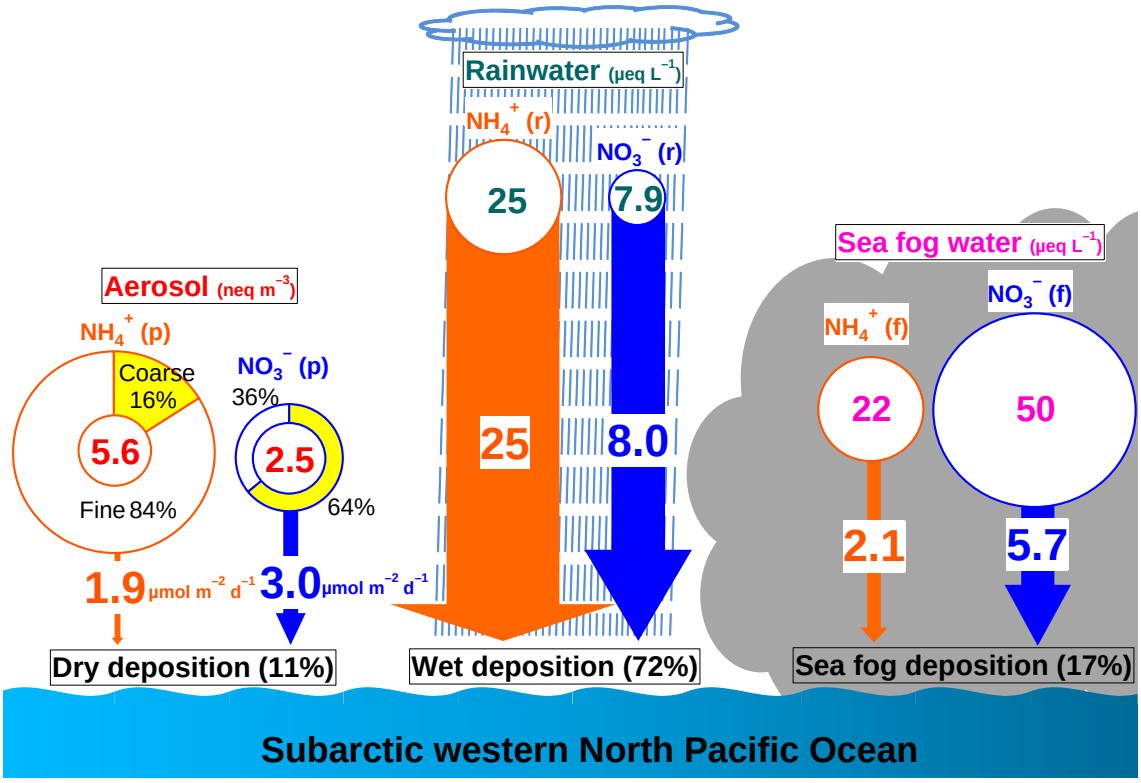

Fig. 4.12. Schematic diagram of atmospheric inorganic N input to the subarctic western North Pacific Ocean during 29 July–19 August 2008. The numbers in circles represent concentrations of NH_4^+ and NO_3^- in aerosols (in neq m^{-3}), rainwater (in μeq L^{-1}) and sea fog water (in μeq L^{-1}). The mean percentages of total (fine + coarse) aerosol concentrations in fine (white) and coarse (yellow) modes for NH_4^+ and NO_3^- are shown in circles for aerosol. The orange and blue arrows and numbers (in μmol m^{-2} d^{-1}) indicate NH_4^+ (orange) and NO_3^- (blue) fluxes via dry, wet and sea fog deposition.

4.10. Potential impact of atmospheric inorganic nitrogen deposition on primary production over the subarctic western North Pacific Ocean

The potential impact of atmospheric deposition on marine ecosystems depends on the nutrient status of the receiving waters, and is related to both the total amount and ratio of atmospherically supplied nutrients and to the limiting nutrient for the existing local water column (Baker et al., 2006). It is known that NH_4^+ and NO_3^- can be readily utilized by a variety of aquatic microorganisms (Gilbert et al., 1991). In order to evaluate the impact of atmospheric N on the marine ecosystem, potential primary production was estimated using the result for total deposition flux of TIN and the Redfield C/N ratio of 6.6. Assuming that phytoplankton can take up all the N coming from atmospheric deposition with no losses, and that there is no co limitation by other nutrients (i.e., P and Fe), total mean deposition flux of atmospheric TIN over the subarctic western North Pacific Ocean (46 ± 48 μmol m^{-2} d^{-1}) was found to be maximally responsible for the carbon uptake of 300 ± 320 μmol C m^{-2} d^{-1}. Elskens et al. (2008) reported that the integrated new primary production in the upper part of the euphotic zone at station K2 (47°N, 161°E) in the subarctic western North Pacific Ocean from 30 July 2005 to 18 August 2005 ranged from 67–119 mg C m^{-2} d^{-1} (5.6–9.9 mmol C m^{-2} d^{-1}). Wong et al. (2002) estimated that the annual new production from the surface (upper 50m) of the subarctic western North Pacific Ocean, which covers the sampling area of this study, to be 32.8–82.8 g C m^{-2} yr^{-1}. To facilitate evaluation, g C m^{-2} yr^{-1} units for the annual new production reported by Wong et al. (2002) were converted to the μmol C m^{-2} d^{-1} units used in this study. Based on these, the result of this study suggests that inorganic N deposited to the subarctic western North Pacific Ocean from the atmosphere can support 1.6–5.3% of the new primary production. Atmospheric inorganic N deposition, however, could be an important N source in the ocean where sporadic atmospheric N deposition events caused by the transport of the continental dust are affected and the supply of deep nutrient-rich water is restricted by the stratification of the surface ocean that is enhanced by global warming.

4.11. Conclusions

The subarctic western North Pacific Ocean (> 40°N) has a high frequency of sea fog, with a maximum of ~50% during the summertime period (June–August). The fog deposition is an important transfer process for atmospheric substances from the atmosphere to the biosphere. It is therefore suggested that sea fog may play a key role in supplying atmospheric nutrients to this region. Nevertheless, no study has been carried out over the subarctic western North Pacific Ocean to quantify sea fog deposition flux for atmospheric N. This is the first study to estimate atmospheric inorganic N fluxes via dry, wet and sea fog deposition over the subarctic western North Pacific Ocean simultaneously. The mean dry, wet and sea fog deposition fluxes for TIN were estimated to be 4.9 ± 2.6 μmol m^{-2} d^{-1}, 33

± 47 μmol m^{-2} d^{-1} and 7.8 ± 8.7 μmol m^{-2} d^{-1}, respectively. Wet deposition delivered more atmospheric inorganic N to the subarctic western North Pacific Ocean than dry and sea fog deposition, contributing ~72% to total deposition flux for TIN (46 ± 48 μmol m^{-2} d^{-1}), although the relative contributions are highly variable.

The mean contribution of sea fog deposition to total deposition flux for TIN was ~17%. Despite the relatively lower contribution of sea fog deposition, in some cases, atmospheric inorganic N input via sea fog deposition exceeded the combined dry and wet deposition fluxes. Thus, it is suggested that sea fog can result in substantial N deposition if the event persists long enough and has sufficient LWC (dense sea fog), and that ignoring sea fog deposition would lead to underestimate of the total influx of atmospheric inorganic N into the subarctic western North Pacific Ocean, especially in summer periods.

A schematic diagram of atmospheric inorganic N input to the subarctic western North Pacific Ocean via dry, wet and sea fog deposition is shown in Fig. 4.12. In dry deposition, NO_3^- was the dominant inorganic N species, accounting for ~57%. This reflects higher deposition velocity of NO_3^- than that of NH_4^+ since NO_3^- is largely associated with coarse mode particles in the marine atmosphere. In comparison, inorganic N supplied to surface waters by atmospheric wet deposition was predominantly by NH_4^+ (72–89% of the wet deposition fluxes for TIN), suggesting that NH_4^+ is more important inorganic N species supplied by wet deposition over the subarctic western North Pacific Ocean. The contributions of NH_4^+ and NO_3^- to the sea fog deposition flux for TIN were ~39% and ~61%, respectively, indicating that sea fog scavenged more effectively not only coarse mode particles (e.g., sea salt particles and $NaNO_3$) that acted as condensation nuclei of sea fog droplets, but also gaseous HNO_3.

In this study, atmospheric inorganic N input via dry, wet and sea fog deposition to the subarctic western North Pacific Ocean was estimated by simplified calculation (e.g., using assumption for sea fog water flux) during limited sampling period in the summer, but these results contributed to the understanding of atmospheric N cycle in open ocean environment. Further studies, however, are required to understand the biogeochemical cycles of N more clearly and should focus on long-term monitoring of atmospheric reactive N species, including organic N, in the subarctic western North Pacific Ocean.

References

Aikawa, M., Hiraki, T., Suzuki, M., Tamaki, M., Kasahara, M., 2007. Separate chemical characterizations of fog water, aerosol, and gas before, during, and after fog events near an industrialized area in Japan. Atmospheric Environment 41, 1950–1959.

Akimoto, H., 2003. Global air quality and pollution. Science 302, 1716–1719.

Ali, K., Momin, G.A., Tiwari, S., Safai, P.D., Chate, D.M., Rao, P.S.P., 2004. Fog and precipitation chemistry at Delhi, North India. Atmospheric Environment 38, 4215–4222.

Andreae, M.O., Crutzen, P.J., 1997. Atmospheric aerosols: biogeochemical sources and role in

atmospheric chemistry. Science 276(5315), 1052–1058.

Andreae, M.O., Merlet, P., 2001. Emission of trace gases and aerosols from biomass burning. Global Biogeochemical Cycles 15, 955–966.

Aneja, V.P., Roelle, P.A., Murray, G.C., Southerland, J., Erisman, J.W., Fowler, D., Asman, W.A.H., Patni, N., 2001. Atmospheric nitrogen compounds II: emissions, transport, transformation, deposition and assessment. Atmospheric Environment 35, 1903–1911.

Baker, A.R., Jickells, T.D., Biswas, K.F., Weston, K., French, M., 2006. Nutrient in atmospheric aerosol particles along the Atlantic Meridional Transect. Deep-Sea Research Part II 53, 1706–1719.

Baker, A.R., Kelly, S.D., Biswas, K.F., Witt, M., Jickells, T.D., 2003. Atmospheric deposition of nutrients to the Atlantic Ocean. Geophysical Research Letters 30, OCE 11/11–OCE 11/14.

Baker, A.R., Lesworth, T., Adams, C., Jickells, T.D., Ganzeveld, L., 2010. Estimation of atmospheric nutrient inputs to the Atlantic Ocean from 50°N to 50°S based on large-scale field sampling: Fixed nitrogen and dry deposition of phosphorus. Global Biogeochemical Cycles 24(3), GB3006/3001–GB3006/3016.

Baker, A.R., Weston, K., Kelly, S.D., Voss, M., Streu, P., Cape, J.N., 2007. Dry and wet deposition of nutrients from the tropical Atlantic atmosphere: Links to primary productivity and nitrogen fixation. Deep Sea Research Part I 54, 1704–1720.

Bardouki, H., Berresheim, H., Vrekoussis, M., Sciare, J., Kouvarakis, G., Oikonomou, K., Schneider, J., Mihalopoulos, N., 2003. Gaseous (DMS, MSA, SO_2, H_2SO_4 and DMSO) and particulate (sulfate and methanesulfonate) sulfur species over the northeastern coast of Crete. Atmospheric Chemistry and Physics 3, 1871–1886.

Brasseur, G.P., Orlando, J.J., Tyndall, G.S., 1999. Atmospheric Chemistry and Global Change, Oxford University Press, Inc., New York, pp. 126.

Burkard, R., Eugster, W., Wrzesinsky, T., Klemm, O., 2002. Vertical divergence of fogwater fluxes above a spruce forest. Atmospheric Research 64, 133–145.

Charlson, R.J., Lovelock, J.E., Andreae, M.O., Warren, S.G., 1987. Oceanic phytoplankton, atmospheric sulfur, cloud albedo and climate. Nature 326, 655–661.

Cho, Y.K., Kim, M.O., Kim, B.C., 2000. Sea fog around the Korean peninsula. Journal of Applied Meteorology 39, 2473–2479.

Collett Jr, J.L., Bator, A., Sherman, D.E., Moore, K.F., Hoag, K.J., Demoz, B.B., Rao, X., Reilly, J.E., 2002. The chemical composition of fogs and intercepted clouds in the United States. Atmospheric Research 64, 29–40.

Collett Jr, J.L., Sherman, D.E., Moore, K.F., Hannigan, M.P., Lee, T., 2001. Aerosol particle processing and removal by fogs: observations in chemically heterogeneous central California radiation fogs. Water, Air, and Soil Pollution: Focus 1, 303–312.

Deboudt, K., Flament, P., Bertho, M.L., 2004. Cd, Cu, Pb and Zn concentrations in atmospheric wet

deposition at a coastal station in Western Europe. Water, Air, and Soil Pollution 151, 335–359.

Duce, R.A., Liss, P.S., Merrill, J.T., Atlas, E.L., Buat-Menard, P., Hicks, B.B., Miller, J.M., Prospero, J.M., Arimoto, R., et al., 1991. The atmospheric input of trace species to the world ocean. Global Biogeochemical Cycles 5, 193–259.

Elbert, W., Hoffmann, M.R., Krämer, M., Schmitt, G., Andreae, M.O., 2000. Control of solute concentrations in cloud and fog water by liquid water content. Atmospheric Environment 34, 1109–1122.

Elskens, M., Brion, N., Buesseler, K., Van Mooy, B. A. S., Boyd, P., Dehairs, F., Savoye, N., Baeyens, W., 2008. Primary, new and export production in the NW Pacific subarctic gyre during the vertigo K2 experiments. Deep-sea Research Part II, 55, 1594–1604.

Fahey, K.M., Pandis, S.N., Collett Jr, J.L., Herckes, P., 2005. The influence of size-dependent droplet composition on pollutant processing by fogs. Atmospheric Environment 39, 4561–4574.

Finlayson-Pitts, B.J., Pitts Jr, J.N., 2000. Chemistry of the Upper and Lower Atmosphere: Theory, Experiments, and Applications, Academic press, California, pp. 800.

Fu, G., Guo, J., Xie, S.-P., Duan, Y., Zhang, M., 2006. Analysis and high-resolution modeling of a dense sea fog event over the Yellow Sea. Atmospheric Research 81, 293–303.

Galloway, J.N., Townsend, A.R., Erisman, J.W., Bekunda, M., Cai, Z., Freney, J.R., Martinelli, L.A., Seitzinger, S.P., Sutton, M.A., 2008. Transformation of the Nitrogen Cycle: Recent Trends, Questions, and Potential Solutions. Science 320, 889–892.

Gao, Y., Arimoto, R., Zhou, M.Y., Merrill, J.T., Duce, R.A., 1992. Relationships between the dust concentrations over eastern Asia and the remote North Pacific. Journal of Geophysical Research—Atmospheres 97, 9867–9872.

Gilbert, P.M., Garside, C., Fuhrman, J.A., Roman, M.R., 1991. Time-dependent coupling of inorganic and organic nitrogen uptake and regeneration in the plume of the Chesapeake Bay estuary and its regulation by large heterotrophs. Limnology and Oceanography 36, 895–909.

Gioda, A., Reyes-Rodríguez, G.J., Santos-Figueroa, G., Collett Jr, J.L., Decesari, S., Ramos, M.D.C.K.V, Bezerra Netto, H.J.C., De Aquino Neto, F.R., Mayol-Bracero, O.L., 2011. Speciation of water-soluble inorganic, organic, and total nitrogen in a background marine environment: Cloud water, rainwater, and aerosol particles. Journal of Geophysical Research—Atmospheres 116, D05203–D05219.

Gondwe, M., Krol, M., Gieskes, W., Klaassen, W., de Baar, H., 2003. The contribution of ocean-leaving DMS to the global atmospheric burdens of DMS, MSA, SO_2, and NSS $SO_4^{=}$. Global Biogeochemical Cycles 17, 25-1–25-18.

Graedel, T.E., Keene, W.C., 1995. Tropospheric budget of reactive chlorine. Global Biogeochemical Cycles 9, 47–77.

Gultepe, I., Tardif, R., Michaelides, S.C., Cermak, J., Bott, A., Bendix, J., Müller, M.D., Pagowski, M.,

Hansen, B., Ellrod, G., Jacobs, W., Toth, G., Cober, S.G., 2007. Fog research: A review of past achievements and future perspectives. Pure and Applied Geophysics 164, 1121–1159.

Herckes, P., Chang, H., Lee, T., Collett Jr, J.L., 2007. Air pollution processing by radiation fogs. Water, Air, Soil Pollution 181, 65–75.

Jacob, D.J., Waldman, J.M., Munger, W., Hoffmann M.R., 1984. A field investigation of physical and chemical mechanisms affecting pollutant concentrations in fog droplets. Tellus 36B, 272–285.

Jickells, T., 2006. The role of air-sea exchange in the marine nitrogen cycle. Biogeosciences 3(3), 271–280.

Jickells, T.D., Kelly, S.D., Baker, A.R., Biswas, K., Dennis, P.F., Spokes, L.J., Witt, M., Yeatman, S.G., 2003. Isotopic evidence for a marine ammonia source. Geophysical Research Letters 30, 27/21–27/24.

Jordan, C.E., Talbot, R.W., 2000. Direct atmospheric deposition of water-soluble nitrogen to the Gulf of Maine. Global Biogeochemical Cycles 14(4), 1315–1329.

Keene, W.C., Pszenny, A.A.P., Galloway, J.N., Hawley, M.E., 1986. Sea-salt corrections and interpretation of constituent ratios in marine precipitation. Journal of Geophysical Research—Atmospheres 91, 6647–6658.

Klemm, O., Wrzesinsky, T., 2007. Fog deposition fluxes of water and ions to a mountainous site in Central Europe. Tellus, Series B 59B, 705–714.

Lange, C.A., Matschullat, J., Zimmermann, F., Sterzik, G., Wienhaus, O., 2003. Fog frequency and chemical composition of fog water—a relevant contribution to atmospheric deposition in the eastern Erzgebirge, Germany. Atmospheric Environment 37, 3731–37 39.

Larsen, J., Neal, C., Webley, P., Freymueller, J., Haney, M., McNutt, S., Schneider, D., Prejean, S., Schaefer, J., Wessels, R., 2009. Eruption of Alaska volcano breaks historic pattern, EOS, Transactions, American Geophysical Union 90(20), 173–175.

Lewis, J.M., Koračin, D., Redmond, K.T., 2004. Sea fog research in the United Kingdom and United States: A historical essay including outlook. Bulletin of the American Meteorological Society 85, 395–408.

Li, P., Li, X., Yang, C., Wang, X., Chen, J., Collett Jr, J.L., 2011. Fog water chemistry in Shanghai. Atmospheric Environment 45, 4034–4041.

Lovett, G.M., Reiners, W.A., Olson, R.K., 1982. Cloud droplet deposition in subalpine balsam fir forests: hydrological and chemical inputs. Science 218, 1303–1304.

Lu, C., Niu, S., Tang, L., Lv, J., Zhao, L., Zhu, B., 2010. Chemical composition of fog water in Nanjing area of China and its related fog microphysics. Atmospheric Research 97, 47–69.

Lu, Z., Dzurisin, D., 2010. Ground surface deformation patterns, magma supply, and magma storage at Okmok volcano, Alaska, from InSAR analysis: 2. Coeruptive deflation, July–August 2008. Journal of Geophysical Research—Solid Earth 115, B00B03–B00B15.

Matsumoto, K., Tominaga, S., Igawa, M., 2011. Measurements of atmospheric aerosols with diameters greater than 10 μm and their contribution to fixed nitrogen deposition in coastal urban environment. Atmospheric Environment 45, 6433–6438.

Millet, M., Sanusi, A., Wortham, H., 1996. Chemical composition of fogwater in an urban area: Strasbourg (France). Environmental Pollution 94, 345–354.

Minami, Y., Ishizaka, Y., 1996. Evaluation of chemical composition in fog water near the summit of a high mountain in Japan. Atmospheric Environment 30, 3363–3376.

Moore, K.F., Sherman, D.E., Reilly, J.E., Collett Jr, J.L., 2004. Drop size-dependent chemical composition in clouds and fogs. Part I. Observations. Atmospheric Environment 38, 1389–1402.

Nakamura, T., Matsumoto, K., Uematsu, M., 2005. Chemical characteristics of aerosols transported from Asia to the East China Sea: an evaluation of anthropogenic combined nitrogen deposition in autumn. Atmospheric Environment 39, 1749–1758.

Pandis, S.N., Seinfeld, J.H., 1989. Mathematical modeling of acid deposition due to radiation fog. Journal of Geophysical Research—Atmospheres 94, 12,911–12,923.

Pandis, S.N., Seinfeld, J.H., 1990. The smog-fog-smog cycle and acid deposition. Journal of Geophysical Research—Atmospheres 95, 18489–18500.

Pandis, S.N., Seinfeld, J.H., Pilinis, C., 1990. Chemical composition differences in fog and cloud droplets of different sizes. Atmospheric Environment 24A, 1957–1969.

Pryor, S.C., Barthelmie, R.J., 2000. Particle dry deposition to water surfaces: Processes and consequences. Marine Pollution Bulletin 41, 220–231.

Quinn, P.K., Charlson, R.J., Bates, T.S., 1988. Simultaneous observations of ammonia in the atmosphere and ocean. Nature 335(6188), 336–338.

Raja, S., Raghunathan, R., Yu, X.-Y., Lee, T., Chen, J., Kommalapati, R.R., Murugesan, K., Shen, X., Yuan, Q., Valsaraj, K.T., Collett Jr, J.L., 2008. Fog chemistry in the Texas-Louisiana Gulf Coast corridor. Atmospheric Environment 42, 2048–2061.

Sasakawa, M., Ooki, A., Uematsu, M., 2003. Aerosol size distribution during sea fog and its scavenge process of chemical substances over the northwestern North Pacific. Journal of Geophysical Research—Atmospheres 108, AAC13/11–AAC13/19.

Sasakawa, M., Uematsu, M., 2002. Chemical composition of aerosol, sea fog, and rainwater in the marine boundary layer of the northwestern North Pacific and its marginal seas. Journal of Geophysical Research—Atmospheres 107, ACH 17/11–ACH 17/19.

Sasakawa, M., Uematsu, M., 2005. Relative contribution of chemical composition to acidification of sea fog (stratus) over the northern North Pacific and its marginal seas. Atmospheric Environment 39, 1357–1362.

Schmale, J., Schneider, J., Jurkat, T., Voigt, C., Kalesse, H., Rautenhaus, M., Lichtenstern, M., Schlager, H., Ancellet, G., Arnold, F., Gerding, M., Mattis, I., Wendisch, M., Borrmann, S., 2010. Aerosol

layers from the 2008 eruptions of Mount Okmok and Mount Kasatochi: In situ upper troposphere and lower stratosphere measurements of sulfate and organics over Europe. Journal of Geophysical Research—Atmospheres 115, D00L07–D00L24.

Spokes, L.J., Yeatman, S.G., Cornell, S.E., Jickells, T.D., 2000. Nitrogen deposition to the eastern Atlantic Ocean. The importance of south-easterly flow. Tellus, Series B: Chemical and Physical Meteorology 52B, 37–49.

Thalmann, E., Burkard, R., Wrzesinsky, T., Eugster, W., Klemm, O., 2002. Ion fluxes from fog and rain to an agricultural and a forest ecosystem in Europe. Atmospheric Research 64, 147–158.

Tokinaga, H., Xie, S.-P., 2009. Ocean tidal cooling effect on summer sea fog over the Okhotsk Sea. Journal of Geophysical Research—Atmospheres 114, D14102–D14118.

Uematsu, M., Duce, R.A., Prospero, J.M., Chen, L., Merrill, J.T., McDonald, R.L., 1983. Transport of mineral aerosol from Asia over the North Pacific Ocean. Journal of Geophysical Research—Atmospheres 88, 5343–5352.

Uematsu, M., Hattori, H., Nakamura, T., Narita, Y., Jung, J., Matsumoto, K., Nakaguchi, Y., Dileep Kumar, M., 2010. Atmospheric transport and deposition of anthropogenic substances from the Asia to the East China Sea. Marine Chemistry 120, 108–115.

Uno, I., Uematsu, M., Hara, Y., He, Y.J., Ohara, T., Mori, A., Kamaya, T., Murano, K., Sadanaga, Y., Bandow, H., 2007. Numerical study of the atmospheric input of anthropogenic total nitrate to the marginal seas in the western North Pacific region. Geophysical Research Letters 34, L17817–L17822.

Wallace, J.M., Hobbs, P.V., 2006. Atmospheric science: An introductory survey, Academic Press, California, pp. 209–269.

Wang, B.-H., 1985. Distributions and variations of sea fog in the world, in Sea Fog. China Ocean Press, Beijing, pp. 51–90.

Wang, Y., Zhuang, G., Tang, A., Yuan, H., Sun, Y., Chen, S., Zheng, A., 2005. The ion chemistry and the source of $PM_{2.5}$ aerosol in Beijing. Atmospheric Environment 39, 3771–3784.

Wong, C.S., Waser, N.A.D., Nojiri, Y., Whitney, F.A., Page, J.S., Zeng, J. 2002. Seasonal cycles of nutrients and dissolved inorganic carbon at high and mid latitudes in the North Pacific Ocean during the Skaugran cruise: determination of new production and nutrient uptake ratios. Deep-Sea Research Part II 49, 5317–5338.

Xie, P., Arkin, P.A., 1997. Global precipitation: A 17-year monthly analysis based on gauge observations, satellite estimates, and numerical model outputs. Bulletin of the American Meteorological Society 78, 2539–2558.

Zhang, Q., Anastasio, C., 2001. Chemistry of fog waters in California's Central Valley—Part 3. Concentrations and speciation of organic and inorganic nitrogen. Atmospheric Environment 35, 5629–5643.

5. Atmospheric inorganic nitrogen in marine aerosol and precipitation and its deposition to the North and South Pacific Oceans

5.1. Introduction

Atmospheric N deposition can be important for marine biological activity over large remote areas of the oceans where N supply by deep nutrient rich water is small. Previous studies have highlighted the significance of atmospheric N and its critical role in oceanic biogeochemical cycling (e.g., Galloway et al., 2004; Dentener et al., 2006; Duce et al., 2008; Gruber and Galloway 2008; Baker et al., 2010; Krishnamurthy et al., 2010; Kim et al., 2011). Extensive use of fossil fuels and N in fertilizer has already impacted coastal as well as open ocean marine ecosystems due to increased N deposition (e.g., Paerl 1997; Spokes and Jickells 2005; Jung et al., 2009; Zhang et al., 2010; Krishnamurthy et al., 2010). Duce et al. (2008) have estimated that in 1860, atmospheric deposition flux of total reactive N (i.e., NO_y and NH_x) to the ocean was ~20 Tg N yr^{-1}, of which ~29% was anthropogenic. By 2000, this had increased to ~67 Tg N yr^{-1}, of which ~80% was anthropogenic. They also pointed out that the effects of increasing atmospheric N deposition were expected to continue to grow in the future.

Although recent studies have estimated impacts of atmospheric N inputs, there are still large uncertainties regarding the global atmospheric N cycle since most studies are based on the results of several models (e.g., Dentener et al., 2006; Duce et al., 2008). The atmospheric N cycle over the oceans contains the most uncertain part (Baker et al., 2010) because the validation of model output was primarily based on comparisons to terrestrial sampling sites (Dentener et al., 2006; Baker et al., 2010). So far, the field observation/data on the deposition flux of atmospheric N are mostly concentrated on the Atlantic Ocean and the Mediterranean Sea (e.g., Spoke et al., 2000; Baker et al., 2007; Sandroni et al., 2007; Baker et al., 2010), with a little data being reported for the Pacific Ocean (e.g., Duce et al., 1991; Nakamura et al., 2005; Matsumoto et al., 2009).

Because of rapid Asian economic growth, emissions of anthropogenic substances (e.g., nitrogen oxides; NO_x) from the Asian continent have significantly increased (Uno et al., 2007). Since the western North Pacific receives a large influx of mineral dust and pollution aerosol from the Asian continent through atmospheric transport (Uematsu et al., 2010), estimating deposition flux of atmospheric N and its impacts on biogeochemical cycles over the western North Pacific have become increasingly important. Nevertheless, few field studies have been carried out over this region to estimate the dry and wet deposition fluxes of atmospheric N, simultaneously. Moreover, atmospheric N in marine aerosols and rain over the South Pacific Ocean, which is expected to receive little influences from terrestrial and anthropogenic substances, has not been extensively investigated.

In this chapter, concentrations and deposition fluxes of atmospheric N over the North and South Pacific Ocean using data obtained from aerosol and rain sampling during the KH-08-2 and MR08-06

cruises in 2008 and 2009 are presented. This study focuses on NH_4^+ and NO_3^-, which are dominant components for N supply to the oceans (Krishnamurthy et al. 2010), since current models of the global atmospheric N cycle generally have been targeted these two inorganic N species (Baker et al. 2010). The results for atmospheric inorganic N deposition from this study should be valuable for filling the data gap, especially for the South Pacific Ocean, and be useful for validation of N deposition flux model on a global ocean scale.

5.2. Deposition flux estimates

Dry deposition fluxes (F_d) were calculated from aerosol concentrations (C_a) in the coarse (c) and fine (f) modes and dry deposition velocities (V_d) for each size mode (Duce et al., 1991; Baker et al., 2007):

$$F_d = C_a^c V_d^c + C_a^f V_d^f \quad (1)$$

Here, V_d of 2 cm s^{-1} for coarse mode and 0.1 cm s^{-1} for fine mode were used since these two values are known to be best estimates, based on experimental and model studies, for dry deposition velocity for coarse and fine modes (Duce et al., 1991; Baker et al., 2003; Nakamura et al., 2005). This estimate results in an uncertainty of a factor of 2–3 in the calculated flux, since deposition velocity includes terms for gravitational settling, impaction and diffusion of particles, all of which vary in complex functions of particle size and meteorological conditions (e.g., wind speed and relative humidity) (Duce et al., 1991).

Wet deposition fluxes (F_w) were estimated from the concentration of the species of interest in rainwater (C_r) and the precipitation rate (P):

$$F_w = C_r P \quad (2)$$

The precipitation rate was calculated from the monthly averaged precipitation rate (mm d^{-1}) using the CMAP model output (http://www.cdc.noaa.gov/cdc/data.cmap.html) (Xie and Arkin 1997).

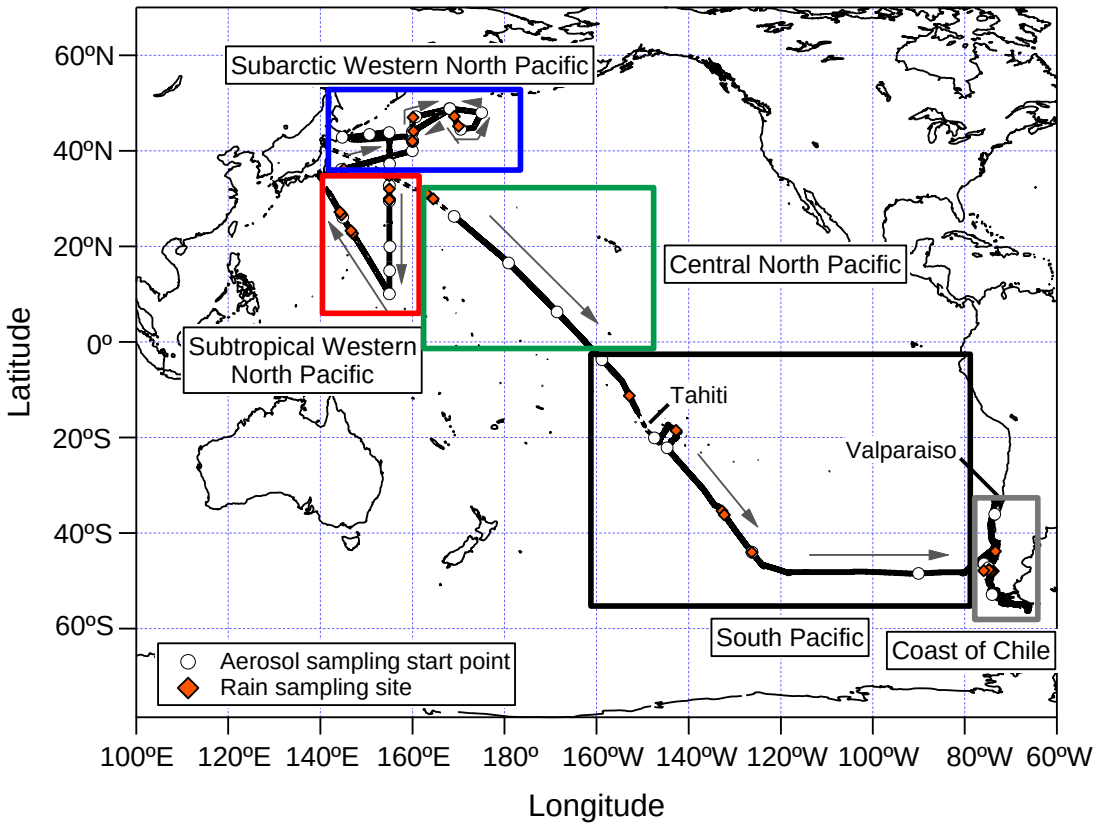

Fig. 5.1. Cruise tracks of the KH-08-2 and MR08-06. White circles and orange diamonds indicate aerosol and rain sampling locations during each cruise, respectively. Each aerosol sampling start point represents the end of the previous sampling period. Dotted line indicates that no aerosol sampling was conducted since the relative wind directions were outside the ranges of the wind-sector controller. The two cruises were classified into five regions (open box) with different colors (subarctic western North Pacific (SAWNP), blue; subtropical western North Pacific (STWNP), red; central North Pacific (CNP), green; South Pacific (SP), black; Coast of Chile (CC), gray).

5.3. Aerosol ammonium and nitrate over the North and South Pacific Ocean

To aid with interpretation, data from the two cruises were divided into five oceanic regions: the subarctic western North Pacific (SAWNP), the subtropical western North Pacific (STWNP), the central North Pacific (CNP), the South Pacific (SP), the coast of Chile (CC) (Fig. 5.1). Mean concentrations of total NH_4^+ and NO_3^- in aerosols collected in the five regions are given in Table 5.1. For comparison with results from this study, previously reported data from other studies conducted in the marine atmosphere are also listed.

Total concentrations of NH_4^+ and NO_3^- in bulk (fine + coarse) aerosols during the two cruises varied from 0.93–12 nmol m^{-3} and 0.44–5.6 nmol m^{-3}, respectively (Figs. 5.2a and 5.2b). Aerosol inorganic N in the entire data set was composed of ~68% NH_4^+ and ~32% NO_3^- (median values for all data), with ~81% and ~45% of each species being present on fine mode aerosol, respectively. The total NH_4^+ and NO_3^- concentrations showed similar trends, with higher concentrations in samples collected over the western North Pacific and lower values over the South Pacific. These distributions likely resulted from large terrestrial emission sources of N in the northern hemisphere, deposition during transport across the ocean, and the intertropical convergence zone (ITCZ) by which cross-equatorial transport is suppressed (Baker et al., 2007).

Mean contributions of NH_4^+ to total inorganic nitrogen (TIN = NH_4^+ + NO_3^-) in aerosols for five regions were: the SAWNP 70 ± 11%, the STWNP 70 ± 5.2%, the CNP 59 ± 15%, the SP 58 ± 6.8% and the CC 67 ± 8.5%.

5.3.1. Effect of sea fog on aerosol NH_4^+ and NO_3^- over the subarctic western North Pacific Ocean

The mean concentrations of aerosol NH_4^+ and NO_3^- in the SAWNP were about 1.3 times and 1.5 times lower than those observed in the northern North Pacific (Mano et al., 2007, unpublished data) and at Shemya Island in the Aleutian island chain (Prospero et al., 1985), respectively (Table 5.1). As mentioned in chapter 4, over a dozen sea fog events occurred and aerosol samples, A03–A06 and A08–A09, were affected by these fog appearance during Leg 1 of the KH-08-2 cruise. The northern North Pacific region (> 40°N) has a high sea fog frequency with a maximum of ~50% during the summertime period from June to August (Wang 1985). Both NO_3^- and Na^+, which mainly existed in coarse mode aerosols (Figs. 5.2b and 5.3a), were more efficiently scavenged by sea fog than NH_4^+, indicating that coarse particles act predominantly as condensation nuclei of sea fog droplets rather than the fine particles (e.g., NH_4^+ and nss-SO_4^{2-}) (Sasakawa et al., 2003). The low mean concentrations of NH_4^+ and NO_3^- in the SAWNP region thus are likely due to strong influences of sea fog, and this result suggests that sea fog over the SAWNP may play a key role in supplying atmospheric N to the ocean in summer since sea fog scavenges gases (e.g., HNO_3) as well as aerosols (Sasakawa and Uematsu 2005).

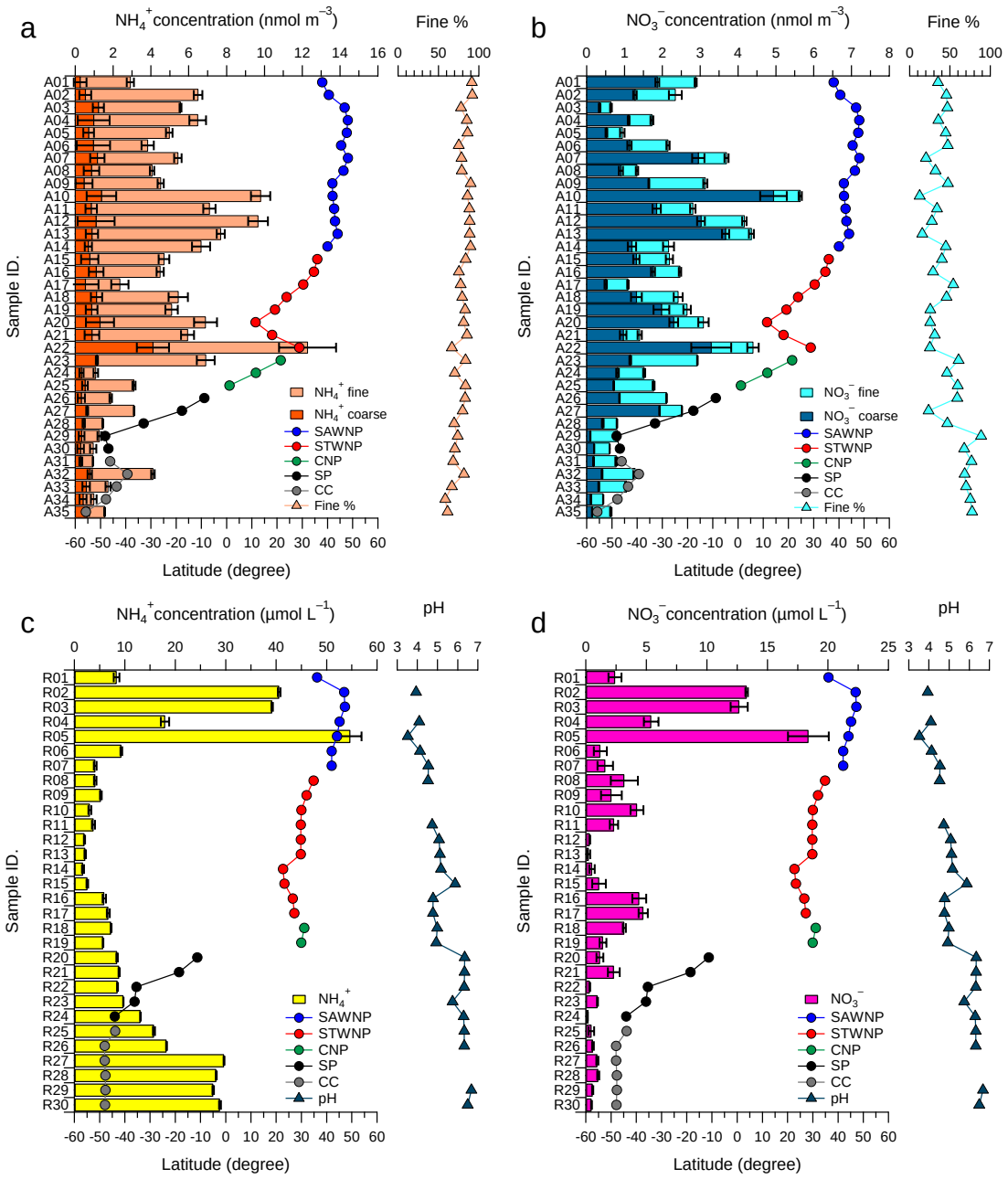

Fig. 5.2. Concentrations of NH_4^+ and NO_3^- against sample I.D in aerosols (a, b) and rains (c, d) collected during the KH-08-2 and MR08-06 cruises. Right sections of NH_4^+ and NO_3^- in aerosols and rainwater panels show the percentage (solid triangle line) of each component in fine (D < 2.5 μm) aerosol particles and the pH values of rainwater, respectively. The latitude of each aerosol and rain sampling location (solid circle line) is shown with different colors (subarctic western North Pacific (SAWNP), blue; subtropical western North Pacific (STWNP), red; central North Pacific (CNP), green; South Pacific (SP), black; Coast of Chile (CC), gray).

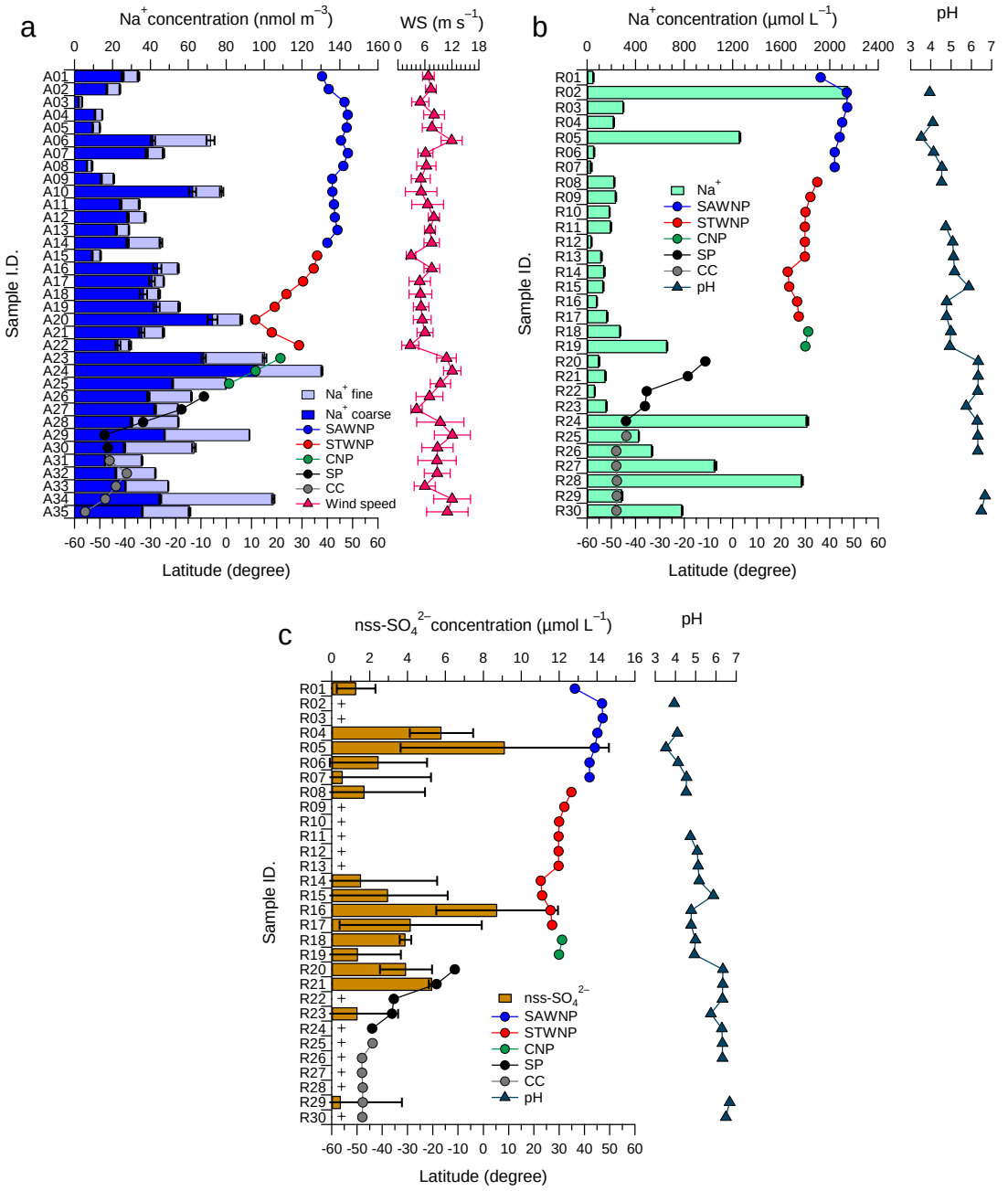

Fig. 5.3. Concentrations of Na^+ and nss-SO_4^{2-} against sample I.D. Na^+ in aerosols (a), Na^+ in rains (b), and nss-SO_4^{2-} in rains (c) collected during the KH-08-2 and MR08-06 cruises. Right sections of Na^+ in aerosols and Na^+ and nss-SO_4^{2-} in rainwater panels show the mean and standard deviation of wind speeds for each aerosol sampling time, and the pH values of rainwater, respectively. Crosses in (c) indicate that the calculated nss-SO_4^{2-} concentrations were negative. The latitude of each aerosol and rain sampling location (solid circle line) is shown with different colors (subarctic western North Pacific (SAWNP), blue; subtropical western North Pacific (STWNP), red; central North Pacific (CNP), green; South Pacific (SP), black; Coast of Chile (CC), gray).

Table 5.1 Mean concentrations of total NH_4^+ and NO_3^- in aerosol, and the mean percentage of each component in fine (D < 2.5 μm) aerosol particles collected in each of the five oceanic regions during the KH-08-2 and MR08-06 cruises, together with referenced data for comparison[a]

		Aerosol							
		NH_4^+ (nmol m^{-3})				NO_3^- (nmol m^{-3})			
Region/Location	Period	Mean[a]	Range	Fine %[a]	n	Mean[a]	Range	Fine %[a]	n
Subarctic western North Pacific (SAWNP)[1]	Jul–Aug 2008	6.1(2.0)	2.9–9.8	85(5.5)	14	2.7(1.4)	0.64–5.6	35(12)	14
Subtropical western North Pacific (STWNP)[1]	Aug–Sep 2008	5.9(2.9)	2.4–12	79(6.0)	8	2.5(1.0)	1.1–4.4	35(11)	8
Central North Pacific (CNP)[1]	Jan 2009	3.7(3.0)	1.1–6.9	79(7.7)	3	2.1(0.75)	1.5–2.9	56(8.0)	3
South Pacific (SP)[1]	Jan–Mar 2009	1.7(0.84)	0.95–3.1	75(6.0)	5	1.4(0.88)	0.61–2.5	57(24)	5
Coast of Chile (CC)[1]	Mar 2009	1.9(1.3)	0.93–4.1	67(8.9)	5	0.84(0.33)	0.44–1.3	73(4.2)	5
Shemya (52°N, 174°E)[2]	1981–1982	-	-	-	-	4.0(3.9)	0.16–18	-	36
Enewetak (11°N, 162°E)[2]	1981–1982	-	-	-	-	3.1(2.7)	0.32–12	-	29
Northern North Pacific (35°N–53°N, 139°E–160°W)[3, b]	Sep 2005	7.8(3.3)	2.5–12	94(3.7)	12	4.0(2.5)	1.2–8.4	22(11)	12
Central North Pacific (0°N–47°N, 122°W-157°W)[4]	Feb–Mar 1984	4.5(3.8)	0.56–16	-	13	2.1(0.93)	0.97–4.0	-	13
Central North Pacific (10°S–53°N, 160°W)[3]	Aug–Sep 2005	5.9(5.5)	1.5–28	93(2.5)	28	2.0(1.8)	0.28–8.6	9.0(8.2)	27
South Pacific (55°S–0°N, 150°W–170°W)[4]	Mar–Apr 1984	4.6(3.1)	1.1–7.8	-	17	1.6(0.93)	0.48–3.9	-	17
South Pacific (50°S–5°N, 160°W–170°W)[5]	Nov 2001–Mar 2002	3.3(-)	2.1–4.4	-	6	-	-	-	-
American Samoa (14°S, 170°W)[6]	1983–1987	-	-	-	-	1.8(0.16)	-	-	215
Palmer, Antarctica (64°S, 64°W)[7]	Apr 1990–Jun 1991	1.4(2.3)	-	-	-	0.29(0.15)	-	-	-

[a]Mean with (standard deviation). [b]Details of the study area are described in Furutani et al. (2010).

References: [1]This study. [2]Prospero et al. (1985). [3]Mano et al. (2007, unpublished data). [4]Parungo et al. (1986). [5]Ooki et al. (2007). [6]Savoie et al. (1989a). [7]Savoie et al. (1993).

5.3.2. Aerosol NH_4^+ over the South Pacific Ocean

The mean NH_4^+ concentration in the SP was a factor of 1.9–2.7 lower than those of previous studies in the SP (Table 5.1). Air masses encountered during the collection of aerosol samples in the SP spent at least 7 days over the ocean (based on 7 day backward trajectories from the NOAA HYSPLIT model) (Fig. 5.4c), permitting input of marine origin aerosols with relatively little terrestrial and anthropogenic input. It is known that NH_4^+ is primarily associated with fine mode aerosol and produced by heterogeneous reactions involving NH_3 derived from intensive agricultural activity (Aneja et al., 2001) and biomass burning (Andreae and Merlet 2001). Ammonia is also emitted into the atmosphere from the ocean as a result of biological activity (Quinn et al., 1988). Both the current data from this study and previous results for NH_4^+ were in the range of modeled annual mean NH_4^+ concentrations over the South Pacific (40–200 ppt; 1.6–8.2 nmol m^{-3} STP) (Dentener and Crutzen 1994). Here, it is considered that the mean NH_4^+ concentration in the SP from this study may be representative of the natural oceanic background level. Dentener and Crutzen (1994) reported that calculated aerosol NH_4^+ concentrations without natural emissions in the SP ranged from 16–19 ppt (0.65–0.78 nmol m^{-3} STP). Those values were a factor of 2.6–7.1 lower than those observed in the SP (Table 5.1). Ooki et al. (2007) estimated that marine biogenic NH_4^+ in accumulation mode aerosols ($D < 1.0$ μm) collected over the South Pacific to be 0.3–3.6 nmol m^{-3}, contributing 21–90% to total NH_4^+ concentration in the accumulation mode. Parungo et al. (1986) reported that concentrations of aerosol NH_4^+ showed maxima at upwelling regions, such as at the equator (7.2 nmol m^{-3}) and near the Chatham Rise (7.8 nmol m^{-3}). Thus, the higher aerosol NH_4^+ concentrations in these two studies than the result from this study are likely due to the influence of oceanic-derived NH_4^+, suggesting that emissions of NH_3 by marine biological activity from the ocean could become a significant source of aerosol NH_4^+ in the South Pacific, and that much of observed aerosol NH_4^+ in the open ocean aerosols could be recycled oceanic NH_3 (Duce et al., 1991).

5.3.3. Contribution of NO_3^- derived from continental sources over the Pacific Ocean

Nitrate is an end product of a series of gas-phase photochemical and heterogeneous reactions involving NO_x primarily derived from fossil fuel combustion (Seinfeld and Pandis 1998). The significant sources of aerosol NO_3^- over oceans are thought to include long-range transport from continental source regions, lightning and injection from the stratosphere (Prospero et al., 1985). The mean NO_3^- concentrations in this study were in reasonable agreement with other values reported for the Pacific Ocean (Table 5.1), with the exception of the value in the SAWNP as mentioned in section 5.3.1. The measured mean NO_3^- concentration (1.4 nmol m^{-3}) over the SP agreed with the 1.8 nmol m^{-3} (0.11 μg m^{-3}) observed at American Samoa (14°S, 170°W) by Savoie et al. (1989a); however, the mean NO_3^- concentration in the CC was a factor of 2 lower than their results, but a factor of 2.9 higher than the

observed value from Antarctica. The concentration of any particular species in the atmosphere is dependent on a number of factors including the distribution and strength of the sources for that species, its transport and transformation in the atmosphere, and the nature of the removal processes (Prospero et al., 1985). The southern oceans are relatively unimpacted by anthropogenic N sources in general or by northern hemisphere sources in particular (Duce et al., 1991). Lightning is an important source of NO_x, especially in the free troposphere (where it is the only natural source) and in remote regions, including the oceans where it accounts for almost the entire source of NO_x (Galloway et al., 2004). Crutzen and Gidel (1983) reported that the modeled HNO_3 concentrations with only NO_x derived from lightning and injection from the stratosphere in the South Pacific (an altitude: 0–6 km) ranged from 5–25 ppt (0.20–1.0 nmol m^{-3} STP), with an average of 13 ppt (0.53 nmol m^{-3} STP). Assuming that the mean HNO_3 concentration reported by Crutzen and Gidel (1983) is converted to aerosol NO_3^-, it was obtained the following total NO_3^- contributions from continental sources in aerosol samples: the SAWNP = 80%, the STWNP = 79%, the CNP = 75%, the SP = 62%, and the CC = 37%. This result suggests that the North Pacific is most likely affected by strong anthropogenic and/or continental NO_3^- sources, and that the NO_3^- derived from lightning and injection from the stratosphere could represent a significant portion of the observed NO_3^- in the South Pacific.

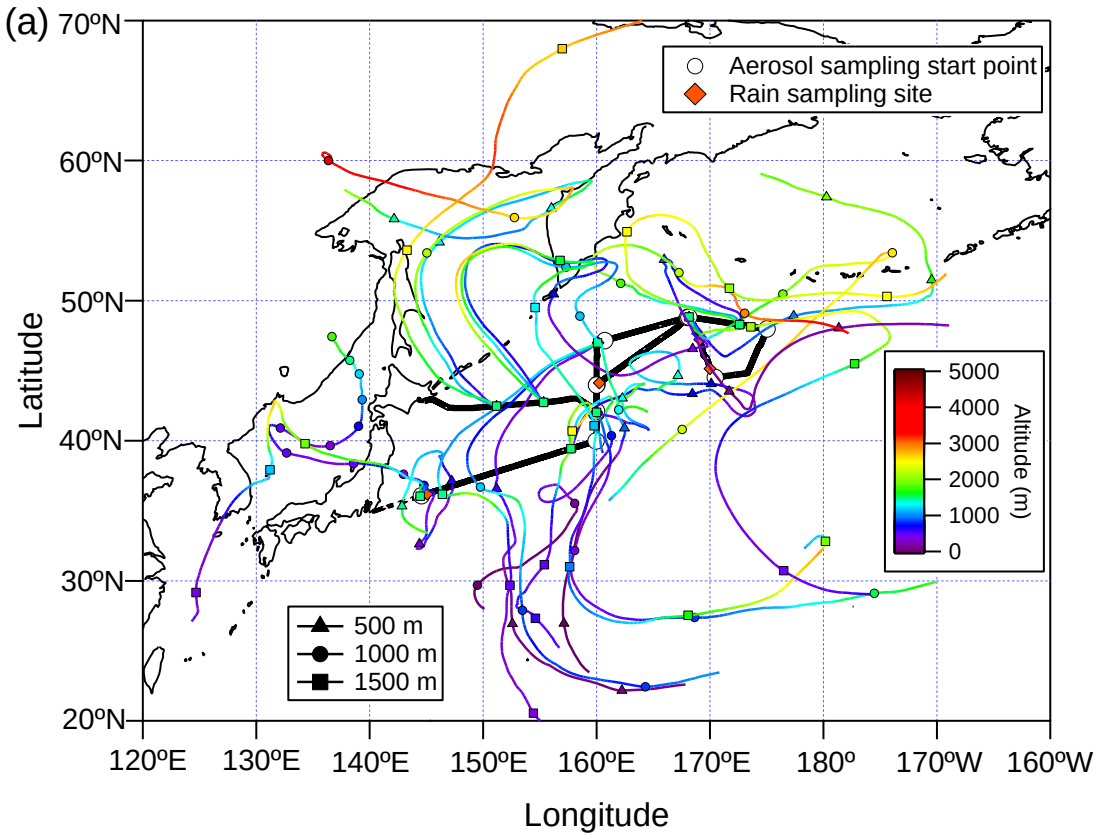
(a)
70ºN
60ºN
50ºN
40ºN
30ºN
20ºN
Latitude
120ºE
130ºE
140ºE
150ºE
160ºE
170ºE
180º
170ºW
160ºW
Longitude
Aerosol sampling start point
Rain sampling site
500 m
1000 m
1500 m
5000
4000
3000
2000
1000
0
Altitude (m)

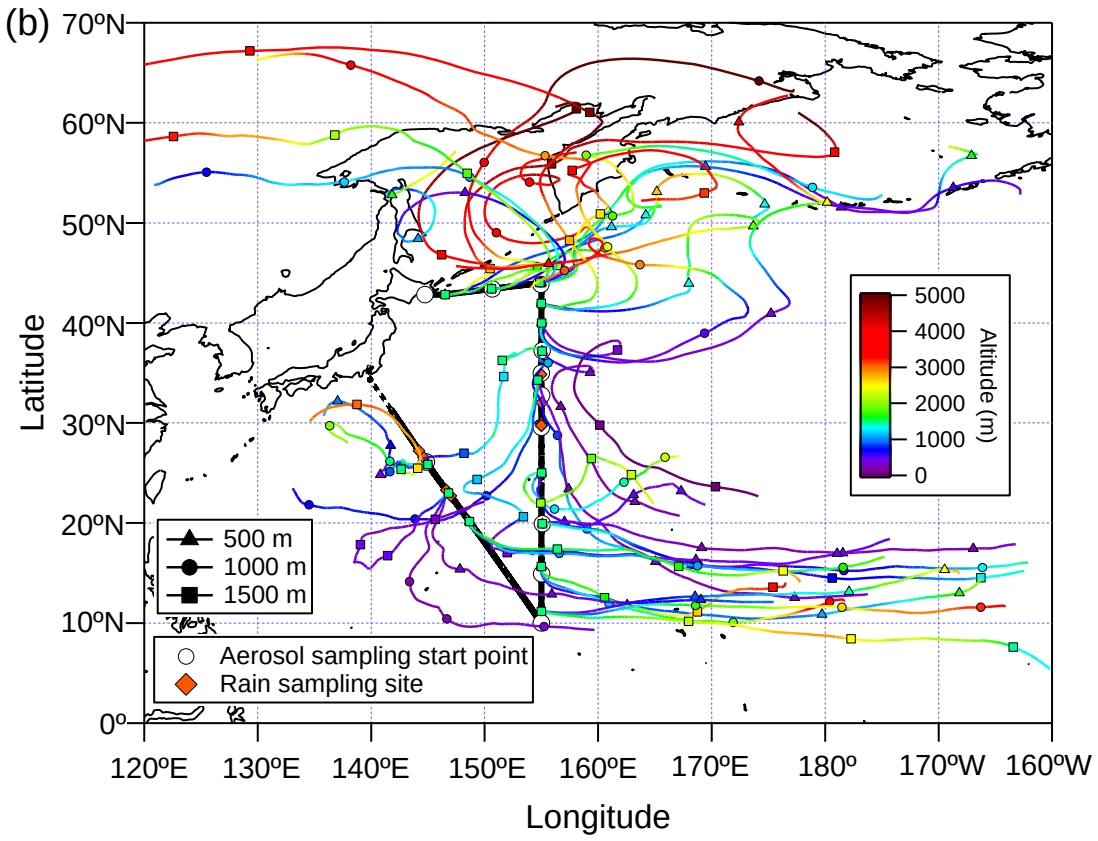
(b)
70ºN
60ºN
50ºN
40ºN
30ºN
20ºN
10ºN
0º
Latitude
120ºE
130ºE
140ºE
150ºE
160ºE
170ºE
180º
170ºW
160ºW
Longitude
500 m
1000 m
1500 m
Aerosol sampling start point
Rain sampling site
5000
4000
3000
2000
1000
0
Altitude (m)

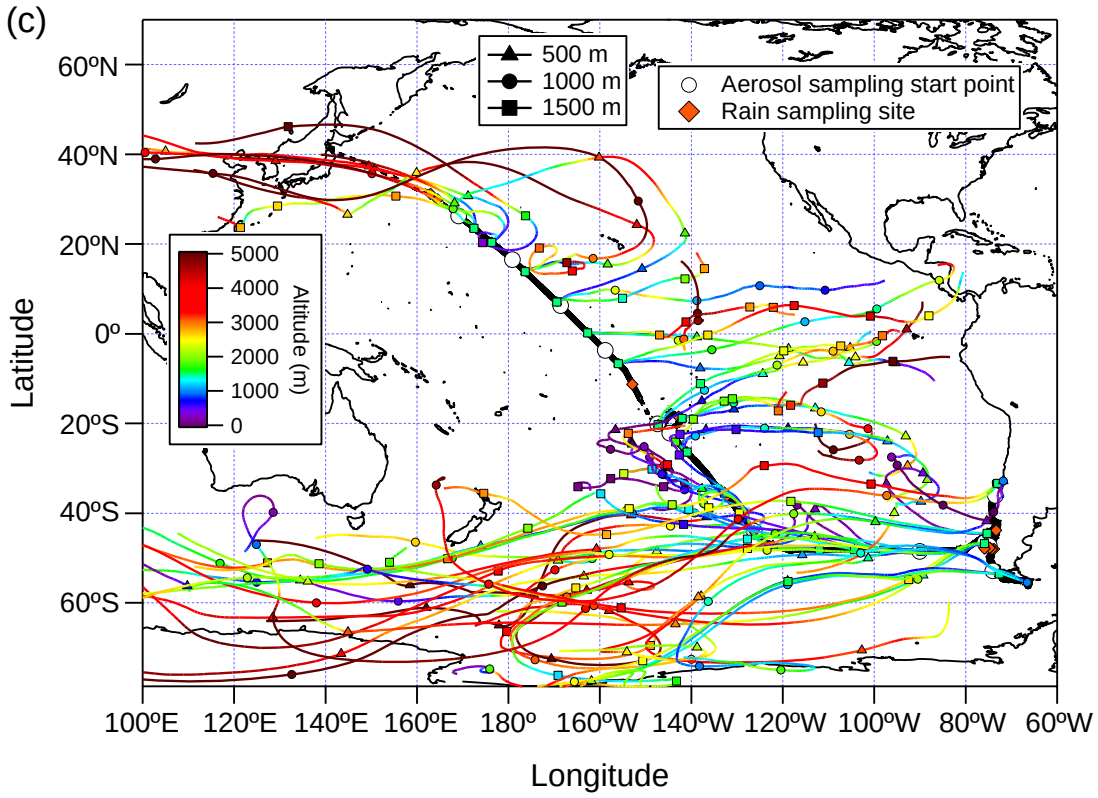

Fig. 5.4. The 168 h (7 days) air mass backward trajectories for starting altitudes of 500 (triangle symbols), 1000 (circle symbols) and 1500 m (square symbols) above ground level (AGL) were calculated from the GDAS database of the National Ocean and Atmospheric Administration (NOAA) and simulated by using the Hybrid Single-Particle Langrangian Integrated Trajectory (HY-SPLIT) model (web site http://ready.arl.noaa.gov/HYSPLIT.php): (a) Leg 1 of KH-08-2; (b) Leg 2 of KH-08-2; (c) MR08-06

5.3.4. NO_3^- in fine mode over the coast of Chile

Overall, NO_3^- mainly was found in coarse mode aerosols, while NH_4^+ was largely associated with the fine mode. Interestingly, it was found that approximately 73 ± 4.2% of NO_3^- collected in the CC existed in fine mode aerosols (Fig. 5.2b), although it is known that NO_3^- in the marine atmosphere is predominantly associated with coarse mode aerosol as a result of a chemical reaction between nitric acid (HNO_3) and sea-salt (Andreae and Crutzen 1997). This facilitates an effective shift of NO_3^- from the fine mode to the coarse mode, enhancing its deposition potential through more effective gravitational settling and increased precipitation scavenging via inertial impaction (Yeatman et al., 2001). Air masses encountered during the collection of aerosol samples in the CC spent at least 7 days over the Southern Ocean (Fig. 5.4c), suggesting that NO_3^- accumulated in the coarse mode could have been removed more rapidly by dry or wet deposition during transport because of the larger particle size (Duce et al., 1991). In addition to rapid removal of NO_3^- in the coarse mode by dry or wet deposition, NO_3^- derived from lightning at high altitudes could experience longer lifetimes and long-range transport away from formation sites, contrary to other sources of NO_x (Shepon et al., 2007). If aerosol NO_3^- is produced by lightning in the free troposphere and by injection from the stratosphere, there are few chances to react with coarse mode sea-salt that is continuously supplied from the sea surface. In this study, the contribution of NO_3^- derived from lightning and injection from the stratosphere to the observed NO_3^- in the CC was estimated to be 63%, as mentioned in section 5.3.3. Therefore, the NO_3^- in fine mode collected in the CC is most likely due to long-range transport and/or injection of NO_3^- produced by lightning from the free troposphere and by intrusion from the stratosphere.

5.4. Ammonium and nitrate in rainwater over the North and South Pacific Oceans

Concentrations of NH_4^+ and NO_3^- in rainwater during the two cruises ranged from 1.7–55 μmol L^{-1} and 0.16–18 μmol L^{-1}, respectively (Figs. 5.2c and 5.2d). Inorganic N in rainwater was composed of ~87% NH_4^+ and ~13% NO_3^- (median values for all data). Mean contributions of NH_4^+ to TIN in rainwater for five regions were: the SAWNP 77 ± 5.3%, the STWNP 67 ± 15%, the CNP 75 ± 7.4%, the SP 91 ± 7.7% and the CC 97 ± 0.74%. These results suggest that NH_4^+ is more abundant in rainwater collected over the North and South Pacific Ocean, and that it is a more important inorganic N species supplied by wet deposition. Because concentration in rainfall are influenced by rainfall amount, rain samples were divided into five regions mentioned above and used the concentration (C_i) and rainfall volume (V) for each sample to calculate volume-weighted mean concentrations (C_v) for each region (Baker et al., 2007):

$$C_v = \sum C_i V_i / \sum V_i \qquad (3)$$

Mean, range and volume-weighted mean (VWM) concentration values for NH_4^+ and NO_3^- determined in rainwater samples for each of the five regions are given in Table 5.2. The mean pH values of rainwater samples are also listed.

5.4.1. Concentrations of NH_4^+ and NO_3^- in rainwater

The difference in inorganic N concentration in rainwater can be attributed to differences in location, regional natural and/or anthropogenic emissions, and meteorological conditions (e.g., rainfall and the origin of air masses) (Zhang et al., 2007). The high NH_4^+ and NO_3^- concentrations were observed in the rainwater samples collected over the SAWNP where air masses originated from the Asian continent and the Kamchatka Peninsula (Fig. 5.4a). In contrast, the NH_4^+ and NO_3^- concentrations drastically decreased when stable easterly trade winds were reaching the sampling sites from the central Pacific Ocean (Fig. 5.4b), permitting input of relatively clean marine air. The mean NH_4^+ concentration in rainwater collected over the STWNP was comparable to the result of Cornell et al. (2001), who reported that the mean NH_4^+ concentration in rainwater collected at Oahu, Hawaii in the summer of 1998 was 3.8 ± 7.5 μmol L^{-1} (Table 5.2). In comparison, the mean concentration of NH_4^+ over the SP was about 40% lower (9.7 ± 1.9 μmol L^{-1}) than the observed NH_4^+ concentration (16 ± 14 μmol L^{-1}) in rainwater collected at Cape Grim, Australia. The mean NH_4^+ concentration in rainwater samples collected over the CC, however, was about 56% higher (25 ± 6.0 μmol L^{-1}) than that at Cape Grim. The data of this study shows evidence that the observed NH_4^+ concentrations in rainwater samples collected over the SP and the CC could be related to the emission of NH_3 from the ocean, a topic discussed later in section 5.4.3. The results for NO_3^- and pH of rainwater in the CNP and the SP were broadly similar to those reported by Parungo et al. (1986), although the collected rainwater sample numbers of this study, especially in the CNP, are small. In comparison, the observed values for NO_3^- in rainwater samples collected at Oahu and Cape Grim were an order of magnitude greater than the NO_3^- concentrations in rainwater collected on shipboard over the Pacific Ocean, probably reflecting the pronounced influence of terrestrial and/or local anthropogenic sources of NO_3^- at Oahu and Cape Grim.

Table 5.2 Mean and volume-weighted mean (VWM) concentration values for NH_4^+ and NO_3^- in rainwater and pH of rainwater collected in each of the five oceanic regions sampled during the KH-08-2 and MR08-06 cruises, together with referenced data for comparison[a]

		Rain										
		NH_4^+ (μmol L^{-1})				NO_3^- (μmol L^{-1})				pH		
Region/Location	Period	Mean[a]	Range	VWM	n	Mean[a]	Range	VWM	n	Mean[a]	Range	n
Subarctic western North Pacific (SAWNP)[1]	Jul–Aug 2008	25(20)	4.1–55	16	7	7.8(6.9)	1.2–18	4.7	7	4.0(0.37)	3.5–4.5	5
Subtropical western North Pacific (STWNP)[1]	Aug–Sep 2008	3.7(1.8)	1.7–6.7	2.2	10	2.3(1.8)	0.24–4.7	0.70	10	5.0(0.42)	4.5–5.9	8
Central North Pacific (CNP)[1]	Jan 2009	6.5(1.1)	5.7–7.3	6.5	2	2.3(1.2)	1.4–3.2	2.4	2	5.0(0.035)	4.9–5.0	2
South Pacific (SP)[1]	Jan–Mar 2009	9.7(1.9)	8.4–13	9.3	5	0.98(0.85)	0.16–2.3	0.71	5	6.2(0.26)	5.7–6.3	5
Coast of Chile (CC)[1]	Mar 2009	25(6.0)	16–30	22	6	0.68(0.24)	0.46–1.0	0.57	6	6.5(0.17)	6.3–6.7	4
Oahu (21°N, 157°W)[2]	Jul-Aug 1998	3.8(7.5)	0.5–4.2	-	17	12(12)	3.3–15	-	17	-	-	-
Central North Pacific (0°N–47°N, 122°W-157°W)[3]	Feb–Mar 1984	-	-	-	-	1.7(1.1)	0.2–3.2	2.0	7	6.0(0.82)	5.4–7.3	7
South Pacific (55°S–0°N, 150°W–170°W)[3]	Mar–Apr 1984	-	-	-	-	1.4(1.1)	0.2–2.9	1.4	8	6.2(0.50)	5.7–7.2	8
Cape Grim (40°S, 144°E)[4]	Nov 2000	16(14)	-	-	6	13(8.2)	-	-	6	-	-	-

[a]Mean with (standard deviation).

References: [1]This study. [2]Cornell et al. (2001). [3]Parungo et al. (1986). [4]Mace et al. (2003a).

5.4.2. Variation of pH in rainwater

The pH ranged from 3.5–6.7, with a median value of 5.1 for the entire data set. The mean pH values of rainwater gradually increased from the SAWNP to the CC (Table 5.2), suggesting that the influence of acidic substances (e.g., NO_3^- and nss-SO_4^{2-}) derived from terrestrial and/or anthropogenic sources had become relatively weak (Figs. 5.2d and 5.3c). In addition, pH values increased with increasing NH_4^+ concentrations in rainwater collected over the SP and the CC (Fig. 5.2c). Ammonia is the only base present in sufficient quantities to neutralize a significant fraction of the sulfuric and nitric acids found in the troposphere, and it plays a key role in determining the pH of cloud condensation nuclei and precipitation (Adams et al., 1999). Moreover, the mean concentration of Na^+ in rainwater collected over the CC (810 ± 540 μmol L^{-1}) was a factor of 1.4 higher than that over the SAWNP (580 ± 820 μmol L^{-1}) (Fig. 5.3b), since sea-salt concentration in the air is generally high in windy conditions (Fig. 5.3a) and the pH value of rainwater which contains high Na^+ concentration has high alkalinity (Parungo et al., 1986). Thus, pH values for rainwater samples collected over the North Pacific are most likely affected by acidic substances, while pH values for South Pacific samples reflect neutralization of acidic substances by NH_4^+ and/or the influence of sea-salt.

5.4.3. Marine biogenic NH_4^+ in rainwater over the South Pacific Ocean

The variation of NH_4^+ and NO_3^- concentrations in rainwater showed similar trends between the SAWNP and the CNP (Figs. 5.2c and 5.2d). Ammonium concentrations in rainwater collected over the SP and the CC, however, gradually increased from 8.4–29 μmol L^{-1}, showing a distinctly different trend from that seen for aerosol NH_4^+. Nitrate concentrations, on the other hand, remained low (0.16–2.3 μmol L^{-1}) in both regions. Upwelling is a particularly conspicuous phenomenon both at the equator where the trade winds cause the surface water transport and in Antarctic waters, between 40°S and 60°S, where strong westerly winds drive the circumpolar current. Upwelled water is rich in nutrients that support biological activity and, consequently, more biogenic gases (e.g., DMS and NH_3) are released from the ocean in these regions (Parungo et al., 1986). During the MR08-06 cruise (January–March 2009), SeaWiFS satellite images (http://oceancolor.gsfc.nasa.gov) revealed persistently high chlorophyll a levels (implying high phytoplankton densities) in the Southern Ocean near Antarctica (Fig. 5.5). Quinn et al. (1990) reported that dimethylsulfide (DMS) and NH_3 had similar flux strengths in the North Pacific from 15°S–55°N, with an average NH_3 to DMS molar flux ratio of 1–1.5.

Ammonia is an important neutralizing species, readily reacting with acids in the atmosphere to form NH_4^+ aerosols that can act as cloud condensation nuclei (CCN) (Spokes et al., 2000). Alternatively, NH_3 can be dissolved directly into cloud or rainwater (Quinn et al., 1987). Dimethylsulfide produced by phytoplankton in the ocean is emitted into the atmosphere, where it undergoes chemical transformation

to eventually form MSA and nss-SO_4^{2-} among other sulfur products (Charlson et al., 1987). Gondwe et al. (2004) reported that MSA/nss-SO_4^{2-} ratio in aerosols tends to be low within the tropics and high around polar regions since MSA production is most effective at low temperatures. In this study, a significant correlation ($r = 0.74$, $p < 0.05$, $n = 10$) was found between NH_4^+ and MSA in rainwater samples collected over the SP and the CC (Fig. 5.6), suggesting that they were derived from similar sources and/or experienced similar transport patterns and removal mechanisms (Kocak et al., 2004). If the single outlying point (i.e., assuming the high NH_4^+ concentration is likely affected by both oceanic and terrestrial sources) is removed from Fig. 5.5, the correlation coefficient (r) between NH_4^+ and MSA increases to 0.89 ($p < 0.01$, $n = 9$). Moreover, NH_4^+ showed no clear relationship with Na^+ in rainwater collected over the SP and the CC (Figs. 5.2c and 5.3b), suggesting that the NH_4^+ observed in these regions were not derived from NH_4^+ in seawater, but from emissions of NH_3 by high biological productivities in the Southern Ocean near Antarctica. In comparison, no significant correlations were found between NH_4^+ and MSA in rainwater collected over the SAWNP ($r = 0.42$, $p > 0.1$, $n = 6$) and the STWNP ($r = 0.33$, $p > 0.5$, $n = 6$) (Fig. 5.6). These results are likely due to the strong influence of terrestrial-derived NH_4^+ in addition to NH_4^+ produced by marine biota over the western North Pacific Ocean. A number of rainwater samples (7 out of 11 samples) collected over the SP and CC had negative nss-SO_4^{2-} values that were associated with extremely high sea-salt concentrations (Fig. 5.3c). Thus, the nss-SO_4^{2-} data in rainwater over the SP and CC could not be interpreted.

Low-pressure systems have the potential to inject air masses rich in nss-SO_4^{2-}, sea-salt, NH_4^+, DMS, MSA and other substances of biogenic origin into the free troposphere (> 2 km). Under these circumstances, effective transport to diverse oceanic sampling sites can occur (Arimoto et al., 2008). As shown in Fig. 5.4c, surface air was elevated to an altitude of 2–5 km by a low-pressure system before the air was transported to sampling sites over the SP and the CC. The elevated air that contains substances such as NH_4^+ and MSA can be transported from source regions to large areas of the open ocean by moving above planetary boundary layer avoiding wet deposition which is a primary removal mechanism for these compounds (Shepon et al., 2007). Thus, the increased NH_4^+ concentrations in rainwater samples collected over the SP and the CC and the differing spatial variations of NH_4^+ in aerosol and rainwater samples collected from the same region are most likely due to removal of NH_4^+ derived from marine biological activity by wet deposition in the free troposphere.

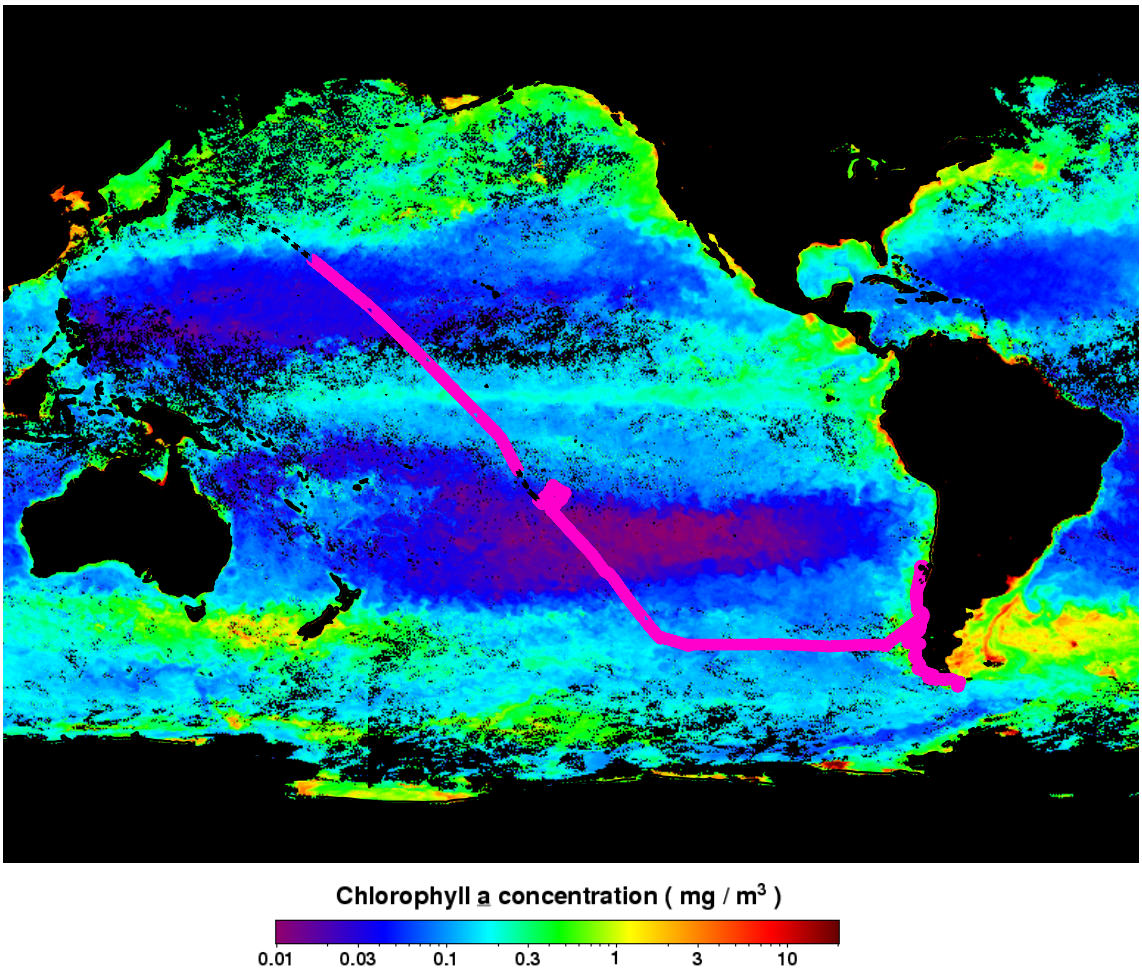

Fig. 5.5. SeaWiFS chlorophyll a image of the North and South Pacific Ocean in February 2009 (web site: http://oceancolor.gsfc.nasa.gov) and cruise track (pink line) of the MR08-06 cruise.

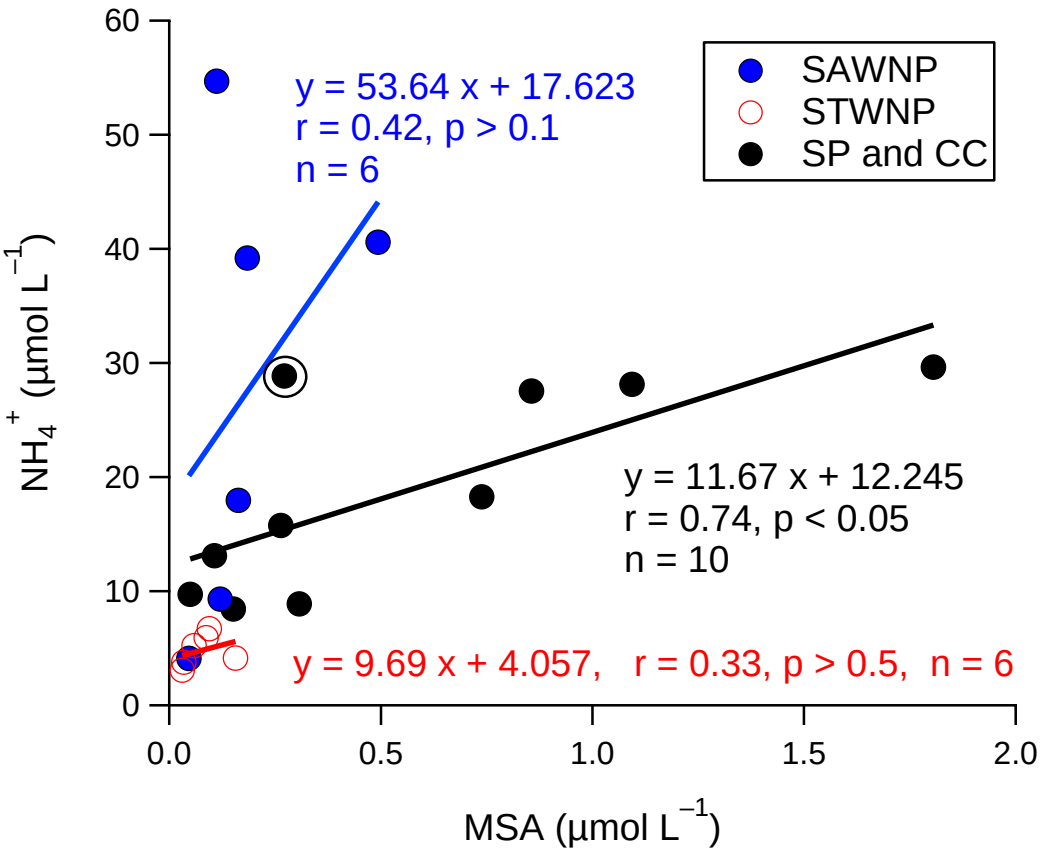

Fig. 5.6. Correlations between NH_4^+ and MSA in rainwater collected over the subarctic western North Pacific (SAWNP, blue solid symbols), the subtropical western North Pacific (STWNP, red open symbols), and the South Pacific and the coast of Chile (SP and CC, black solid symbols). MSA was not detected in 6 of the 30 rainwater samples, and these samples were excluded from statistical analyses. Circled point shows outlier described in the text.

5.5. Dry and wet deposition fluxes of atmospheric inorganic nitrogen to the Pacific Ocean

Variations of dry and wet deposition fluxes for NH_4^+ and NO_3^- during the two cruises are shown in Figs. 5.7a–5.7d. The estimated dry deposition fluxes for atmospheric inorganic N species varied from 0.55–7.8 μmol m^{-2} d^{-1} for NH_4^+ to 0.22–8.6 μmol m^{-2} d^{-1} for NO_3^-, contributing ~46% by NH_4^+ and ~54% by NO_3^- to the dry deposition flux for TIN (median values for all data). Mean dry deposition fluxes for NH_4^+ and NO_3^- estimated in the five regions ranged from 0.81–2.7 μmol m^{-2} d^{-1} and 0.45–3.3 μmol m^{-2} d^{-1}, respectively (Table 5.3). Although the mean concentration of NH_4^+ in all aerosols collected over the Pacific Ocean was approximately 1–2 times higher than that for total NO_3^- (Table 5.1), inorganic N supplied to surface waters by atmospheric dry deposition was mainly from NO_3^-, except in the CC, since NO_3^- was largely associated with coarse mode particles which deposit more rapidly.

Wet deposition of atmospheric inorganic N was highly variable from one event to the next depending on the concentrations of NH_4^+ and NO_3^- in the precipitation as well as the frequency and amount of precipitation. Wet deposition fluxes of atmospheric inorganic N species varied from 3.5 to 119 μmol m^{-2} d^{-1} for NH_4^+ and from 0.30 to 36 μmol m^{-2} d^{-1} for NO_3^-, accounting for ~83% by NH_4^+ and ~17% by NO_3^- of TIN from wet deposition flux (median values for all data). While NO_3^- was the dominant inorganic N species in dry deposition, inorganic N supplied to surface waters by atmospheric wet deposition was predominantly by NH_4^+ (42–99% of the wet deposition fluxes for TIN). It is worth noting that atmospheric NH_4^+ input does not always supply entirely "new" N to the ocean since NH_4^+ is a recycled component between the atmosphere and the ocean as mentioned in sections 5.3.2 and 5.4.3. This suggests that much of the estimated deposition flux of NH_4^+ could consist of recycled oceanic material, and that NH_4^+ is a more important N species to understand the biogeochemical cycle of N between the ocean and the atmosphere.

While dry deposition is a continuous process occurring at all times over all surfaces, wet deposition is highly episodic. The relative importance of wet and dry deposition obviously varies greatly on short time scales since rainfall is episodic and varies spatially on longer time scales with global rainfall patterns (Jickells 2006). Mean total (dry + wet) deposition fluxes of atmospheric TIN in the Pacific Ocean between 48°N and 55°S were estimated to be 32–64 μmol m^{-2} d^{-1}, with 66–99% of this in the form of wet deposition. This indicates that wet deposition plays an important role in the supply of atmospheric inorganic N to the Pacific Ocean compared to dry deposition, although the relative contributions are highly variable among regions (Table 5.3). The estimates of the proportion of atmospheric N input contributed by wet deposition were comparable to previously published values: the Pacific 86% (Duce et al., 1991), the Atlantic 78–85% (Baker et al., 2010), and the world oceans 71% (Duce et al., 1991).

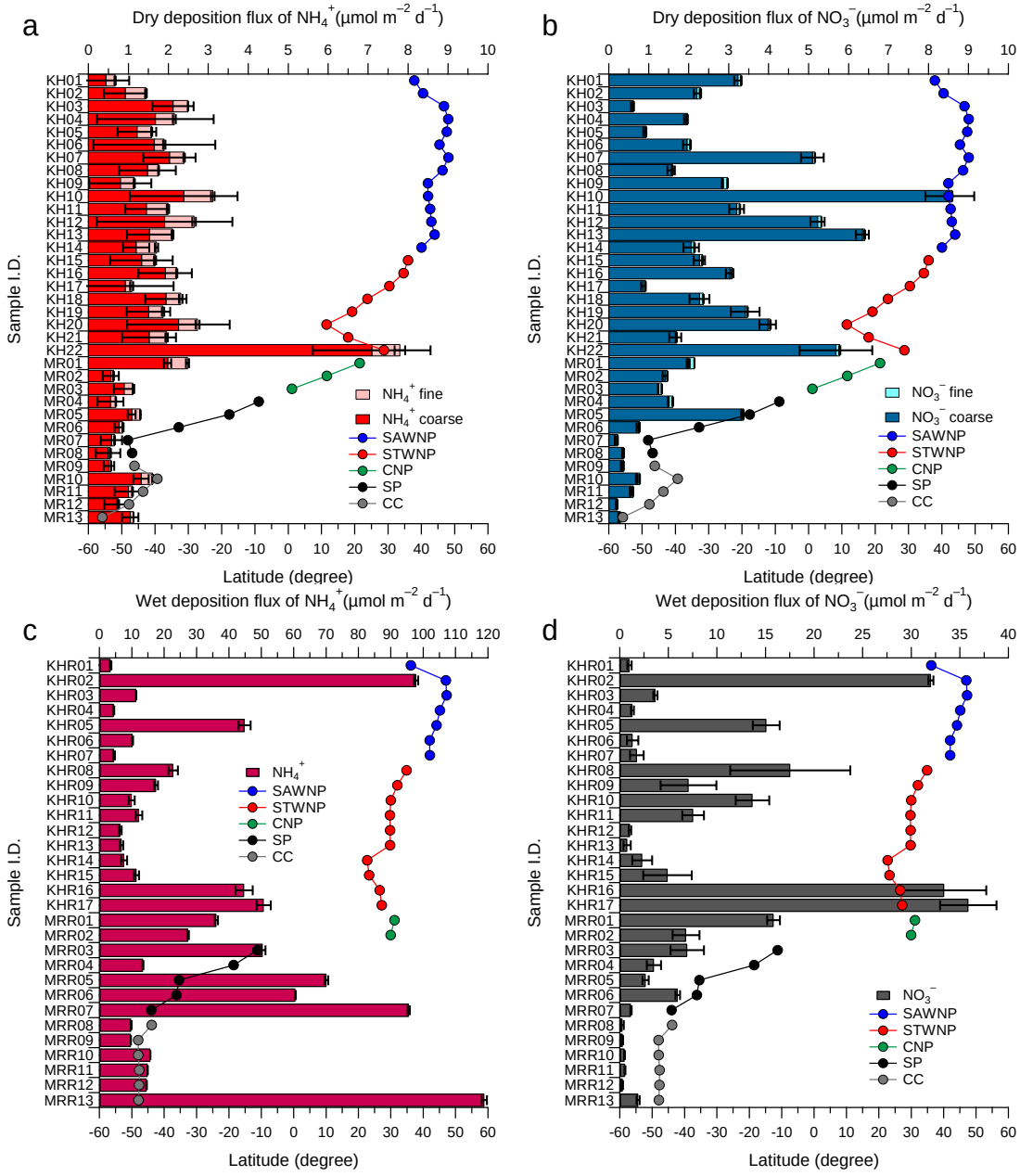

Fig. 5.7. Dry (a, b) and wet (c, d) deposition fluxes of NH_4^+ and NO_3^- against sample I.D for aerosols and rains collected during the KH-08-2 and MR08-06 cruises. The latitude of each aerosol and rain sampling location (solid circle line) is shown with different colors (subarctic western North Pacific (SAWNP), blue; subtropical western North Pacific (STWNP), red; central North Pacific (CNP), green; South Pacific (SP), black; Coast of Chile (CC), gray).

Table 5.3 Dry, wet and total deposition fluxes of NH_4^+ and NO_3^-, and the contribution of wet deposition to total inorganic N (TIN) input in each of the five oceanic regions during the KH-08-2 and MR08-06 cruises with values from Duce et al. (1991) for reference[a]

		Dry deposition flux ($\mu mol\ m^{-2}\ d^{-1}$)			Wet deposition flux ($\mu mol\ m^{-2}\ d^{-1}$)			Total deposition flux ($\mu mol\ m^{-2}\ d^{-1}$)			TIN[b] in wet deposition (%)
Region	Period	NH_4^+	NO_3^-	TIN[b]	NH_4^+	NO_3^-	TIN[b]	NH_4^+	NO_3^-	TIN[b]	
Subarctic western North Pacific (SAWNP)[1]	Jul–Aug 2008	1.9(0.63)	3.3(2.3)	5.3(2.6)	25(35)	8.0(12)	33(47)	27(35)	11(12)	38(47)	27–98
Subtropical western North Pacific (STWNP)[1]	Aug–Sep 2008	2.7(2.1)	3.0(1.5)	5.7(3.5)	19(16)	12(13)	31(29)	22(16)	15(13)	37(29)	35–98
Central North Pacific (CNP)[1]	Jan 2009	1.4(0.96)	1.6(0.44)	3.1(1.4)	32(6.2)	11(6.4)	43(13)	33(6.3)	13(6.4)	46(13)	88–96
South Pacific (SP)[1]	Jan–Mar 2009	0.81(0.30)	1.3(1.3)	2.1(1.6)	58(30)	4.1(2.4)	62(69)	59(30)	5.4(2.7)	64(69)	78–99
Coast of Chile (CC)[1]	Mar 2009	1.0(0.40)	0.45(0.24)	1.5(0.60)	31(43)	0.64(0.62)	31(44)	32(43)	1.1(0.66)	32(44)	81–99
North Pacific[1]	Jul–Sep 2008, Jan 2009	2.1(1.3)	3.0(1.9)	5.1(2.3)	23(24)	11(12)	34(27)	25(24)	14(12)	39(27)	66–98
South Pacific[1]	Jan–Mar 2009	0.92(0.35)	0.86(0.98)	1.8(1.0)	43(39)	2.2(2.4)	45(39)	44(39)	3.1(2.6)	47(39)	79–99
North Pacific[2, c]	1981–1987	1.5(-)	1.8(-)	3.3(-)	13(-)	7.4(-)	20(-)	15(-)	9.2(-)	23(-)	87
South Pacific[2, c]	1983–1987	0.58(-)	0.78(-)	1.4(-)	5(-)	3.1(-)	8.1(-)	5.6(-)	3.9(-)	9.5(-)	85

[a]Mean with (standard deviation).

[b]TIN represents total inorganic nitrogen. In this study, total inorganic nitrogen is defined as including NO_3^- and NH_4^+; i.e. TIN = NO_3^- + NH_4^+.

References: [1]This study. [2]Duce et al. (1991).

[c]Because of the limited data for NH_3 and NH_4^+ over the Pacific Ocean, Duce et al. (1991) used a few of available data reported by previous studies (references therein).

5.5.1. Previous flux estimate over the Pacific Ocean

The estimates of atmospheric inorganic N fluxes over the Pacific Ocean were related to those of Duce et al. (1991), who estimated dry and wet deposition fluxes of atmospheric inorganic N by extrapolating land-based observations to the Pacific (Table 5.3). To facilitate direct comparison, the deposition fluxes of atmospheric inorganic N species for combined oceanic regions that represent the North (SAWNP–CNP in this study) and the South Pacific (SP–CC in this study) were averaged, and mg N m^{-2} yr^{-1} units for dry and wet deposition fluxes reported by Duce et al. (1991) were converted to the μmol m^{-2} d^{-1} units used in this study. The estimates from this study for dry and wet deposition fluxes of atmospheric inorganic N species over the Pacific Ocean appeared to be higher than the values of Duce et al. (1991), with the exception of the value for the mean wet deposition flux of NO_3^- in the South Pacific. There is a difference between methods for estimating dry deposition flux. Duce et al. (1991) used constant dry deposition velocity values of 0.1 and 0.3 cm s^{-1} for NH_4^+ and NO_3^-, respectively (Baker et al., 2010), whereas atmospheric aerosols were separated according to their aerodynamic diameters into fine (D < 2.5 μm) and coarse (D > 2.5 μm) modes and velocities of 0.1 cm s^{-1} for fine mode and 2 cm s^{-1} for coarse mode were used in this study. This ambiguity in values used for dry deposition velocities leads to the greatest uncertainty in dry flux estimates, since atmospheric inorganic N species occur on a range of different size fractions (Spokes et al., 2000). It is worth noting that they used data for NH_4^+ and NO_3^- in aerosols observed during a long-term field campaign (e.g., Sea-Air Exchange Program; SEAREX) or referred previously published values to estimate deposition fluxes of atmospheric inorganic N, while only the results observed during two cruises conducted in the Pacific Ocean during the summer periods in both hemispheres were used in this study. Previous studies (e.g. Adams et al. 1999; Zhang et al. 2007; Zhang et al. 2011) reported that there is some seasonality in NO_x emissions from fossil fuel combustion (highest in winter) and NH_3 from chemical fertilizer application and livestock breeding (highest in spring/summer). Similar considerations probably apply to seasonal variations in emissions from fossil fuel combustion and agricultural sources in the southern hemisphere (Baker et al., 2010). Kundu et al. (2010) observed similar seasonal trends of atmospheric NH_4^+ and NO_3^- in aerosols, collected at Gosan (33°N, 126°E) on Jeju Island, Korea from April 2003–April 2004, showing high concentrations in spring and winter when most air masses were transported from the heavily polluted regions in East Asia, and low values in summer due to an increased clean air mass transport from the North Pacific Ocean. Prospero and Savoie (1989) reported that the highest monthly mean NO_3^- concentration in aerosols, collected at Midway (28°N, 177°W) from 1981–1987, was observed in May (0.44 μg m^{-3}; 7.1 nmol m^{-3}) and the lowest in July (0.18 μg m^{-3}; 2.9 nmol m^{-3}), showing similar seasonal trend to that of mineral dust observed at the same site. Savoie et al. (1989b) also reported that the highest NO_3^- concentrations, observed at New Caledonia (22°S, 166°E) and Norfolk Island (29°S, 167°E) from 1983–1987, generally occurred from September to January when the

transport of dust from Australia was the greatest. Given the sampling period of this study, atmospheric inorganic N input estimates of this study would indicate lower limits.

Similar to estimates for dry deposition flux, the choice of precipitation rates based on limited data causes the greatest uncertainty in wet deposition flux estimates, particularly in the open ocean (Spokes et al., 2000). Baker et al. (2010 and references therein), using the method for estimating wet deposition flux that was chose to use in this study, argued that the uncertainty arising from selection of precipitation rate is minor since the precipitation rate data agreed relatively well with other studies in terms of total rainfall amount. Therefore, it is suggest that the higher wet deposition fluxes for atmospheric inorganic N species in this study are likely due to the lack of data for atmospheric inorganic N in rainwater collected over the Pacific Ocean rather than the uncertainty inherent in precipitation rate, especially since Duce et al. (1991) based their estimated deposition fluxes for atmospheric inorganic N on extrapolations of land-based observations as mentioned above. To properly estimate dry and wet deposition fluxes of atmospheric N in the Pacific, future work should therefore focus on long-term monitoring of atmospheric N.

5.5.2. Atmospheric water-soluble organic nitrogen

Atmospheric water-soluble organic nitrogen (Org N_{ws}) (or dissolved organic nitrogen; DON) has recently drawn increasing attention as a significant additional source of "new" N input to both coastal and oceanic regions since atmospheric Org N_{ws} (or DON) is available for the uptake by primary producers (Cornell et al., 1995, 2001, 2003; Peierls and Paerl 1997; Mace et al., 2003a, 2003b; Nakamura et al., 2006). It is known that Org N_{ws} constitutes approximately 30% of total reactive N deposition (Duce et al., 2008), although the impact of Org N_{ws} on the marine ecosystem depends on the sources, composition and abundance (Cornell et al., 2003; Shi et al., 2010; Miyazaki et al., 2011). Due to the limited scope of this study, Org N_{ws} (or DON) was not measured, and therefore the current estimate of total deposition fluxes of atmospheric N over the Pacific Ocean, in particular bioavailable N, is underestimated. Assuming that the proportion of Org N_{ws} (or DON) in dry and wet deposition fluxes of atmospheric TIN is ~30%, the total deposition fluxes of atmospheric N could be underestimated by ~21–24%. The uncertainties associated with this assumption emphasize the need for further research on atmospheric Org N_{ws} (or DON) (Duce et al., 2008).

5.5.3. Potential impact of atmospheric inorganic nitrogen deposition on primary production over the Pacific Ocean

The potential impact of atmospheric deposition on marine systems depends on the nutrient status of the receiving waters, and is related to both the total amount and ratio of atmospherically supplied

nutrients and to the limiting nutrient for the existing local water column (Baker et al., 2006). It is known that NH_4^+ and NO_3^- can be readily utilized by a variety of aquatic microorganisms (Gilbert et al., 1991). In order to evaluate the impact of atmospheric N on the marine ecosystem, potential primary production was estimated using our results for total deposition fluxes of TIN and the Redfield C/N ratio of 6.6. Assuming that phytoplankton can take up all the N coming from atmospheric deposition with no losses, and that there is no co-limitation by other nutrients (i.e., P and Fe), total mean deposition fluxes of atmospheric inorganic N over the Pacific Ocean were found to be maximally responsible for the carbon uptake of 210–420 μmol C m^{-2} d^{-1} in the Pacific Ocean. Carr et al. (2006) using a primary production algorithm round robin model to compute mixed depth-integrated primary production from satellite measurements of ocean color within latitudinal bands (i.e., > 40°N, 10°–40°N, 10°S–10°N, 10°–40°S and < 40°S) in the Pacific Ocean, estimated that the area-integrated primary production for the Pacific Ocean varied between 0.30 and 0.42 g C m^{-2} d^{-1} (25–35 mmol C m^{-2} d^{-1}). Based on this, the results from this study suggested that inorganic N deposited to the Pacific Ocean from the atmosphere can support 0.86–1.7% of the total primary production. Atmospheric inorganic N deposition, however, could be an important N source in the ocean where sporadic atmospheric N deposition events caused by the transport of the continental dust are affected and the supply of deep nutrient-rich water is restricted by the stratification of the surface ocean that is enhanced by global warming.

5.6. Conclusions

Atmospheric inorganic N input to the Pacific was determined using the results from aerosols and rainwater collected during the KH-08-2 and MR08-06 cruises in 2008 and 2009. Distribution of aerosol NH_4^+ and NO_3^- showed similar trends, with high concentrations over the western North Pacific and lower values over the South Pacific, resulting from stronger influences of terrestrial sources of atmospheric N in the northern hemisphere and the intertropical convergence zone. Contributions of NH_4^+ to total inorganic N in aerosols for five regions over the Pacific Ocean were found to represent 58–70%. On the other hand, NO_3^- was the dominant atmospheric inorganic N species in dry deposition, accounting for ~54% (median value for all data), reflecting higher deposition velocity of NO_3^- than that of NH_4^+ since NO_3^- is largely associated with coarse mode particles in the marine atmosphere (Graedel and Keene 1995; Andreae and Crutzen 1997).

Wet deposition of inorganic N to surface waters was predominantly by NH_4^+ (42–99% of the wet deposition fluxes for total inorganic N), suggesting that NH_4^+ is more abundant in rainwater over the North and South Pacific Ocean, and that it is more important inorganic N species supplied by wet deposition. The significant correlation between NH_4^+ and MSA in rainwater collected over the South Pacific suggested that emissions of NH_3 by marine biological activity from the ocean could become a significant source of NH_4^+ over the South Pacific, and that much of observed NH_4^+ could be recycled

oceanic NH_3. Consequently, simple application of atmospheric NH_4^+ concentration for the estimate of atmospheric deposition flux of N may lead to overestimate of "new" N input due to its recycling between the atmosphere and the ocean (Duce et al., 1991).

Total deposition fluxes of atmospheric inorganic N over the Pacific Ocean were estimated to be 32–64 μmol m^{-2} d^{-1}, accounting for 66–99% by wet deposition. This result indicates that wet deposition plays an important role in the supply of atmospheric inorganic N to the Pacific Ocean compared to dry deposition, although the relative contributions of wet deposition are highly variable. The deposition fluxes reported in this study, however, should be considered a lower limit on the direct total atmospheric N flux to the Pacific Ocean, since only the results observed during the summer periods, when the influences of mineral dust are weak in both hemispheres, were used in this study. Nevertheless, the estimates of atmospheric inorganic N deposition fluxes over the Pacific Ocean in this study provide a useful contribution to the understanding of the atmospheric N cycle in open ocean environments. To improve understanding of the N biogeochemical cycle, future fieldwork should focus on long-term monitoring of atmospheric reactive N species in the Pacific Ocean.

References

Adams, P.J., Seinfeld, J.H., Koch, D.M., 1999. Global concentrations of tropospheric sulfate, nitrate, and ammonium aerosol simulated in a general circulation model. Journal of Geophysical Research—Atmosphere 104(D11), 13791–13823.

Andreae, M.O., Crutzen, P.J., 1997. Atmospheric aerosols: biogeochemical sources and role in atmospheric chemistry. Science 276(5315), 1052–1058.

Andreae, M.O., Merlet, P., 2001. Emission of trace gases and aerosols from biomass burning. Global Biogeochemical Cycles 15(4), 955–966.

Aneja, V.P., Roelle, P.A., Murray, G.C., Southerland, J., Erisman, J.W., Fowler, D., Asman, W.A.H., Patni, N., 2001. Atmospheric nitrogen compounds II: emissions, transport, transformation, deposition and assessment. Atmospheric Environment 35(11), 1903–1911.

Arimoto, R., Zeng, T., Davis, D., Wang, Y., Khaing, H., Nesbit, C., Huey, G., 2008. Concentrations and sources of aerosol ions and trace elements during ANTCI-2003. Atmospheric Environment 42(12), 2864–2876.

Baker, A.R., Jickells, T.D., Biswas, K.F., Weston, K., French, M., 2006. Nutrient in atmospheric aerosol particles along the Atlantic Meridional Transect. Deep-Sea Research Part II 53, 1706–1719.

Baker, A.R., Kelly, S.D., Biswas, K.F., Witt, M., Jickells, T.D., 2003. Atmospheric deposition of nutrients to the Atlantic Ocean. Geophysical Research Letters 30(24), OCE 11/11–OCE 11/14.

Baker, A.R., Lesworth, T., Adams, C., Jickells, T.D., Ganzeveld, L., 2010. Estimation of atmospheric

nutrient inputs to the Atlantic Ocean from 50°N to 50°S based on large-scale field sampling: fixed nitrogen and dry deposition of phosphorus. Global Biogeochemical Cycles 24(3), GB3006/3001–GB3006/3016.

Baker, A.R., Weston, K., Kelly, S.D., Voss, M., Streu, P., Cape, J.N., 2007. Dry and wet deposition of nutrients from the tropical Atlantic atmosphere: Links to primary productivity and nitrogen fixation. Deep-Sea Research Part I 54(10), 1704–1720.

Carr, M.-E., Friedrichs, M.A.M., Schmeltz, M., Aita, M.N, Antoine, D., Arrigo, K.R., Asanuma, I., Aumont, O., Barber, R., Behrenfeld, M., Bidigare, R., Buitenhuis, E.T., Campbell, J., Ciotti, A., Dierssen, H., Dowell, M., Dunne, J., Esaias, W., Gentili, B., Gregg, W., Groom, S., Hoepffner, N., Ishizaka, J., Kameda, T., Le Qu, C., Lohrenz, S., Marra, J., Melin, F., Moore, K., Morel, A., Reddy, T.E., Ryan, J., Scardi, M., Smyth, T., Turpie, K., Tilstone, G., Waters, K., Yamanaka, Y., 2006. A comparison of global estimates of marine primary production from ocean color. Deep-Sea Research Part II 53, 741–770.

Charlson, R.J., Lovelock, J.E., Andreae, M.O., Warren, S.G., 1987. Oceanic phytoplankton, atmospheric sulfur, cloud albedo and climate. Nature 326(6114), 655–661.

Chen, Y., Siefert, R.L., 2004. Seasonal and spatial distributions and dry deposition fluxes of atmospheric total and labile iron over the tropical and subtropical North Atlantic Ocean. Journal of Geophysical Research—Atmosphere 109, D09305–D09318.

Cornell, S., Mace, K., Coeppicus, S., Duce, R., Huebert, B., Jickells, T., Zhuang, L.Z., 2001. Organic nitrogen in Hawaiian rain and aerosol. Journal of Geophysical Research—Atmosphere 106(D8), 7973–7983.

Cornell, S., Rendell, A., Jickells, T., 1995. Atmospheric inputs of dissolved organic nitrogen to the oceans. Nature 376, 243–246.

Cornell, S.E., Jickells, T.D., Cape, J.N., Rowland, A.P., Duce, R.A., 2003. Organic nitrogen deposition on land and coastal environments: a review of methods and data. Atmospheric Environment 37, 2173–2191.

Crutzen, P.J., Gidel, L.T., 1983. A two-dimensional photochemical model of the atmosphere. 2: The tropospheric budgets of the anthropogenic chlorocarbons, carbon monoxide, methane, chloromethane and the effect of various nitrogen oxides (NO_x) sources on tropospheric ozone. Journal of Geophysical Research 88(C11), 6641–6661.

Dentener, F., Drevet, J., Lamarque, J.F., Bey, I., Eickhout, B., Fiore, A.M., Hauglustaine, D., Horowitz, L.W., Krol, M., Kulshrestha, U.C., Lawrence, M., Galy-Lacaux, C., Rast, S., Shindell, D., Stevenson, D., Van, N.T., Atherton, C., Bell, N., Bergman, D., Butler, T., Cofala, J., Collins, B., Doherty, R., Ellingsen, K., Galloway, J., Gauss, M., Montanaro, V., Muller, J.F., Pitari, G., Rodriguez, J., Sanderson, M., Solmon, F., Strahan, S., Schultz, M., Sudo, K., Szopa, S., Wild, O., 2006. Nitrogen and sulfur deposition on regional and global scales: a multimodel evaluation. Global Biogeochemical

Cycles 20(4), GB4003/4001–GB4003/4021.

Dentener, F.J., Crutzen, P.J., 1994. A three-dimensional model of the global ammonia cycle. Journal of Atmospheric Chemistry 19(4), 331–369.

Duce, R.A., LaRoche, J., Altieri, K., Arrigo, K.R., Baker, A.R., Capone, D.G., Cornell, S., Dentener, F., Galloway, J., Ganeshram, R.S., Geider, R.J., Jickells, T., Kuypers, M.M., Langlois, R., Liss, P.S., Liu, S.M., Middelburg, J.J., Moore, C.M., Nickovic, S., Oschlies, A., Pedersen, T., Prospero, J., Schlitzer, R., Seitzinger, S., Sorensen, L.L., Uematsu, M., Ulloa, O., Voss, M., Ward, B., Zamora, L., 2008. Impacts of atmospheric anthropogenic nitrogen on the open ocean. Science 320(5878), 893–897.

Duce, R.A., Liss, P.S., Merrill, J.T., Atlas, E.L., Buat-Menard, P., Hicks, B.B., Miller, J.M., Prospero, J.M., Arimoto, R., Church, T.M., Ellis, W., Galloway, J.N., Hansen, L., Jickells, T.D., Knap, A.H., Reinhardt, K.H., Schneider, B., Soudine, A., Tokos, J.J., Tsunogai, S., Wollast, R., Zhou, M., 1991. The atmospheric input of trace species to the world ocean. Global Biogeochemical Cycles 5(3), 193–259.

Furutani, H., Meguro, A., Iguchi, H., Uematsu, M., 2010. Geographical distribution and sources of phosphorus in atmospheric aerosol over the North Pacific Ocean. Geophysical Research Letters 37, L03805–L03810.

Galloway, J.N., Dentener, F.J., Capone, D.G., Boyer, E.W., Howarth, R.W., Seitzinger, S.P., Asner, G.P., Cleveland, C.C., Green, P.A., Holland, E.A., Karl, D.M., Michaels, A.F., Porter, J.H., Townsend, A.R., Voeroesmarty, C.J., 2004. Nitrogen cycles: past, present, and future. Biogeochemistry 70(2), 153–226.

Gilbert, P.M., Garside, C., Fuhrman, J.A., Roman, M.R., 1991. Time-dependent coupling of inorganic and organic nitrogen uptake and regeneration in the plume of the Chesapeake Bay estuary and its regulation by large heterotrophs. Limnology and Oceanography 36, 895–909.

Gondwe, M., Krol, M., Klaassen, W., Gieskes, W., de, B.H., 2004. Comparison of modeled versus measured MSA:nss$SO_4^=$ ratios: A global analysis. Global Biogeochemical Cycles 18(2), GB2006/2001–GB2006/2018.

Graedel, T.E., Keene, W.C., 1995. Tropospheric budget of reactive chlorine. Global Biogeochemical Cycles 9, 47–77.

Gruber, N., Galloway, J.N., 2008. An earth-system perspective of the global nitrogen cycle. Nature 451 (7176), 293–296.

Jickells, T., 2006. The role of air-sea exchange in the marine nitrogen cycle. Biogeosciences 3(3), 271–280.

Jung, J., Jang, Y., Arimoto, R., Uematsu, M., Lee, G., 2009. Atmospheric nitrogen deposition and its impact to Lake Sihwa in South Korea from January 2004 to September 2005. Geochemical Journal 43, 305–314.

Kim, T.-W., Lee, K., Najjar, R.G., Jeong, H.-D., Jeong, H.J., 2011. Increasing N abundance in the

Northwestern Pacific Ocean due to atmospheric nitrogen deposition. Science 334, 505–509.

Kocak, M., Kubilay, N., Mihalopoulos, N., 2004. Ionic composition of lower tropospheric aerosols at a Northeastern Mediterranean site: implications regarding sources and long-range transport. Atmospheric Environment 38(14), 2067–2077.

Krishnamurthy, A., Moore, J.K., Mahowald, N., Luo, C., Zender, C.S., 2010. Impacts of atmospheric nutrient inputs on marine biogeochemistry. Journal of Geophysical Research—Biogeosciences 115(G1), G01006/01001–G01006/01013.

Kundu, S., Kawamura, K., Lee, M., 2010. Seasonal variation of the concentrations of nitrogenous species and their nitrogen isotopic ratios in aerosols at Gosan, Jeju Island: Implications for atmospheric processing and source changes of aerosols. Journal of Geophysical Research—Atmosphere 115, D20305–D20323.

Mace, K.A., Duce, R.A., Tindale, N.W., 2003a. Organic nitrogen in rain and aerosol at Cape Grim, Tasmania, Australia. Journal of Geophysical Research—Atmosphere 108(D11), ACH3/1–ACH3/14.

Mace, K.A., Kubilay, N., Duce, R.A., 2003b. Organic nitrogen in rain and aerosol in the eastern Mediterranean atmosphere: an association with atmospheric dust. Journal of Geophysical Research—Atmosphere 108, ACH 5/1–ACH 5/11.

Matsumoto, K., Minami, H., Uyama, Y., Uematsu, M., 2009. Size partitioning of particulate inorganic nitrogen species between the fine and coarse mode ranges and its implication to their deposition on the surface ocean. Atmospheric Environment 43(28), 4259–4265.

Miyazaki, Y., Kawamura, K., Jung, J., Furutani, H., Uematsu, M., 2011. Latitudinal distributions of organic nitrogen and organic carbon in marine aerosols over the western North Pacific. Atmospheric Chemistry and Physics 11, 3037–3049.

Nakamura, T., Matsumoto, K., Uematsu, M., 2005. Chemical characteristics of aerosols transported from Asia to the East China Sea: an evaluation of anthropogenic combined nitrogen deposition in autumn. Atmospheric Environment 39(9), 1749–1758.

Nakamura, T., Ogawa, H., Maripi, D.K., Uematsu, M., 2006. Contribution of water soluble organic nitrogen to total nitrogen in marine aerosols over the East China Sea and western North Pacific. Atmospheric Environment 40, 7259–7264.

Ooki, A., Uematsu, M., Noriki, S., 2007. Size-resolved sulfate and ammonium measurements in marine boundary layer over the North and South Pacific. Atmospheric Environment 41(1), 81–91.

Paerl, H.W., 1997. Coastal eutrophication and harmful algal blooms: importance of atmospheric deposition and groundwater as "new" nitrogen and other nutrient sources. Limnology and Oceanography 42, 1154–1165.

Parungo, F.P., Nagamoto, C.T., Rosinski, J., Haagenson, P.L., 1986. A study of marine aerosols over the Pacific Ocean. Journal of Atmospheric Chemistry 4(2), 199–226.

Peierls, B.L., Paerl, H.W., 1997. Bioavailability of atmospheric organic nitrogen deposition to coastal

phytoplankton. Limnology and Oceanography 42(8), 1819–1823.

Prospero, J.M., Savoie, D.L., 1989. Effect of continental sources on nitrate concentrations over the Pacific Ocean. Nature 339(6227), 687–689.

Prospero, J.M., Savoie, D.L., Nees, R.T., Duce, R.A., Merrill, J., 1985. Particulate sulfate and nitrate in the boundary layer over the North Pacific Ocean. Journal of Geophysical Research—Atmosphere 90(D6), 10,586–10,596.

Quinn, P.K., Bates, T.S., Johnson, J.E., Covert, D.S., Charlson, R.J., 1990. Interactions between the sulfur and reduced nitrogen cycles over the Central Pacific Ocean. Journal of Geophysical Research—Atmosphere 95(D10), 16405–16416.

Quinn, P.K., Charlson, R.J., Bates, T.S., 1988. Simultaneous observations of ammonia in the atmosphere and ocean. Nature 335(6188), 336–338.

Quinn, P.K., Charlson, R.J., Zoller, W.H., 1987. Ammonia, the dominant base in the remote marine troposphere: a review. Tellus, Series B 39B(5), 413–425.

Sandroni, V., Raimbault, P., Migon, C., Garcia, N., Gouze, E., 2007. Dry atmospheric deposition and diazotrophy as sources of new nitrogen to northwestern Mediterranean oligotrophic surface waters. Deep-Sea Research Part I 54, 1859–1870.

Sasakawa, M., Ooki, A., Uematsu, M., 2003. Aerosol size distribution during sea fog and its scavenge process of chemical substances over the northwestern North Pacific. Journal of Geophysical Research—Atmosphere 108(D3), AAC13/11–AAC13/19.

Sasakawa, M., Uematsu, M., 2005. Relative contribution of chemical composition to acidification of sea fog (stratus) over the northern North Pacific and its marginal seas. Atmospheric Environment 39(7), 1357–1362.

Savoie, D.L., Prospero, J.M., Larsen, R.J., Huang, F., Izaguirre, M.A., Huang, T., Snowdon, T.H., Custals, L., Sanderson, C.G., 1993. Nitrogen and sulfur species in Antarctic aerosols at Mawson, Palmer Station, and Marsh (King George Island). Journal of Atmospheric Chemistry 17(2), 95–122.

Savoie, D.L., Prospero, J.M., Merrill, J.T., Uematsu, M., 1989a. Nitrate in the atmospheric boundary layer of the tropical South Pacific: implications regarding sources and transport. Journal of Atmospheric Chemistry 8(4), 391–415.

Savoie, D.L., Prospero, J.M., Nees, R.T., 1987. Nitrate, non-sea-salt sulfate, and mineral aerosol over the northwestern Indian Ocean. Journal of Geophysical Research—Atmosphere 92(D1), 933–942.

Savoie, D.L., Prospero, J.M., Saltzman, E.S., 1989b. Nitrate, non-seasalt sulfate and methanesulfonate over the Pacific Ocean. In: Riley, J.P, Chester, R., Duce, R.A. (eds.) Chemical Oceanography Volume 10, pp. 219–250. Academic Press Publication, California.

Seinfeld, J.H., Pandis, S.N., 1998. Atmospheric Chemistry and Physics: From Air Pollution to Climate Change. John Wiley & Sons, New York.

Shepon, A., Gildor, H., Labrador, L.J., Butler, T., Ganzeveld, L.N., Lawrence, M.G., 2007. Global

reactive nitrogen deposition from lightning NO_x. Journal of Geophysical Research—Atmosphere 112(D6), D06304/06301–D06304/06314.

Shi, J., Gao, H., Qi, J., Zhang, J., Yao, X., 2010. Sources, compositions, and distributions of water-soluble organic nitrogen in aerosols over the China Sea. Journal of Geophysical Research—Atmosphere 115, D17303–D17315.

Spokes, L.J., Jickells, T.D., 2005. Is the atmosphere really an important source of reactive nitrogen to coastal waters? Continental Shelf Research 25, 2022–2035.

Spokes, L.J., Yeatman, S.G., Cornell, S.E., Jickells, T.D., 2000. Nitrogen deposition to the eastern Atlantic Ocean. The importance of south-easterly flow. Tellus Series B 52B(1), 37–49.

Uematsu, M., Hattori, H., Nakamura, T., Narita, Y., Jung, J., Matsumoto, K., Nakaguchi, Y., Kumar, M.D.:=, 2010. Atmospheric transport and deposition of anthropogenic substances from the Asia to the East China Sea. Marine Chemistry 120(1-4), 108–115.

Uno, I., Uematsu, M., Hara, Y., He, Y.J., Ohara, T., Mori, A., Kamaya, T., Murano, K., Sadanaga, Y., Bandow, H., 2007. Numerical study of the atmospheric input of anthropogenic total nitrate to the marginal seas in the western North Pacific region. Geophysical Research Letters 34(17), L17817/17811–L17817/17816.

Wang, B.-H., 1985. Distributions and variations of sea fog in the world, in Sea Fog. pp. 51–90. China Ocean Press, Beijing.

Xie, P., Arkin, P.A., 1997. Global precipitation: A 17-year monthly analysis based on gauge observations, satellite estimates, and numerical model outputs. Bulletin of the American Meteorological Society 78, 2539–2558.

Yeatman, S.G., Spokes, L.J., Jickells, T.D., 2001. Comparisons of coarse-mode aerosol nitrate and ammonium at two polluted coastal sites. Atmospheric Environment 35(7), 1321–1335.

Zhang, G., Zhang, J., Liu, S., 2007. Characterization of nutrients in the atmospheric wet and dry deposition observed at the two monitoring sites over Yellow Sea and East China Sea. Journal of Atmospheric Chemistry 57(1), 41–57.

Zhang, J., Zhang, G.S., Bi, Y.F., Liu, S.M., 2011. Nitrogen species in rainwater and aerosols of the Yellow and East China seas: Effects of the East Asian monsoon and anthropogenic emissions and relevance for the NW Pacific Ocean. Global Biogeochemical Cycles 25, GB3020–GB3033.

Zhang, Y., Yu, Q., Ma, W., Chen, L., 2010. Atmospheric deposition of inorganic nitrogen to the eastern China seas and its implications to marine biogeochemistry. Journal of Geophysical Research—Atmosphere 115, D00K10–D00K19.

6. Summary and Conclusions

There are still large uncertainties regarding the quantitative estimation of the global atmospheric N cycle over the oceans since most studies are based on the results of several models and the observations in the remote island sites. Moreover, the validation of model output was primarily based on comparisons to terrestrial sampling sites. In addition, the field observation/data on the deposition flux of atmospheric N are mostly concentrated on the Atlantic Ocean and the Mediterranean Sea, with a little data being reported for the Pacific Ocean. In this study, atmospheric inorganic N deposition flux was determined using the measurement results for NH_4^+ and NO_3^- in aerosols, rainwater and sea fog water collected over the North and South Pacific Ocean in 2008 and 2009. The simultaneous sampling of aerosol, rainwater and sea fog water carried out in this study, allowed a better estimate of atmospheric inorganic N deposition flux to the Pacific Ocean and its impact on marine biogeochemical cycle. The results from this study provide a significant new observational data on atmospheric inorganic N deposition over the Pacific Ocean, which should be valuable for filling the data gap and be useful for validation of atmospheric N deposition flux model on a global ocean scale.

The mean dry deposition fluxes for atmospheric TIN over the Pacific Ocean were estimated to be 64 ± 31 μmol m^{-2} d^{-1} in the semi-pelagic western North Pacific, 5.3 ± 2.6 μmol m^{-2} d^{-1} in the subarctic western North Pacific, 5.7 ± 3.5 μmol m^{-2} d^{-1} in the subtropical western North Pacific, 3.1 ± 1.4 μmol m^{-2} d^{-1} in the central North Pacific, 2.1 ± 1.6 μmol m^{-2} d^{-1} in the South Pacific and 1.5 ± 0.60 μmol m^{-2} d^{-1} in the coast of Chile. This result suggests that the increase in emissions of anthropogenic N derived from terrestrial sources (i.e., agricultural activity and fossil fuel consumption) in the northern hemisphere, has affected atmospheric N supply to the open ocean. In the North and South Pacific Ocean, the concentrations of aerosol NH_4^+ showed higher values than those of NO_3^-, but dry deposition fluxes of NO_3^- were estimated to be higher than those of NH_4^+. This was caused by the difference of particle size between aerosol NH_4^+ and NO_3^-. The results for size distributions of these two species showed that NH_4^+ was largely associated with nss-SO_4^{2-} existed in fine particles, whereas NO_3^- was mainly contained in coarse sea salt particles by the adsorption of gaseous HNO_3. Particle size is one of the critical factors to contribute to atmospheric inorganic N input via dry deposition to the Pacific Ocean.

Compared to dry deposition, there have been few studies on wet deposition flux of atmospheric inorganic N estimated using the concentrations of NH_4^+ and NO_3^- in rainwater collected over the Pacific Ocean. The mean wet deposition fluxes for atmospheric TIN over the Pacific Ocean were estimated to be 33 ± 47 μmol m^{-2} d^{-1} in the subarctic western North Pacific, 31 ± 29 μmol m^{-2} d^{-1} in the subtropical western North Pacific, 43 ± 13 μmol m^{-2} d^{-1} in the central North Pacific, 62 ± 69 μmol m^{-2} d^{-1} in the South Pacific and 31 ± 44 μmol m^{-2} d^{-1} in the coast of Chile. Wet deposition was the dominant removal process for atmospheric inorganic N, contributing 66–99% to total (dry + wet) atmospheric inorganic N input to the Pacific Ocean. So far, deposition fluxes for atmospheric N over the South Pacific Ocean

have been considered to be minor; however, total deposition fluxes of atmospheric TIN over the South Pacific Ocean (i.e., including the value in the coast of Chile) were estimated to be 47 ± 39 μmol m^{-2} d^{-1}, with 79–99% of this in the form of wet deposition. In this study, it is suggested that higher deposition fluxes for atmospheric inorganic N over the South Pacific Ocean are likely due to the lack of data for atmospheric inorganic N in rainwater collected over the South Pacific Ocean since previous studies on atmospheric inorganic N deposition fluxes are based on extrapolations of land-based observations. While NO_3^- was the dominant atmospheric inorganic N species in dry deposition, wet deposition of inorganic N to surface waters was predominantly by NH_4^+ (42–99% of the wet deposition fluxes for TIN), indicating that NH_4^+ is more important inorganic N species supplied by wet deposition. In this study, the significant correlation was found between NH_4^+ and MSA in rainwater collected over the South Pacific Ocean, suggesting that emissions of NH_3 by marine biological activity from the ocean could become a significant source of NH_4^+ over the South Pacific Ocean. This result therefore reveals that much of the estimated wet deposition fluxes of NH_4^+ over the South Pacific could consist of marine biogenic NH_4^+, and that NH_4^+ is a more important N species to understand the biogeochemical cycle of N between the atmosphere and the ocean.

The subarctic western North Pacific Ocean (> 40°N) has a high frequency of sea fog, with a maximum of ~50% during the summertime period (June–August). The fog deposition is an important transfer process for atmospheric substances from the atmosphere to the biosphere. It is therefore suggested that sea fog may play a key role in supplying atmospheric nutrients to this region. Nevertheless, no study has been carried out over the subarctic western North Pacific Ocean to quantify sea fog deposition flux for atmospheric N. This is the first study to estimate atmospheric inorganic N fluxes via dry, wet and sea fog deposition simultaneously. The mean dry, wet and sea fog deposition fluxes for atmospheric TIN were estimated to be 4.9 ± 2.6 μmol m^{-2} d^{-1}, 33 ± 47 μmol m^{-2} d^{-1} and 7.8 ± 8.7 μmol m^{-2} d^{-1}, respectively. While dry and wet deposition was the entire process to deliver inorganic N species from the atmosphere to the ocean in the other regions of the Pacific Ocean, the subarctic western North Pacific received additional atmospheric inorganic N influx by sea fog that scavenges more efficiently HNO_3 gas as well as aerosol NO_3^- in coarse mode particles. Wet deposition delivered more atmospheric inorganic N to the subarctic western North Pacific Ocean than dry and sea fog deposition, contributing ~72% to total deposition flux for TIN (46 ± 48 μmol m^{-2} d^{-1}), although the relative contributions are highly variable. The mean contribution of sea fog deposition to total deposition flux for TIN was ~17%. Despite the relatively lower contribution of sea fog deposition, in some cases, atmospheric inorganic N input via sea fog deposition exceeded the combined dry and wet deposition fluxes. Thus, it is suggested that sea fog can result in substantial N deposition if the event persists long enough and has sufficient LWC (dense sea fog), and that ignoring sea fog deposition would lead to underestimate of the total influx of atmospheric inorganic N into the subarctic western North Pacific Ocean, especially in summer periods.

In this study, the impact of atmospheric inorganic N deposition on primary production over the Pacific Ocean was evaluated using the Redfield C/N ratio of 6.6. The results from this study suggested that even the high atmospheric inorganic N deposition events seen in this region are not large enough to trigger phytoplankton blooms. This may be because productivity in the Pacific Ocean is controlled by internal recycling of N. However, the sporadic atmospheric deposition events caused by dust storms can supply a large amount of N to the surface ocean over a very short period. In addition, since the emissions of anthropogenic atmospheric reactive N by rapid growth in human population and industrial activity are increasing, atmospheric deposition could become an important source of nutrients in the ocean where the supply of deep nutrient rich water is restricted by the stratification of the surface ocean that is enhanced by global warming. To improve understanding of the biogeochemical cycle of N and the contribution of atmospheric N deposition to primary production in the Pacific Ocean, future work therefore should focus on long-term monitoring of atmospheric reactive N, including organic N as well as other nutrients such as phosphorus and iron.

Acknowledgement

I am deeply indebted to my adviser Professor Mitsuo Uematsu, Atmosphere and Ocean Research Institute (AORI), the University of Tokyo, whose valuable comments, stimulating suggestions and encouragements helped me in all the time of research for and writing of this thesis. He provided many opportunities to participate in the research cruises and to present the result of this study at the domestic and international conferences. He also created a productive and distraction-free environment that allowed me to concentrate on this work. His perpetual energy and enthusiasm in research had motivated all his advisees, including me. In addition, he was always accessible and willing to help his students with their research. I am grateful to Dr. Hiroshi Furutani for his friendship, considerable assistance during the research cruises, stimulating discussions and helping me to broaden my view. His remarks and constructive criticisms have certainly improved the quality of this work. I would like to express my sincere gratitude to Dr. William L. Miller, the University of Georgia, the United States of America, who was invited to AORI as a visiting professor, for his helpful comments and a critical reading of the manuscript. I would like to thank Professor Shigenobu Takeda, Nagasaki University and Associate Professor Hajime Obata, AORI, for providing a rainwater sampler. Without their help, I was not able to collect rainwater samples. Professor Kazuhiro Kogure, Professor Ichiro Yasuda, Professor Atsushi Tsuda, Associate Professor Hajime Obata deserve special thanks as my thesis committee members and advisors.

I am grateful to the captains and crews of R/V *Hakuho Maru*, R/V *Mirai* and R/V *Tansei Maru* for their enthusiastic assistance in collecting aerosol, rainwater and sea fog water samples during the KH-08-2, MR08-06 and KH-09-5 cruises. I would also like to express my great appreciation to the principal investigators Professor Mitsuo Uematsu (Leg 1 of the KH-08-2 cruise), Associate Professor Hiroshi Ogawa (Leg 2 of the KH-08-2 cruise), AORI, Dr. Natsue Abe (Leg 1 of the MR08-06 cruise), Japan Agency for Marine-Earth Science and Technology (JAMSTEC), Dr. Naomi Harada (Leg 2 and Leg 3 of the MR08-06 cruise), JAMSTEC and Professor Mitsuo Uematsu (the KT-09-5 cruise) for their thoughtful assistance. My grateful thanks are also extended to Dr. Yasushi Narita, Dr. Yoko Iwamoto and Dr. Fumiyoshi Kondo for their professional guidance for observation on the ship and valuable support. Thanks also to Ms. Sujaree Bureekul, Mr. Hiroyasu Nakayama, Mr. Daisuke Morimoto, Mr. Ryou Kawata, Ms. Yoshiko Murashima, Ms. Mayu Iimura, Mr. Taejin Kim, Ms. Mary Mar P. Noblezada and the colloquium members of inorganic group at AORI, for their help for observation, laboratory work and discussion. They also presented me with memorable days during my life in Japan.

This study was supported by funds from the Grant-in-Aid for Scientific Research in Priority Areas “Western Pacific Air-Sea Interaction Study (W-PASS)” under Grant No.18067005 from the Ministry of Education, Culture, Sports, Science and Technology (MEXT), Japan. This work was partly supported by the Sasakawa Scientific Research Grant from The Japan Science Society. This research is a contribution to the Surface Ocean Lower Atmosphere Study (SOLAS) Core Project of the International Geosphere-

Biosphere Programme (IGBP). I have been financially supported by University of Tokyo Fellowship and research assistant of AORI. In particular, I would like to thank Professor Mitsuo Uematsu for hiring me as a research assistant.

My deepest gratitude goes to my family for their unflagging love and support throughout my life. I could not have written this dissertation without their support. I am indebted to my wife, Miseon Lee, for her devotion and support. She had never complained about all the hardships. I have no suitable word that can fully describe her love and support. My father-in-law and mother-in-law deserve special thanks for supporting me in various ways. They always pray for me and help to care for my two sons, Minjun Jung and Hyunjun Jung.

Last but not least, thanks be to my God who is always with me and strengthen me. You have helped me to receive the Ph. D degree at the University of Tokyo. May your name be exalted, honored, and glorified.